arXiv:hep-ph/0505042v2 26 Jul 2005

MPP-2005-23
PSI-PR-05-05
hep-ph/0505042

Electroweak corrections to charged-current $e^+e^- \to 4\,$fermion processes

—

technical details and further results

A. Denner[1], S. Dittmaier[2], M. Roth[2] and L.H. Wieders[1,3]

[1] *Paul Scherrer Institut, Würenlingen und Villigen*
CH-5232 Villigen PSI, Switzerland

[2] *Max-Planck-Institut für Physik (Werner-Heisenberg-Institut)*
D-80805 München, Germany

[3] *Institute for Theoretical Physics*
University of Zürich, CH-8057 Zürich, Switzerland

Abstract:

The complete electroweak $\mathcal{O}(\alpha)$ corrections have been calculated for the charged-current four-fermion production processes $e^+e^- \to \nu_\tau\tau^+\mu^-\bar{\nu}_\mu$, $u\bar{d}\mu^-\bar{\nu}_\mu$, and $u\bar{d}s\bar{c}$. Here, technical details of this calculation are presented. These include the algebraic reduction of spinor chains to a few standard structures and the consistent implementation of the finite width of the W boson. To this end, a generalization of the complex-mass scheme to the one-loop level is proposed, and the practical application of this method is described. Finally, the effects of the complete $\mathcal{O}(\alpha)$ corrections to various differential cross sections of physical interest are discussed and compared to predictions based on the double-pole approximation, revealing that the latter approximation is not sufficient to fully exploit the potential of a future linear collider in an analysis of W-boson pairs at high energies.

May 2005

1 Introduction

W-pair production is an important process for testing the Electroweak Standard Model (SM). On the one hand, it allows to measure the mass of the W boson, a fundamental parameter of the SM, precisely. On the other hand, it is sensitive to the triple non-abelian gauge couplings and, in particular at high energies, allows to test the non-abelian structure of the SM accurately, owing to the delicate gauge cancellations in its lowest-order matrix elements.

Experimentally, W-pair production has been studied intensively at LEP2 with quite high precision [1]. The total cross section was measured from threshold up to a centre-of-mass (CM) energy of 207 GeV leading to a combined experimental accuracy of $\sim 1\%$. While the W-boson mass M_W was determined from the threshold cross section with an error of $\sim 200\,\mathrm{MeV}$ and by reconstructing the W bosons from their decay products within $\sim 40\,\mathrm{MeV}$, deviations from the SM triple gauge-boson couplings were constrained within a few per cent. More precise experimental investigations of W-pair production will be possible at a future International $\mathrm{e}^+\mathrm{e}^-$ Linear Collider (ILC) [2, 3, 4]. Owing to the high luminosity of such a collider, the accuracy of the cross section measurement will be at the per-mille level, and the precision of the W-mass determination is expected to be $\sim 10\,\mathrm{MeV}$ [5] by direct reconstruction and $\sim 7\,\mathrm{MeV}$ from a threshold scan of the total W-pair-production cross section [2, 3]. The higher energy of the ILC will enable much more precise measurements of the triple gauge-boson couplings, improving the sensitivity of LEP2 by more than an order of magnitude.

Because of its theoretical importance, W-pair production found early interest. The lowest-order amplitudes for on-shell W-pair production were already considered at the end of the 1970's [6]. The electroweak corrections to on-shell W-pair production have been calculated by four different groups [7, 8] shortly after and supplemented by hard photon radiation [9]. Already at that time, these calculations were at the forefront of the technical developments in higher-order calculations. Later, the structure of these corrections has been investigated by constructing improved Born approximations [10] and high-energy approximations [11]. With the advent of LEP2 it became quickly clear that the decays of the W bosons into fermion pairs had to be included. The electroweak corrections to the on-shell W-boson decay were given in Ref. [12]. Different types of programs (ranging from semianalytical codes to Monte Carlo generators) for lowest-order predictions for $\mathrm{e}^+\mathrm{e}^- \to 4f$ were developed [13] (see also Refs. [14, 15, 16] and references therein) and subsequently supplemented by universal corrections thus reaching an accuracy of about 2%. The universal corrections included running couplings, initial-state radiation, and also the effects of the Coulomb singularity for off-shell W-pair production [17]. Since the accuracy of 2% was not sufficient for LEP2, the $\mathcal{O}(\alpha)$ corrections to $\mathrm{e}^+\mathrm{e}^- \to \mathrm{WW} \to 4f$ were calculated in the double-pole approximation (DPA), where only the leading terms in an expansion about the resonance poles of the two W-boson propagators were taken into account [18, 19, 20, 21, 22]. These corrections were implemented into the event generators YFSWW [19] and RacoonWW [20, 21, 23]. A discussion of the remaining theoretical uncertainties of these calculations is presented in Refs. [16, 24]. In view of the improved precision of the ILC, a further reduction of the uncertainties from missing radiative corrections is necessary. This requires, in particular, the calculation of the full one-loop corrections for W-pair-mediated $\mathrm{e^+e^-} \to 4f$ processes.

Such a calculation poses a number of theoretical challenges.[1] Neglecting diagrams involving couplings of Higgs bosons to light fermions, which are proportional to the fermion masses, already for the simplest final states $\mathrm{e^+e^-} \to \nu_\tau \tau^+ \mu^- \bar{\nu}_\mu$, $\mathrm{u\bar{d}}\mu^-\bar{\nu}_\mu$, and $\mathrm{u\bar{d}s\bar{c}}$ about 1200 Feynman diagrams contribute (counting the contributions of the three fermion generations in the loops only once), and for the most complicated final state $\nu_\mathrm{e}\mathrm{e^+e^-}\bar{\nu}_\mathrm{e}$, there are about 6000 diagrams. The large number and the complexity of the diagrams require to develop improved reduction algorithms, in order to keep the expressions manageable and to produce an efficient and numerically stable computer code.

Because of the complicated multi-particle final state, the appearing loop integrals in general cannot be evaluated with standard methods. Using the Passarino–Veltman reduction to calculate the tensor integrals leads to serious numerical problems when the Gram determinants that appear in the denominators become small. This usually happens near the boundary of phase space but can also occur within phase space because of the indefinite Minkowski metric. Thus, in order to obtain numerically stable results, one has to devise and implement alternative methods for the calculation of the tensor integrals, at least, in the critical regions.

The inclusion of the finite gauge-boson decay width constitutes a further important problem in the calculation of radiative corrections to W-pair-mediated four-fermion production. An appropriate description of resonances in perturbation theory requires a Dyson summation of self-energy insertions in the resonant propagators. It is well known that this procedure in general violates gauge invariance, i.e. destroys Slavnov–Taylor and Ward identities and disturbs the cancellation of gauge-parameter dependences, because different perturbative orders are mixed [26, 27]. Several solutions have been described for lowest-order predictions. The early attempts have been summarized in Ref. [28], and some of the schemes have been compared in Ref. [29]. More recent approaches include the "pole-scheme" [30, 31], the "fermion-loop scheme" [27, 29, 32, 33], the use of effective Lagrangians [34, 35][2], and the "complex-mass scheme" (CMS) [23]. Apart from the pole expansions, none of these approaches has been elaborated beyond tree level so far. The pole scheme provides a gauge-invariant answer in terms of an expansion about the resonance, but is only applicable sufficiently far above the W-pair threshold. However, in the full calculation we are after a unified description that is valid everywhere in phase space, without any matching between different treatments for different regions. Some problems related to the finite width appearing in a calculation of radiative corrections to $\mathrm{e^+e^-} \to \mu^-\bar{\nu}_\mu\mathrm{u\bar{d}}$ are illustrated in Ref. [36]. Here we propose to solve these problems by using a generalization of the CMS, which was introduced in Ref. [23] for lowest-order calculations, to the one-loop level.

In this paper we present details of our solutions to the above-mentioned problems. We discuss, in particular, our methods for the algebraic reduction of the one-loop amplitude and describe the use of the CMS at the one-loop level. In addition, we provide numerical results for the effects of the complete $\mathcal{O}(\alpha)$ corrections to the processes $\mathrm{e^+e^-} \to \nu_\tau\tau^+\mu^-\bar{\nu}_\mu$, $\mathrm{u\bar{d}}\mu^-\bar{\nu}_\mu$, and $\mathrm{u\bar{d}s\bar{c}}$ for various differential cross sections of physical interest. The effects of the complete corrections on the total cross section without cuts have already been discussed in Ref. [37].

---

[1] Some of the problems appearing in a first attempt of such a calculation were already described in Ref. [25].

[2] The recently proposed approach [35] to describe unstable particles within an effective field theory is equivalent to a pole expansion.

The paper is organized as follows: In Section 2 we fix our conventions and sketch the general strategy of our calculation. Our methods for the reduction of spinor chains to a few standard structures are described in Section 3. Section 4 is devoted to the description of the complex-mass scheme for loop calculations with complex masses. In Section 5, we discuss the corrections for various distributions. We note that Sections 3, 4, and 5 can be read independently. Section 6 contains our conclusions.

2 Strategy of the calculation

The actual calculation builds upon the RacoonWW approach [20, 21], where real-photonic corrections are based on full matrix elements and virtual corrections are treated in DPA. Real and virtual corrections are combined either using two-cutoff phase-space slicing or employing the dipole subtraction method as formulated in Ref. [38] for photon radiation. We also include leading-logarithmic initial-state radiation (ISR) beyond $\mathcal{O}(\alpha)$ in the structure-function approach (see Ref. [14] and references therein). The presented calculation only differs from RacoonWW in the treatment of the (IR and collinear finite part of the) virtual corrections. Therefore, we only describe the calculation of the complete $\mathcal{O}(\alpha)$ virtual corrections in the following.

2.1 Notation and conventions

We consider the process

$$\mathrm{e}^+(p_+,\sigma_+) + \mathrm{e}^-(p_-,\sigma_-) \;\to\; f_1(k_1,\sigma_1) + \bar{f}_2(k_2,\sigma_2) + f_3(k_3,\sigma_3) + \bar{f}_4(k_4,\sigma_4). \qquad (2.1)$$

The arguments label the momenta $p_\pm$, k_i $(i = 1,2,3,4)$ and helicities $\sigma_\pm$, $\sigma_i = \pm 1/2$ of the corresponding particles. We often use only the signs to denote the helicities. The particle momenta obey the mass-shell conditions $p_\pm^2 = m_\mathrm{e}^2$ and $k_i^2 = m_i^2$. The masses of the external fermions are neglected whenever possible, i.e. everywhere but in the mass-singular logarithms. For later use, the following set of kinematical invariants is defined:

$$s = (p_1 + p_2)^2, \qquad s_{ij} = (k_i + k_j)^2, \qquad t_{\pm i} = (p_\pm - k_i)^2, \qquad i,j = 1,2,3,4. \qquad (2.2)$$

In this paper we consider only final states where f_1 and f_3 are different fermions excluding electrons and electron neutrinos; f_2 and f_4 are their isospin partners, respectively. This corresponds to the CC11 family in the classification of Ref. [15]. It represents the gauge-invariant subclass of general $\mathrm{e^+e^-} \to 4f$ processes that includes all diagrams with pairs of potentially resonant W bosons. In this class, the lowest-order and one-loop amplitudes vanish unless $\sigma = \sigma_- = -\sigma_+$, $\sigma_1 = -\sigma_2$, and $\sigma_3 = -\sigma_4$. Moreover, the helicities of the outgoing fermions are fixed, $\sigma_{1,3} = -\sigma_{2,4} = -1/2$, owing to the left-handed coupling of the W bosons. In general this does not hold for other $\mathrm{e^+e^-} \to 4f$ final states and diagrams. We set the quark-mixing matrix to the unit matrix, but in the limit of small masses for the external fermions a non-trivial quark-mixing matrix can be easily taken into account by rescaling the cross sections for definite flavours accordingly.

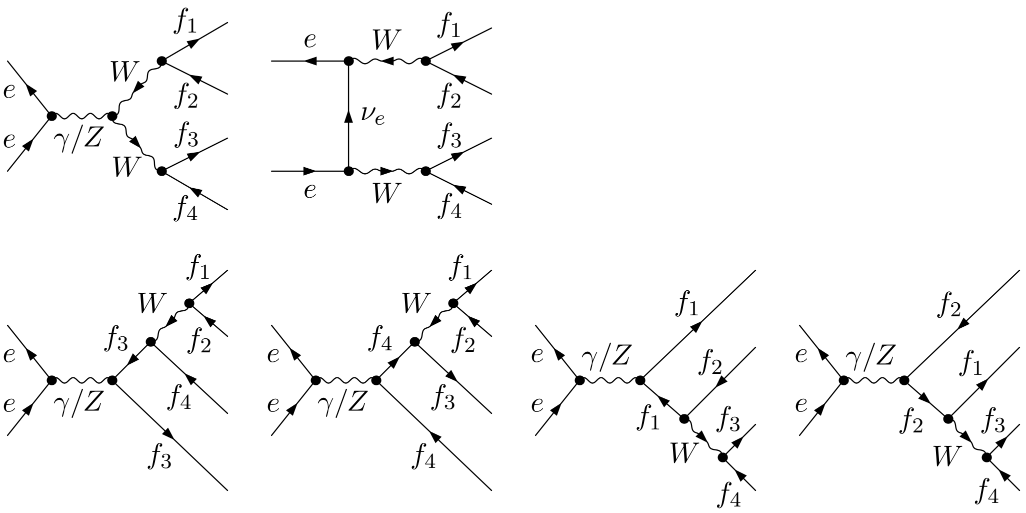

Figure 1: Lowest-order diagrams for $\mathrm{e^+e^-} \to f_1\bar{f}_2f_3\bar{f}_4$

The lowest-order cross section reads

$$\sigma_0 = \frac{1}{2s}\int \mathrm{d}\Phi_4 \sum_{\sigma=\pm\frac{1}{2}} \frac{1}{4}(1+2P_-\sigma)(1-2P_+\sigma)\,|\mathcal{M}_0^{\sigma--}|^2. \tag{2.3}$$

Here $\mathcal{M}_0^{\sigma\sigma_1\sigma_3}$ denotes the lowest-order matrix element, $P_\pm$ the polarization degrees of the $\mathrm{e}^\pm$ beams, and $\mathrm{d}\Phi_4$ the 4-particle phase-space volume element

$$\mathrm{d}\Phi_4 = \left(\prod_{i=1}^{4}\frac{\mathrm{d}^3\mathbf{k}_i}{(2\pi)^3 2k_i^0}\right)(2\pi)^4\delta\left(p_+ + p_- - \sum_{j=1}^{4}k_j\right). \tag{2.4}$$

2.2 Survey of one-loop diagrams

The virtual corrections receive contributions from self-energy, vertex, box, pentagon, and hexagon diagrams. In this section, we survey the diagrams contributing to the massless charged-current processes $\mathrm{e^+e^-} \to f_1\bar{f}_2f_3\bar{f}_4$, where f_1 and f_3 are different fermions, excluding electrons and electron neutrinos, and f_2 and f_4 their respective isospin partners.

The contributions from self-energy and vertex corrections are obtained by inserting self-energies and vertex corrections in all propagators and vertices of the tree-level diagrams shown in Figure 1. When inserting a self-energy in a γ/Z line one obtains $\gamma\gamma$ and ZZ self-energies as well as γZ and $Z\gamma$ mixing-energies. Since we neglect the masses of the external fermions, all diagrams that involve Higgs-boson couplings to these fermions obviously vanish. Nevertheless there remain diagrams containing contributions to the $H\gamma$, HZ, and ϕW mixing energies and to the Hee and ϕff vertices with on-shell fermions, where ϕ denotes the would-be Goldstone boson corresponding to the W boson. One can easily verify that these contributions also vanish in the limit of vanishing masses for the external fermions.

The diagrams for the appearing $ee\gamma$, eeZ, $e\nu_eW$, γWW, and ZWW vertex functions are listed in Ref. [8], where the process $\mathrm{e^+e^-} \to \mathrm{W^+W^-}$ was treated at one loop. The diagrams for the other $\gamma f\bar{f}$, $Zf\bar{f}$, $Wf\bar{f}'$ vertex functions are simply obtained from the latter by obvious substitutions and adding some diagrams with internal Z bosons replaced by photons, which are absent for the $e\nu_e W$ vertex because of the vanishing charge of the neutrino. The diagrams for the gauge-boson and fermion self-energies can be found in Ref. [39]. For all these vertex functions, the corresponding counterterm diagrams must be included.

The generic contributions of the different vertex functions with more than three external legs are shown in Figure 2. These are all ultraviolet (UV) finite. There are 40 hexagon diagrams, 112 pentagon diagrams, and 227 (220) box diagrams in the conventional 't Hooft–Feynman gauge (background-field gauge [40]). A set of hexagon diagrams is shown in Figure 3 and one set of pentagon diagrams for the $Zf_1f_2f_3f_4$ vertex function in Figure 4. In both cases there are three further sets of diagrams that are obtained by reversing the fermion flow in one or both of the fermion lines of the outgoing fermions and by exchanging $f_1 \leftrightarrow f_2$ and/or $f_3 \leftrightarrow f_4$. Those for the $\gamma f_1f_2f_3f_4$ vertex function are simply obtained by replacing the external Z boson by a photon in the diagrams for the $Zf_1f_2f_3f_4$ vertex function. A set of diagrams for the eef_1f_2W vertex function is listed in Figure 5 and a further set is obtained from those by reversing the fermion flow in the fermion chain of the outgoing fermions and by exchanging $f_1 \leftrightarrow f_2$. The diagrams for the eef_3f_4W vertex function can be obtained from the latter by obvious substitutions. The box diagrams of the ZWf_1f_2 vertex function are depicted in Figure 6 and those for the ZWf_3f_4 vertex can again be obtained from those. The diagrams for the γWf_1f_2 and γWf_3f_4 boxes are obtained by replacing the external Z boson by a photon and omitting the diagrams with internal H lines. The diagrams for the $eeWW$, $f_1f_2f_3f_4$, and eef_1f_1 boxes are compiled in Figures 7, 8, and 9. The $e\nu_e f_1f_2$ and $e\nu_e f_3f_4$ box functions are special cases of the $f_1f_2f_3f_4$ box function.

2.3 Calculational framework

The amplitudes are generated with FeynArts, using the two independent versions 1 and 3, as described in Refs. [41] and [42], respectively. The algebraic manipulations are performed using two independent in-house programs implemented in Mathematica, one of which builds upon FormCalc [43].

All contributions to the matrix elements involve three spinor chains, corresponding to the three different fermion–antifermion pairs, which are contracted with each other and with four-momenta in many different ways. There are $\mathcal{O}(10^3)$ different spinor structures to calculate for $\mathrm{e}^+\mathrm{e}^- \to f_1\bar{f}_2f_3\bar{f}_4$ so that an algebraic reduction to a standard form which involves only very few standard chains is desirable. We have worked out algorithms that reduce all occurring spinor chains to $\mathcal{O}(10)$ standard structures, the standard matrix elements (SMEs), without introducing coefficients that lead to numerical problems. These algorithms are described in Section 3.

It is convenient to separate the matrix elements into invariant coefficient functions F_n, containing the loop integrals, and SMEs $\hat{\mathcal{M}}_n$, containing all spinorial objects and the dependence on the helicities of the external particles [44]. After the reduction of the spinor structures, the amplitudes take the form

$$\mathcal{M}^{\sigma\sigma_1\sigma_3} = \sum_n F_n^{\sigma\sigma_1\sigma_3}(\{s, s_{ij}, t_{\pm i}\})\hat{\mathcal{M}}_n^{\sigma\sigma_1\sigma_3}(p_+, p_-, k_1, k_2, k_3, k_4). \qquad (2.5)$$

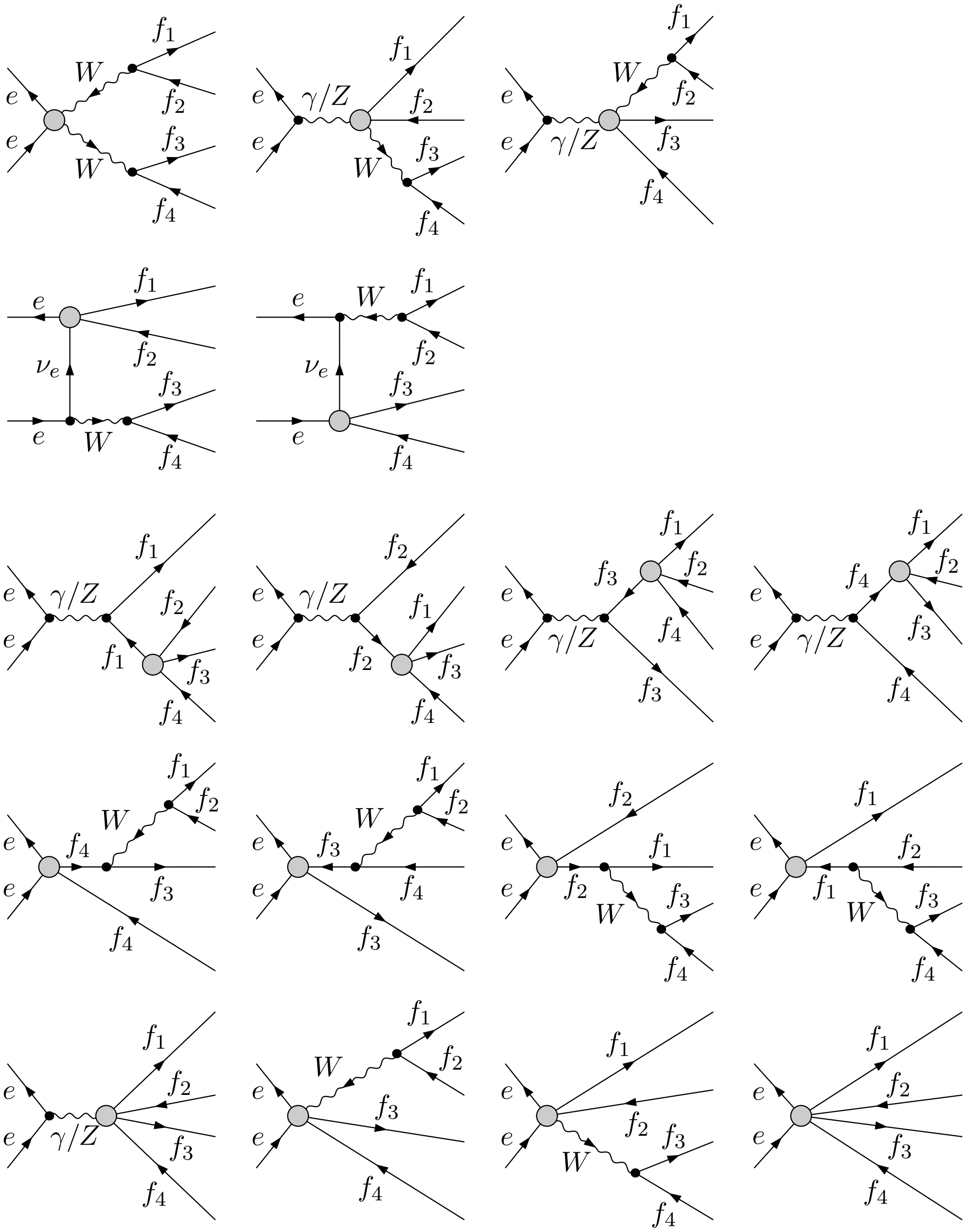

Figure 2: Contributions of vertex functions with at least four external legs to $e^+e^- \to f_1\bar{f}_2f_3\bar{f}_4$

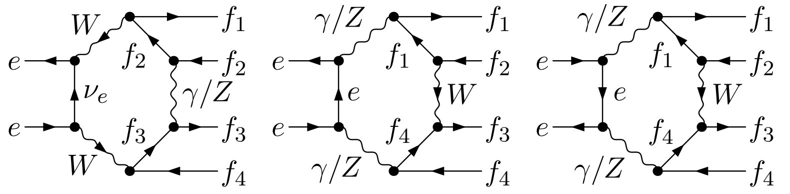

Figure 3: Ten hexagon diagrams for $e^+e^- \to f_1\bar{f}_2f_3\bar{f}_4$. The remaining 30 hexagon diagrams are obtained by reversing the fermion flow in one or both of the fermion lines of the outgoing fermions and by exchanging $f_1 \leftrightarrow f_2$ and/or $f_3 \leftrightarrow f_4$.

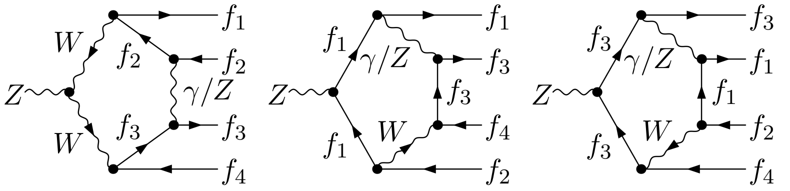

Figure 4: Six pentagon diagrams contributing to the $Zf_1f_2f_3f_4$ vertex function. The remaining 18 diagrams are obtained by reversing the fermion flow in one or both of the fermion lines of the outgoing fermions and by exchanging $f_1 \leftrightarrow f_2$ and/or $f_3 \leftrightarrow f_4$.

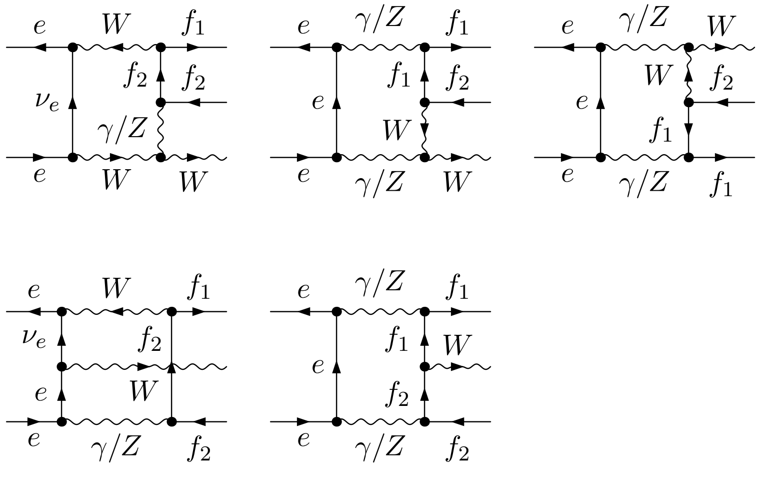

Figure 5: A set of 16 diagrams contributing to the eef_1f_2W vertex function. The remaining 16 diagrams contributing to this vertex function are obtained from those by reversing the fermion flow in the fermion line of the outgoing fermions and by exchanging $f_1 \leftrightarrow f_2$.

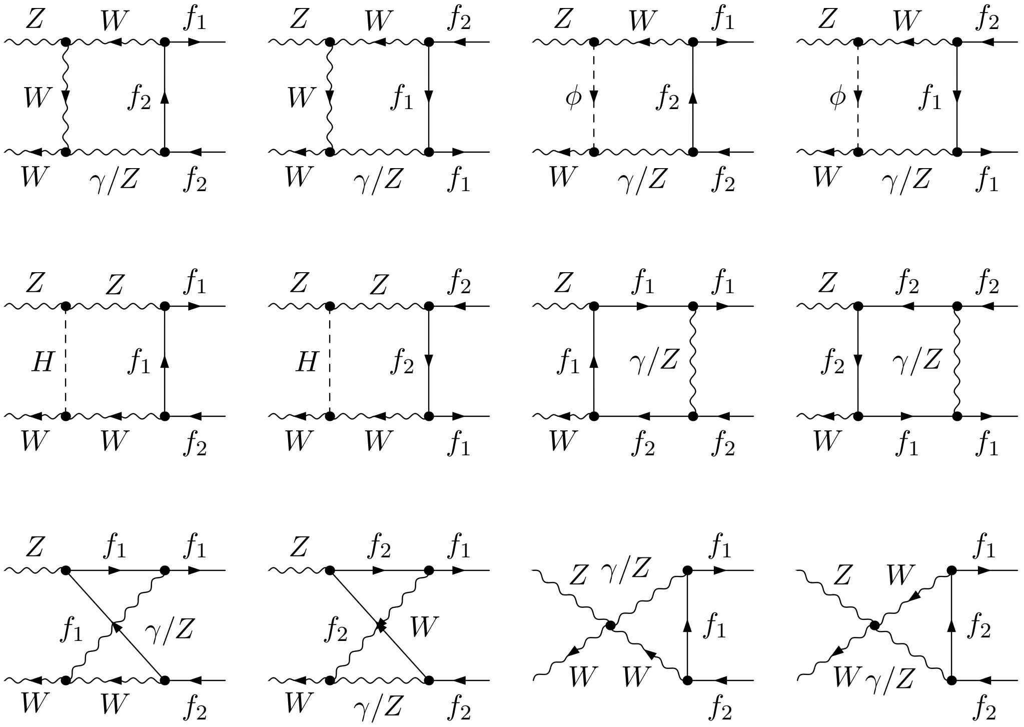

Figure 6: Diagrams contributing to the ZWf_1f_2 vertex function

The invariant functions F_n are linear combinations of one-loop integrals with coefficients that depend on scalar kinematical variables, particle masses, and coupling factors.

The calculation of the virtual corrections has been repeated using the background-field method [40], where the individual contributions from self-energy, vertex, box, and pentagon corrections differ from their counterparts in the conventional formalism, apart from those that involve only fermion–gauge-boson couplings in the loops. The total one-loop corrections of the conventional and of the background-field approach were found to be in numerical agreement.

The contribution of the virtual corrections to the cross section is given by

$$\delta\sigma_{\mathrm{virt}} = \frac{1}{2s}\int \mathrm{d}\Phi_4 \sum_{\sigma=\pm\frac{1}{2}} \frac{1}{4}(1+2P_-\sigma)(1-2P_+\sigma)\,2\,\mathrm{Re}\left\{\mathcal{M}_1^{\sigma--}\left(\mathcal{M}_0^{\sigma--}\right)^*\right\}, \tag{2.6}$$

where $\mathcal{M}_1^{\sigma\sigma_1\sigma_3}$ denotes the one-loop contributions to the helicity amplitudes.

2.4 Calculation of loop integrals

For the calculation of the loop integrals we use an improved version of the standard approach. All coefficient integrals are algebraically reduced to a set of master integrals. The reduction formulas are implemented into Fortran codes, and the reduction is performed

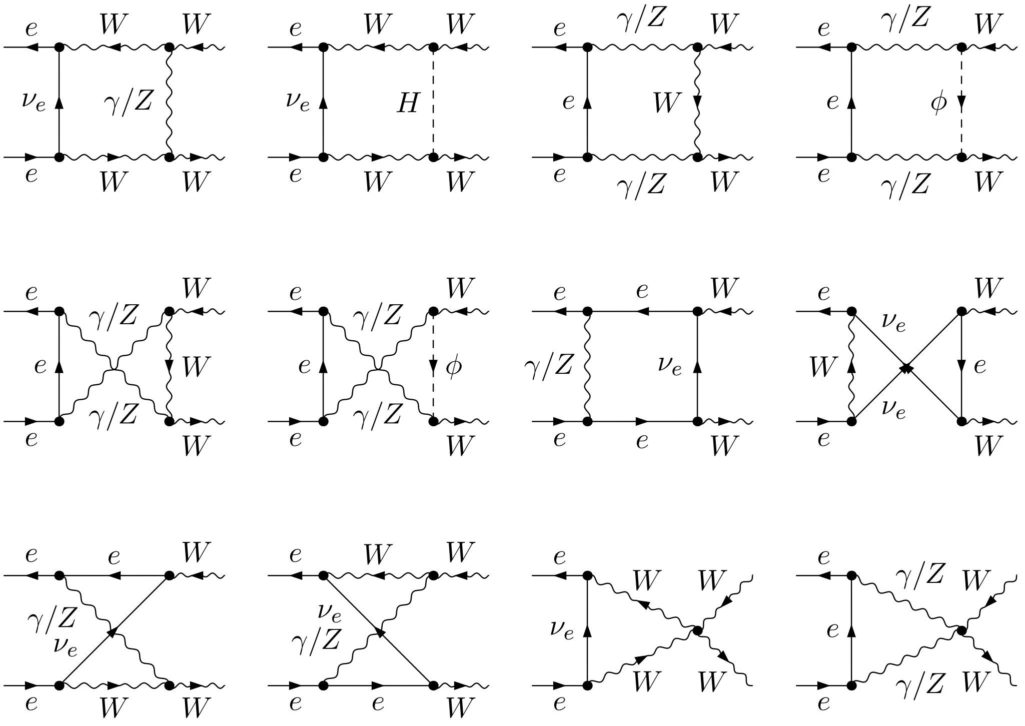

Figure 7: Diagrams contributing to the $eeWW$ vertex function

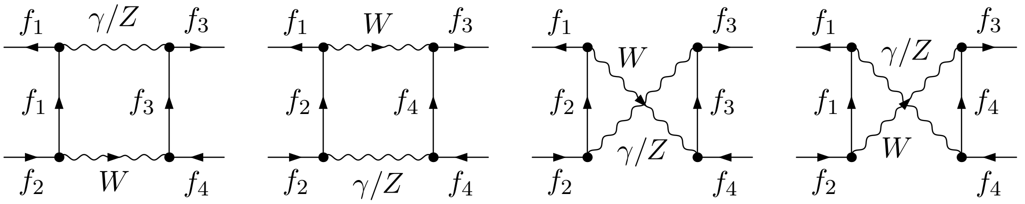

Figure 8: Diagrams contributing to the $f_1f_2f_3f_4$ vertex function

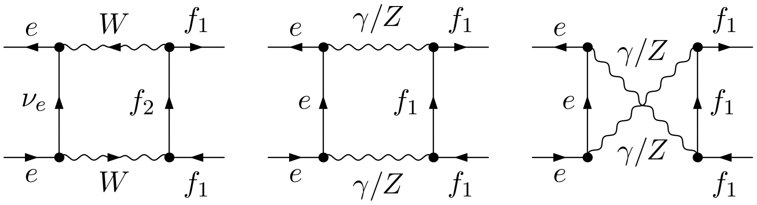

Figure 9: Diagrams contributing to the eef_1f_1 vertex function

numerically. Finally, the master integrals are either calculated from explicit formulas or from numerical integration as explained below.

Let us first describe our standard approach that we use as long as it yields numerically stable results. The 6-point integrals are directly expressed in terms of six 5-point functions, as described in Refs. [44, 45]. The 5-point integrals are written in terms of five 4-point functions following the method of Ref. [46]. The 3-point and 4-point tensor integrals are algebraically reduced to the (standard) scalar 1-point, 2-point, 3-point, and 4-point functions, which are the master integrals, with the Passarino–Veltman algorithm [47]. Finally, the remaining scalar integrals are evaluated based on generalizations of the methods and results of Refs. [48, 49, 50]. UV divergences are regulated dimensionally and IR divergences with an infinitesimal photon mass[3] m_γ.

The standard approach leads to serious numerical problems when the Gram determinants, which appear in the denominator of the Passarino–Veltman reduction, become small. This happens usually near the boundary of phase space but also occurs within phase space because of the indefinite Minkowski metric. Since we use Passarino–Veltman reduction only for 3-point and 4-point functions, the dangerous Gram determinants are those involving two or three momenta. Our reduction of 5- and 6-point functions, on the other hand, does not involve inverse Gram determinants composed of external momenta. Instead, it involves so-called (modified) Cayley determinants, the zeroes of which are related to the Landau singularities of the (sub-)diagrams. We did not encounter numerical problems with these determinants. For the 2-point tensor coefficients numerically stable explicit results exist for arbitrary momenta [47].

For the regions where the Gram determinants become small, we have worked out two alternative calculational methods. The precise description of these will be given elsewhere. Here, we sketch only the basic strategy. One method makes use of expansions of the tensor coefficients about the limit of vanishing Gram determinants. Using this, again all tensor coefficients can be expressed in terms of the standard scalar 1-point, 2-point, 3-point, and 4-point functions. In the second, alternative method we evaluate a specific tensor coefficient, the integrand of which is logarithmic in Feynman parametrization, by numerical integration. Then the remaining coefficients as well as the standard scalar integral (numerator equal to one) are algebraically derived from this coefficient. This reduction again involves only inverse Cayley determinants, but no inverse Gram determinants. In this approach, the set of master integrals is not given by the standard scalar integrals anymore. For some specific 3-point integrals, where the Cayley determinant vanishes exactly, analytical results have been worked out that allow for a stable numerical evaluation.

2.5 Checks on the calculation

In order to prove the reliability of our results, we have performed a number of checks, as described in more detail in Ref. [37]. We have checked the structure of the (UV, soft, and collinear) singularities, the matching between virtual and real corrections, and the gauge independence (by repeating the calculation in a different gauge). The most convincing check for ourselves is the fact that we worked out the whole calculation in two independent ways, resulting in two independent computer codes the results of which are in good agreement. All algebraic manipulations, including the generation of Feynman diagrams, have been done using independent programs. In particular, one calculation uses the strategy described in Section 3.2 for the reduction of the spinor structures, the other the strategy presented in Section 3.3. For the calculation of the loop integrals we use the two independent in-house libraries which employ the different calculational methods sketched in Section 2.4 for the numerical stabilization.

---

[3] At one loop the photon-mass regularization is equivalent to dimensional regularization ($D = 4 - 2\varepsilon$) with reference mass μ via the correspondence $\ln(m_\gamma^2) \leftrightarrow 1/\varepsilon + \ln(4\pi\mu^2) - \gamma_{\mathrm{E}}$ as long as collinear singularities are regularized with fermion masses.

3 Algebraic reduction of spinor chains

One-loop amplitudes for processes with six external fermions involve $\mathcal{O}(10^3)$ different spinor structures, which are products of three spinor chains. These structures are, however, not independent, but can be related by using the Dirac algebra, the Dirac equation, momentum conservation, and relations that follow from the four-dimensionality of space–time. Of course, the latter relations can only be used after cancelling UV divergences, which are regularized dimensionally in our work.

Below we describe two strategies that can be exploited to express any product of three spinor chains for a reaction involving six external massless fermions (and no external bosons) in terms of very few standard structures. Note that none of the following steps leads to Gram determinants in denominator factors, which potentially spoil the numerical stability[4]. For generic reasons we take all six fermion momenta p_i as incoming ($\sum_{i=1}^{6} p_i = 0$) and use the following shorthand notation for a spinor chain,

$$\Big[A\Big]^{\pm}_{ab} = \bar{v}_a(p_a)\, A\, \omega_\pm\, u_b(p_b)\,, \tag{3.1}$$

where $\bar{v}_a(p_a)$ and $u_b(p_b)$ are the usual spinors for the (anti-)fermions and

$$\omega_\pm = \frac{1}{2}(1 \pm \gamma_5) \tag{3.2}$$

the chirality projectors. Since we deal with massless fermions, the matrices A, which act in Dirac space, always consist of a product of an odd number of Dirac matrices γ^μ. The quantities that we want to simplify have the general structure

$$\bar{v}_1(p_1)A\omega_\rho u_2(p_2) \;\times\; \bar{v}_3(p_3)B\omega_\sigma u_4(p_4) \;\times\; \bar{v}_5(p_5)C\omega_\tau u_6(p_6) \;\equiv\; \Big[A\Big]^{\rho}_{12}\Big[B\Big]^{\sigma}_{34}\Big[C\Big]^{\tau}_{56}. \tag{3.3}$$

We start out by deriving and summarizing some basic relations that are used in the reduction.

3.1 Basic relations

3.1.1 Identities for Dirac matrices

The four-dimensionality of space–time leads to the Chisholm identity

$$\gamma^\alpha\gamma^\beta\gamma^\gamma = g^{\alpha\beta}\gamma^\gamma - g^{\alpha\gamma}\gamma^\beta + g^{\beta\gamma}\gamma^\alpha + \mathrm{i}\epsilon^{\alpha\beta\gamma\delta}\gamma_\delta\gamma_5, \tag{3.4}$$

---

[4] Inverse Gram determinants, e.g., appear in the reduction proposed in Ref. [51].

which can be used to express products $\gamma^\alpha\gamma^\beta\gamma^\gamma$ of Dirac matrices in terms of single Dirac matrices dressed by γ_5 factors and totally antisymmetric tensors $\epsilon^{\alpha\beta\gamma\delta}$ (we adopt the convention $\epsilon^{0123} = +1$).

If at least two Dirac chains are involved, this identity can be applied to shift factors of Dirac matrices from one chain to another without introducing ϵ-tensors, provided the two chains are Lorentz contracted with each other:

$$\begin{aligned}
\gamma^\mu\gamma^\alpha\gamma^\beta \otimes \gamma_\mu &\overset{(3.4)}{=} \Big(g^{\mu\alpha}\gamma^\beta - g^{\mu\beta}\gamma^\alpha + g^{\alpha\beta}\gamma^\mu + \mathrm{i}\epsilon^{\mu\alpha\beta\nu}\gamma_\nu\gamma_5\Big) \otimes \gamma_\mu \\
&= \gamma^\beta \otimes \gamma^\alpha - \gamma^\alpha \otimes \gamma^\beta + g^{\alpha\beta}\gamma^\mu \otimes \gamma_\mu - \gamma_\nu\gamma_5 \otimes \Big(\mathrm{i}\epsilon^{\nu\alpha\beta\mu}\gamma_\mu\gamma_5\Big)\gamma_5 \\
&\overset{(3.4)}{=} \gamma^\beta \otimes \gamma^\alpha - \gamma^\alpha \otimes \gamma^\beta + g^{\alpha\beta}\gamma^\mu \otimes \gamma_\mu + \gamma^\alpha\gamma_5 \otimes \gamma^\beta\gamma_5 - \gamma^\beta\gamma_5 \otimes \gamma^\alpha\gamma_5 \\
&\quad + g^{\alpha\beta}\gamma^\mu\gamma_5 \otimes \gamma_\mu\gamma_5 - \gamma_\mu\gamma_5 \otimes \gamma^\mu\gamma^\alpha\gamma^\beta\gamma_5. \qquad (3.5)
\end{aligned}$$

Here and in the following the symbol $\otimes$ denotes the direct product in Dirac space, i.e. Dirac matrices are not sandwiched between Dirac spinors in this case. Relation (3.5) can be expressed in a very compact way after introducing the chirality projectors (3.2) and rearranging the order of some Dirac matrices,

$$\begin{aligned}
\gamma^\mu\gamma^\alpha\gamma^\beta\omega_\pm \otimes \gamma_\mu\omega_\pm &= \gamma^\mu\omega_\pm \otimes \gamma_\mu\gamma^\beta\gamma^\alpha\omega_\pm, \\
\gamma^\alpha\gamma^\beta\gamma^\mu\omega_\pm \otimes \gamma_\mu\omega_\pm &= \gamma^\mu\omega_\pm \otimes \gamma^\beta\gamma^\alpha\gamma_\mu\omega_\pm, \\
\gamma^\mu\gamma^\alpha\gamma^\beta\omega_\pm \otimes \gamma_\mu\omega_\mp &= \gamma^\mu\omega_\pm \otimes \gamma^\alpha\gamma^\beta\gamma_\mu\omega_\mp, \\
\gamma^\alpha\gamma^\beta\gamma^\mu\omega_\pm \otimes \gamma_\mu\omega_\mp &= \gamma^\mu\omega_\pm \otimes \gamma_\mu\gamma^\alpha\gamma^\beta\omega_\mp. \qquad (3.6)
\end{aligned}$$

The second and the fourth relations are equivalent forms of the other two.

Equations (3.6) lead to analogous relations for direct products of Dirac chains with more than one contraction.[5] For two contractions we get

$$\begin{aligned}
\gamma^\mu\gamma^\alpha\gamma^\nu\omega_\pm \otimes \gamma_\mu\gamma^\beta\gamma_\nu\omega_\pm &= 4g^{\alpha\beta}\gamma^\mu\omega_\pm \otimes \gamma_\mu\omega_\pm, \\
\gamma^\mu\gamma^\alpha\gamma^\nu\omega_\pm \otimes \gamma_\mu\gamma^\beta\gamma_\nu\omega_\mp &= 4\gamma^\beta\omega_\pm \otimes \gamma^\alpha\omega_\mp. \qquad (3.7)
\end{aligned}$$

The first of these relations is obtained by multiplying the second chain of the first relation of (3.6) by $\gamma^\gamma\gamma_\beta$ from the right and renaming the indices $\beta \to \nu$ and $\gamma \to \beta$ after some obvious algebra. The second relation is found analogously.

Relations for direct products of Dirac chains with three contractions directly result from (3.7) upon contraction with $g_{\alpha\beta}$,

$$\begin{aligned}
\gamma^\mu\gamma^\nu\gamma^\rho\omega_\pm \otimes \gamma_\mu\gamma_\nu\gamma_\rho\omega_\pm &= 16\gamma^\mu\omega_\pm \otimes \gamma_\mu\omega_\pm, \\
\gamma^\mu\gamma^\nu\gamma^\rho\omega_\pm \otimes \gamma_\mu\gamma_\nu\gamma_\rho\omega_\mp &= 4\gamma^\mu\omega_\pm \otimes \gamma_\mu\omega_\mp. \qquad (3.8)
\end{aligned}$$

Relations for more than three contractions could be derived from the above results recursively, but are not needed in our case.

---

[5] Such relations can also be found in Ref. [52].

3.1.2 Identities for products of spinor chains

Further interesting relations follow if we sandwich the Dirac matrices in the above relations between spinors and perform some simplifications. For instance, if we contract the second relation in (3.7) with $p_{1,\alpha} p_{3,\beta}$, then from the r.h.s. multiply the first chain of Dirac matrices by A and the second by B, where here A and B stand for the unit matrix $\mathbf{1}$ or any product of an even number of Dirac matrices, and finally attach the external spinors, we obtain

$$\Big[\gamma^\mu \not{p}_1 \gamma^\nu A\Big]^{\pm}_{12} \Big[\gamma_\mu \not{p}_3 \gamma_\nu B\Big]^{\mp}_{34} = 4\Big[\not{p}_3 A\Big]^{\pm}_{12} \Big[\not{p}_1 B\Big]^{\mp}_{34}. \tag{3.9}$$

On the l.h.s. we can eliminate $\not{p}_1$ and $\not{p}_3$ by the respective Dirac equations and obtain $4(p_1p_3)\Big[\gamma^\nu A\Big]^{\pm}_{12} \Big[\gamma_\nu B\Big]^{\mp}_{34}$. Three similar relations can be derived from (3.7) with other suitable contractions. The resulting four relations read

$$\begin{aligned}
\Big[A\not{p}_3\Big]^{\pm}_{12} \Big[\not{p}_2 B\Big]^{\pm}_{34} &= (p_2p_3)\Big[A\gamma^\mu\Big]^{\pm}_{12} \Big[\gamma_\mu B\Big]^{\pm}_{34}, \\
\Big[\not{p}_4 A\Big]^{\pm}_{12} \Big[B\not{p}_1\Big]^{\pm}_{34} &= (p_1p_4)\Big[\gamma^\mu A\Big]^{\pm}_{12} \Big[B\gamma_\mu\Big]^{\pm}_{34}, \\
\Big[\not{p}_3 A\Big]^{\pm}_{12} \Big[\not{p}_1 B\Big]^{\mp}_{34} &= (p_1p_3)\Big[\gamma^\mu A\Big]^{\pm}_{12} \Big[\gamma_\mu B\Big]^{\mp}_{34}, \\
\Big[A\not{p}_4\Big]^{\pm}_{12} \Big[B\not{p}_2\Big]^{\mp}_{34} &= (p_2p_4)\Big[A\gamma^\mu\Big]^{\pm}_{12} \Big[B\gamma_\mu\Big]^{\mp}_{34}.
\end{aligned} \tag{3.10}$$

3.1.3 Decomposition of the metric tensor

In four dimensions the metric tensor $g^{\mu\nu}$ can be decomposed in terms of four independent orthonormal four-vectors n^μ_j,

$$g^{\mu\nu} = \sum_{i,j=0}^{3} g^{ij}\, n^\mu_i\, n^\nu_j\,, \tag{3.11}$$

with orthonormal components $n^\mu_i\, n_{j,\mu} = g_{ij}$, where $g_{ij} = g^{ij} = \mathrm{diag}(1,-1,-1,-1)$, as described in the appendices of Refs. [53, 54]. The four four-vectors n^μ_i can be constructed from three linearly-independent momenta p_i, p_j, p_k. In the case of massless momenta, $p_i^2 = p_j^2 = p_k^2 = 0$, they can be defined as

$$\begin{aligned}
n^\mu_0(p_i,p_j,p_k) &= \frac{1}{\sqrt{2\,(p_ip_j)}}\,\Big(p^\mu_i + p^\mu_j\Big)\,, \qquad n^\mu_1(p_i,p_j,p_k) = \frac{1}{\sqrt{2\,(p_ip_j)}}\,\Big(p^\mu_i - p^\mu_j\Big)\,, \\
n^\mu_2(p_i,p_j,p_k) &= -\frac{1}{\sqrt{2\,(p_ip_j)\,(p_ip_k)\,(p_jp_k)}}\,\Big[(p_jp_k)\,p^\mu_i + (p_ip_k)\,p^\mu_j - (p_ip_j)\,p^\mu_k\Big]\,, \\
n^\mu_3(p_i,p_j,p_k) &= -\frac{1}{\sqrt{2\,(p_ip_j)\,(p_ip_k)\,(p_jp_k)}}\,\epsilon^{\mu\alpha\beta\gamma}\,p_{i,\alpha}\,p_{j,\beta}\,p_{k,\gamma}\,.
\end{aligned} \tag{3.12}$$

The decomposition of the metric tensor (3.11) can be used to disconnect contractions of spinor chains or other objects. Note that the construction of the four vectors n_i from the three independent vectors p_i, p_j, p_k, in particular the definition of n_3, avoids an inverse

Gram determinant in (3.11); if we decomposed the metric into four totally independent momenta, the result would get the Gram determinant of those four momenta in the denominator.

3.1.4 Identities involving ϵ-tensors

The fact that there is no totally antisymmetric tensor of rank 5 in four space–time dimensions leads to the Schouten identity

$$\epsilon_{[\alpha\beta\gamma\delta}\, g_{\mu]\nu} = 0\,, \tag{3.13}$$

where $[\ldots]$ means antisymmetrization in $\alpha, \beta, \gamma, \delta$, and μ.

The product of totally antisymmetric tensors can be expressed as a determinant of metric tensors,

$$\epsilon^{\alpha\beta\gamma\delta}\epsilon^{\mu\nu\rho\sigma} = -\begin{vmatrix} g^{\alpha\mu} & g^{\alpha\nu} & g^{\alpha\rho} & g^{\alpha\sigma} \\ g^{\beta\mu} & g^{\beta\nu} & g^{\beta\rho} & g^{\beta\sigma} \\ g^{\gamma\mu} & g^{\gamma\nu} & g^{\gamma\rho} & g^{\gamma\sigma} \\ g^{\delta\mu} & g^{\delta\nu} & g^{\delta\rho} & g^{\delta\sigma} \end{vmatrix}\,. \tag{3.14}$$

3.2 Strategy for reducing spinor structures

In this section we describe one algorithm for the reduction of spinor chains. A second one is described in Section 3.3. The algorithm described here reduces all spinor chains to a minimal set. Although this algorithm is applicable more generally, we refer in the description to the massless charged-current $6f$ processes $\mathrm{e}^+\mathrm{e}^-\bar{f}_1 f_2 \bar{f}_3 f_4 \to 0$, where f_1 and f_3 are different fermions excluding electrons and electron neutrinos and f_2 and f_4 their isospin partners.

Step 1 *Reduction of contractions between spinor chains*

As first step in the reduction, spinor chains contracted with other spinor chains or ϵ-tensors are disconnected.[6] This is achieved by introducing a decomposition of the metric tensor (3.11) between contracted Dirac matrices or contractions between a totally antisymmetric tensor and a Dirac matrix:

$$\begin{aligned} \gamma_\mu \otimes \gamma^\mu \;&=\; g^{\mu\nu}\,\gamma_\mu \otimes \gamma_\nu \;\overset{(3.11)}{=}\; \sum_{i,j=0}^{3} g^{ij}\,\not{n}_i \otimes \not{n}_j\,, \\ \epsilon^{\mu\nu\rho\sigma}\,\gamma_\mu \;&=\; \epsilon^{\mu\nu\rho\sigma}\,g_{\mu\alpha}\,\gamma^\alpha \;\overset{(3.11)}{=}\; \epsilon^{\mu\nu\rho\sigma} \sum_{i,j=0}^{3} g^{ij}\,n_{i,\mu}\,\not{n}_j\,. \end{aligned} \tag{3.15}$$

The choice of momenta for a suitable decomposition of the metric tensor depends on the positions of the contracted matrices in the spinor chains. Preferably the momenta p_i, p_j, p_k entering (3.12) and thus (3.11) are selected in such a way that the Dirac equations

---

[6] The explicit ϵ-tensors result from calculating the traces of Dirac matrices in diagrams with closed fermion loops.

$\bar{v}(p_i)\slashed{p}_i = 0 = \slashed{p}_i u(p_i)$ or the mass-shell condition $\slashed{p}_i^2 = p_i^2 = 0$ can be used most directly, i.e. without unnecessary anticommutations of Dirac matrices by means of the Dirac algebra, since additional terms come with it. Therefore, we count the number of anticommutations of the slashed momenta $\slashed{p}_i$, introduced by the decomposition of the metric tensor, with Dirac matrices of the chain that would be necessary in order to apply the Dirac equation or the mass-shell condition. We choose the three momenta with the fewest necessary anticommutations.[7]

The following substeps are recursively applied until no contractions of spinor chains are left:

- Disconnect a single Lorentz contraction between two spinor chains or between a totally antisymmetric tensor and a spinor chain by (3.15).
- Use the Dirac algebra together with the Dirac equation or the mass-shell condition $\slashed{p}_i^2 = 0$ in order to shorten spinor chains.
- Replace contractions between totally antisymmetric tensors and n_3:

  $$\epsilon^{\mu\alpha\beta\gamma}\, n_{3,\mu}(p_i, p_j, p_k) \overset{(3.14)}{=} \frac{1}{\sqrt{2\,(p_i p_j)\,(p_i p_k)\,(p_j p_k)}}\, p_i^{[\alpha}\, p_j^{\beta}\, p_k^{\gamma]}\,, \qquad (3.16)$$

  where $[\ldots]$ means antisymmetrization in α, β, and γ.
- Eliminate $\slashed{n}_3$ in spinor chains by using

  $$\slashed{n}_3(p_i, p_j, p_k) \overset{(3.4)}{=} -\frac{\mathrm{i}\left[\slashed{p}_i\slashed{p}_j\slashed{p}_k - (p_i p_j)\,\slashed{p}_k + (p_i p_k)\,\slashed{p}_j - (p_j p_k)\,\slashed{p}_i\right]\gamma_5}{\sqrt{2\,(p_i p_j)\,(p_i p_k)\,(p_j p_k)}}\,. \qquad (3.17)$$

After this step, the (disconnected) spinor chains we are left with are of the form $[\slashed{p}_j]^{\pm}_{ab}$ with $j \neq a, b$ and $[\slashed{p}_i\,\slashed{p}_j\,\slashed{p}_k]^{\pm}_{ab}$ with pairwise different i, j, k, a, b for processes involving six external fermions. Since there are many different types of multiple contractions of spinor chains, we can only illustrate this reduction step, and particularly the first substep, in three representative examples:

$$\begin{aligned}
\left[\gamma^{\mu}\right]^{\sigma}_{ab}\left[\gamma_{\mu}\right]^{\tau}_{cd} &\overset{(3.15)}{=} \sum_{i,j=0}^{3} g^{ij}\left[\slashed{n}_i(p_a, p_b, p_c)\right]^{\sigma}_{ab}\left[\slashed{n}_j(p_a, p_b, p_c)\right]^{\tau}_{cd} \\
&\overset{(3.17)}{=} \frac{1}{2}\left[\slashed{p}_c\right]^{\sigma}_{ab}\left(\frac{1}{(p_a p_c)}\left[\slashed{p}_a\right]^{\tau}_{cd} + \frac{1}{(p_b p_c)}\left[\slashed{p}_b\right]^{\tau}_{cd}\right) \\
&\quad - \frac{1}{2}\left[\slashed{p}_c\gamma_5\right]^{\sigma}_{ab}\left(\frac{1}{(p_a p_c)}\left[\slashed{p}_a\gamma_5\right]^{\tau}_{cd} - \frac{1}{(p_b p_c)}\left[\slashed{p}_b\gamma_5\right]^{\tau}_{cd}\right)
\end{aligned}$$

---

[7] More precisely: If the metric tensor between two spinor chains is eliminated, we count the necessary anticommutations for each momentum in both spinor chains, say N_1 and N_2 with $N_1 \leq N_2$, and set N_2 to infinity if the momentum does not appear in one of the chains. Then we choose the momenta with smallest $N_1 - 1/N_2$. If, on the other hand, the metric tensor between a spinor chain and an ϵ-tensor is replaced, we proceed analogously, but set the number of necessary anticommutations to zero for those momenta that are already contracted with the ϵ-tensor and to infinity otherwise.

$$= \left[\not p_c\right]^{\sigma}_{ab} \left(\frac{1}{(p_a p_c)} \left[\not p_a\right]^{\tau}_{cd} \delta_{\sigma,-\tau} + \frac{1}{(p_b p_c)} \left[\not p_b\right]^{\tau}_{cd} \delta_{\sigma,\tau} \right), \tag{3.18}$$

$$\begin{aligned}
\left[\gamma^{\mu}\right]^{+}_{12} \left[\not p_2\, \gamma_{\mu}\, \gamma_{\nu}\right]^{-}_{34} \left[\gamma^{\nu}\right]^{-}_{56} &\overset{(3.15)}{=} \sum_{i,j=0}^{3} g^{ij} \left[\not n_i(p_2, p_1, p_3)\right]^{+}_{12} \left[\not p_2\, \not n_j(p_2, p_1, p_3)\, \gamma_{\nu}\right]^{-}_{34} \left[\gamma^{\nu}\right]^{-}_{56} \\
&\overset{(3.17)}{=} -\frac{1}{(p_1 p_3)} \left[\not p_3\right]^{+}_{12} \left[\not p_1\, \not p_2\, \gamma_{\nu}\right]^{-}_{34} \left[\gamma^{\nu}\right]^{-}_{56} \\
&\overset{(3.15)}{=} -\frac{1}{(p_1 p_3)} \left[\not p_3\right]^{+}_{12} \sum_{i,j=0}^{3} g^{ij} \left[\not p_1\, \not p_2\, \not n_i(p_2, p_4, p_5)\right]^{-}_{34} \left[\not n_j(p_2, p_4, p_5)\right]^{-}_{56} \\
&\overset{(3.17)}{=} -\frac{1}{(p_1 p_3)\,(p_4 p_5)} \left[\not p_3\right]^{+}_{12} \left[\not p_1\, \not p_2\, \not p_5\right]^{-}_{34} \left[\not p_4\right]^{-}_{56},
\end{aligned} \tag{3.19}$$

$$\begin{aligned}
\mathrm{i}\, \epsilon^{\mu\alpha\gamma\delta}\, p_{1,\alpha}\, p_{3,\gamma}\, p_{4,\delta} \left[\gamma_{\mu}\right]^{-}_{12} &\overset{(3.15)}{=} \mathrm{i}\, \epsilon^{\mu\alpha\gamma\delta}\, p_{1,\alpha}\, p_{3,\gamma}\, p_{4,\delta} \sum_{i,j=0}^{3} g^{ij}\, n_{i,\mu}(p_1, p_2, p_3) \left[\not n_j(p_1, p_2, p_3)\right]^{-}_{12} \\
&\underset{(3.17)}{\overset{(3.16)}{=}} \frac{1}{2\,(p_2 p_3)} \left[\not p_3\right]^{-}_{12} \Big((p_1 p_2)\,(p_3 p_4) - (p_1 p_3)(p_2 p_4) + (p_1 p_4)(p_2 p_3) \\
&\qquad\qquad - \mathrm{i}\, \epsilon^{\alpha\beta\gamma\delta}\, p_{1,\alpha}\, p_{2,\beta}\, p_{3,\gamma}\, p_{4,\delta} \Big) \\
&= \frac{1}{2\,(p_2 p_3)} \left[\not p_3\right]^{-}_{12} A^{+-++}_{1\,2\,3\,4},
\end{aligned} \tag{3.20}$$

where we introduced the abbreviation

$$A^{a\,b\,c\,d}_{i\,j\,k\,l} = a\,(p_i p_j)\,(p_k p_l) + b\,(p_i p_k)\,(p_j p_l) + c\,(p_i p_l)\,(p_j p_k) - d\,\mathrm{i}\,\epsilon_{i\,j\,k\,l} \tag{3.21}$$

with $\epsilon_{i\,j\,k\,l} = \epsilon_{\alpha\beta\gamma\delta}\, p_i^{\alpha} p_j^{\beta} p_k^{\gamma} p_l^{\delta}$ and upper index combinations $(-++\pm)$, $(+-+\pm)$, and $(++-\pm)$ for $(a\,b\,c\,d)$.

Step 2 *Reduction of a spinor chain to standard form*

Since all spinor structures are disconnected after the first step, we can focus on single spinor chains in this step, i.e. spinor chains of the form $[B]^{\sigma}_{ab}$ where all Dirac matrices in B are contracted with momenta. These spinor chains can be reduced to the standard form $[\not p]^{\pm}_{ab}$ with a freely chosen momentum $p = p_n$, $p_n \neq p_a, p_b$, by recursively applying the following substeps:

- For $p_m \neq p_a, p_b, p$, replace $\not p_m$ by

$$\not p_m \overset{(3.11)}{=} p_{m,\mu} \sum_{i,j=0}^{3} g^{ij}\, n_i^{\mu}\, \not n_j \tag{3.22}$$

- Eliminate $\not n_3$ via (3.17).
- Use the Dirac algebra together with the Dirac equation or the mass-shell condition $\not p_i^2 = 0$ in order to shorten the spinor chain.

Since for our case only two different types of spinor chains are left after the first step, we can demonstrate the reduction procedure of the two cases in full detail. The first case is reduced as:

$$\begin{aligned}
\Big[\not{p}_m\Big]^{\pm}_{ab} &\overset{(3.22)}{=} p_{m,\mu} \sum_{i,j=0}^{3} g^{ij}\, n_i^{\mu}(p_a,p_b,p_n)\, \Big[\not{n}_j(p_a,p_b,p_n)\Big]^{\pm}_{ab} \\
&\overset{(3.17)}{=} \frac{(p_a p_n)\,(p_b p_m) - (p_a p_b)\,(p_n p_m) + (p_a p_m)\,(p_n p_b) \pm \mathrm{i}\,\epsilon_{a\,n\,b\,m}}{2\,(p_a p_n)\,(p_b p_n)} \Big[\not{p}_n\Big]^{\pm}_{ab} \\
&\overset{(3.21)}{=} \frac{1}{2\,(p_a p_n)\,(p_b p_n)}\, A^{+-+\mp}_{a\,n\,b\,m} \Big[\not{p}_n\Big]^{\pm}_{ab}\,.
\end{aligned} \tag{3.23}$$

The second case can be reduced to the first case as follows:

$$\begin{aligned}
\Big[\not{p}_m\,\not{p}_l\,\not{p}_k\Big]^{\pm}_{ab} &\overset{(3.22)}{=} p_{l,\mu} \sum_{i,j=0}^{3} g^{ij}\, n_i^{\mu}(p_m,p_k,p_b)\, \Big[\not{p}_m\,\not{n}_j(p_m,p_k,p_b)\,\not{p}_k\Big]^{\pm}_{ab} \\
&\overset{(3.17)}{=} \frac{(p_b p_m)\,(p_l p_k) - (p_b p_l)\,(p_m p_k) + (p_b p_k)\,(p_m p_l)}{2\,(p_b p_m)(p_b p_k)} \Big[\not{p}_m\,\not{p}_b\,\not{p}_k\Big]^{\pm}_{ab} \\
&\qquad - \mathrm{i}\,\frac{\epsilon_{b\,m\,l\,k}}{2\,(p_b p_m)(p_b p_k)} \Big[\not{p}_m \gamma_5 \not{p}_b \not{p}_k\Big]^{\pm}_{ab} \\
&= \frac{(p_b p_m)\,(p_l p_k) - (p_b p_l)\,(p_m p_k) + (p_b p_k)\,(p_m p_l) \mp \mathrm{i}\,\epsilon_{b\,m\,l\,k}}{(p_b p_m)} \Big[\not{p}_m\Big]^{\pm}_{ab} \\
&\overset{(3.21)}{=} \frac{1}{(p_b p_m)}\, A^{+-+\pm}_{b\,m\,l\,k} \Big[\not{p}_m\Big]^{\pm}_{ab}\,.
\end{aligned} \tag{3.24}$$

Thus, we end up with spinor chains in standard form and prefactors S containing only scalar products of external momenta $(p_i p_j)$, $\epsilon_{i\,j\,k\,l}$, and the abbreviations (3.21). Note that (3.24) could be applied recursively to longer spinor chains.

Thus, for processes with six external fermions, all Dirac structures occurring in one-loop amplitudes, i.e. all structures of the form (3.3), can be brought to the form

$$S\,\Big[\not{p}_3\Big]^{\rho}_{12}\,\Big[\not{p}_1\Big]^{\sigma}_{34}\,\Big[\not{p}_1\Big]^{\tau}_{56}\,, \tag{3.25}$$

where we have chosen the momenta p_3, p_1, and p_1 in the spinor chains by convention. Accordingly, the SMEs can be chosen as

$$\hat{\mathcal{M}}^{\rho\sigma\tau} = \Big[\not{p}_3\Big]^{\rho}_{12}\,\Big[\not{p}_1\Big]^{\sigma}_{34}\,\Big[\not{p}_1\Big]^{\tau}_{56}\,, \tag{3.26}$$

and there is only one SME for each helicity combination of the external fermions. For purely W-mediated charged-current processes, there are only two non-vanishing helicity combinations and thus only two different SMEs.

Step 3 *Simplification of scalar factors*

After the reduction steps above, each spinor structure has the form (3.26) with prefactors S containing products of scalars products $(p_i p_j)$ in the denominator, and possibly polynomials of scalar products, of $\epsilon_{i\,j\,k\,l}$, and of $A^{a\,b\,c\,\pm}_{i\,j\,k\,l}$ in the numerator. These prefactors can be simplified further by means of relations we describe now.

The quantity $A^{abc\pm}_{ijkl}$ defined in (3.21) transforms under exchange of two momenta, corresponding to two of the indices $(ijkl)$, as

$$A^{a\,b\,c\,\pm}_{i\,j\,k\,l} = A^{a\,c\,b\,\mp}_{j\,i\,k\,l} = A^{a\,c\,b\,\mp}_{i\,j\,l\,k} = A^{c\,b\,a\,\mp}_{k\,j\,i\,l} = A^{c\,b\,a\,\mp}_{i\,l\,k\,j} = A^{b\,a\,c\,\mp}_{l\,j\,k\,i} = A^{b\,a\,c\,\mp}_{i\,k\,j\,l}\,, \tag{3.27}$$

and is therefore invariant under exchange of two distinct pairs of momenta,

$$A^{a\,b\,c\,\pm}_{i\,j\,k\,l} = A^{a\,b\,c\,\pm}_{j\,i\,l\,k} = A^{a\,b\,c\,\pm}_{k\,l\,i\,j} = A^{a\,b\,c\,\pm}_{l\,k\,j\,i}\,. \tag{3.28}$$

Owing to these relations, any $A^{a\,b\,c\,\pm}_{i'j'k'l'}$, where $(i'j'k'l')$ is an arbitrary permutation of $(i\,j\,k\,l)$, can be transformed into one of the six elements

$$A^{-++\pm}_{i\,j\,k\,l}\,,\; A^{+-+\pm}_{i\,j\,k\,l}\,,\; \text{ or }\; A^{++-\pm}_{i\,j\,k\,l}\,. \tag{3.29}$$

In the following, we use only these independent quantities (3.29), i.e. for each set of indices $(i\,j\,k\,l)$ of $A^{a\,b\,c\,\pm}_{i\,j\,k\,l}$ we define a standard order.

The identity for products of totally antisymmetric tensors (3.14) leads to relations among the $A^{a\,b\,c\,\pm}_{i\,j\,k\,l}$. Relations for products of $A^{a\,b\,c\,\pm}_{i\,j\,k\,l}$ with the same momenta are

$$\begin{aligned}
A^{-++\pm}_{i\,j\,k\,l}\,A^{-++\mp}_{i\,j\,k\,l} &= 4\,(p_ip_k)(p_jp_l)\,(p_ip_l)(p_jp_k)\,,\\
A^{+-+\pm}_{i\,j\,k\,l}\,A^{+-+\mp}_{i\,j\,k\,l} &= 4\,(p_ip_j)(p_kp_l)\,(p_ip_l)(p_jp_k)\,,\\
A^{++-\pm}_{i\,j\,k\,l}\,A^{++-\mp}_{i\,j\,k\,l} &= 4\,(p_ip_j)(p_kp_l)\,(p_ip_k)(p_jp_l)\,,
\end{aligned} \tag{3.30}$$

and

$$\begin{aligned}
A^{+-+\pm}_{i\,j\,k\,l}\,A^{++-\pm}_{i\,j\,k\,l} &= -2\,(p_ip_j)(p_kp_l)\,A^{-++\mp}_{i\,j\,k\,l}\\
A^{-++\pm}_{i\,j\,k\,l}\,A^{++-\pm}_{i\,j\,k\,l} &= -2\,(p_ip_k)(p_jp_l)\,A^{+-+\mp}_{i\,j\,k\,l}\,,\\
A^{-++\pm}_{i\,j\,k\,l}\,A^{+-+\pm}_{i\,j\,k\,l} &= -2\,(p_ip_l)(p_jp_k)\,A^{++-\mp}_{i\,j\,k\,l}\,.
\end{aligned} \tag{3.31}$$

Note that in these and the following formulas double Latin indices are not summed. In (3.30) and (3.31) the second and third lines are obtained from the first by the substitutions $(j \leftrightarrow k)$ and $(i \leftrightarrow k)$, respectively, and subsequent transformation to the six elements (3.29).

Relations for products of $A^{a\,b\,c\,\pm}_{i\,j\,k\,l}$ which differ in one momentum read

$$A^{-++\pm}_{i\,j\,k\,l} = \frac{1}{2\,(p_ip_m)(p_jp_m)}\,A^{-++\pm}_{i\,j\,k\,m}\,A^{-++\mp}_{i\,j\,l\,m} = \frac{1}{2\,(p_kp_m)(p_lp_m)}\,A^{++-\pm}_{i\,k\,l\,m}\,A^{++-\mp}_{j\,k\,l\,m}\,, \tag{3.32}$$

and

$$A^{+-+\pm}_{i\,j\,k\,l}A^{++-\pm}_{i\,j\,k\,m} = -\frac{(p_ip_j)}{(p_ip_m)}A^{-++\mp}_{i\,j\,k\,m}A^{-++\pm}_{i\,k\,l\,m} = \frac{(p_ip_j)}{(p_lp_m)}A^{++-\mp}_{i\,k\,l\,m}A^{+-+\mp}_{j\,k\,l\,m} = -\frac{(p_ip_j)}{(p_jp_l)}A^{-++\mp}_{i\,j\,k\,l}A^{-++\pm}_{j\,k\,l\,m}\,. \tag{3.33}$$

Two further relations can be obtained from each of the equations in (3.32) and (3.33) via the substitutions $(j \leftrightarrow k)$ and $(i \leftrightarrow k)$. Three further sets of relations can finally be constructed by substituting $(l \leftrightarrow m)$ in all these relations derived from (3.33).

Step 3 consists of two parts:

- First, we try to eliminate *sums* containing $A^{a\,b\,c\,\pm}_{i\,j\,k\,l}$, $(p_i p_j)\,(p_k p_l)$, $\epsilon_{i\,j\,k\,l}$, and products thereof. To this end, we use the Schouten identity (3.13), the relations (3.30)–(3.33), and linear relations like $A^{+-+\pm}_{i\,j\,k\,l} = 2\,(p_i p_j)\,(p_k p_l) - A^{++-\mp}_{i\,j\,k\,l}$ or $(p_i p_j)\,(p_k p_l) \pm \mathrm{i}\,\epsilon_{i\,j\,k\,l} = A^{++-\mp}_{i\,j\,k\,l} - (p_i p_k)\,(p_j p_l) + (p_i p_l)\,(p_j p_k)$ that follow from the definition of the $A^{a\,b\,c\,\pm}_{i\,j\,k\,l}$ (3.21). All these relations are applied recursively to parts of S in (3.26) as long as they lead to simplifications.

  When starting from structures of the form (3.3), we succeeded in this way to eliminate all sums, and the resulting S involve only products of $A^{a\,b\,c\,\pm}_{i\,j\,k\,l}$ and scalar products in the numerator, and products of scalar products in the denominator.

- Second, the *products* of $A^{a\,b\,c\,\pm}_{i\,j\,k\,l}$ are simplified further and brought into a standard form by using the relations (3.30)–(3.33).

Typical results are

$$\begin{aligned}
\Big[\gamma^\mu\gamma^\nu\gamma^\rho\Big]^\sigma_{12}\Big[\gamma_\mu\gamma_\nu\gamma_\rho\Big]^\tau_{34} &= \frac{4}{(p_1p_3)}\,\Big[\not{p}_3\Big]^\sigma_{12}\Big[\not{p}_1\Big]^\tau_{34}\left(\frac{2\,A^{-++\sigma}_{1\,2\,3\,4}}{(p_1p_4)\,(p_2p_3)}\,\delta_{\sigma,\tau}+\delta_{\sigma,-\tau}\right),\\
\Big[\not{p}_3\not{p}_5\gamma^\mu\Big]^-_{12}\Big[\gamma_\mu\Big]^-_{56} &= 0\,,\\
\Big[\not{p}_3\gamma^\mu\gamma^\nu\Big]^+_{12}\,\Big[\gamma_\mu\gamma^\rho\gamma^\kappa\Big]^-_{34}\Big[\gamma_\nu\gamma_\rho\gamma_\kappa\Big]^-_{56} &= 0\,,\\
\Big[\not{p}_3\gamma^\mu\gamma^\nu\Big]^\sigma_{12}\Big[\gamma_\nu\gamma^\rho\gamma^\kappa\Big]^-_{34}\Big[\gamma_\mu\gamma_\rho\gamma_\kappa\Big]^-_{56} &= \frac{-4\,A^{-+++}_{1\,3\,4\,5}\,A^{+-++}_{1\,3\,4\,6}}{(p_1p_3)\,(p_1p_4)\,(p_1p_5)\,(p_1p_6)\,(p_3p_4)}\Big[\not{p}_3\Big]^\sigma_{12}\Big[\not{p}_1\Big]^-_{34}\Big[\not{p}_1\Big]^-_{56}\\
&\quad\times\Big(\delta_{\sigma,-}+2\,\delta_{\sigma,+}\Big)\,,\\
\Big[\not{p}_3\gamma^\mu\gamma^\nu\gamma^\rho\gamma^\kappa\Big]^-_{12}\,\Big[\gamma_\nu\gamma_\rho\gamma_\kappa\Big]^-_{34}\,\Big[\gamma_\mu\Big]^-_{56} &= \frac{8\,A^{-++-}_{1\,2\,3\,4}\,A^{-++-}_{1\,3\,5\,6}}{(p_1p_3)\,(p_1p_4)\,(p_1p_5)\,(p_1p_6)\,(p_2p_3)}\,\Big[\not{p}_3\Big]^-_{12}\Big[\not{p}_1\Big]^-_{34}\Big[\not{p}_1\Big]^-_{56}\,,\\
-\mathrm{i}\epsilon^{\mu\nu\rho\sigma}\,p_{1,\sigma}\,\Big[\gamma_\mu\Big]^+_{12}\,\Big[\gamma_\nu\Big]^-_{34}\,\Big[\gamma_\rho\Big]^-_{56} &= \frac{A^{+-+-}_{1\,2\,3\,5}}{2\,(p_1p_3)\,(p_1p_5)\,(p_2p_3)}\,\Big[\not{p}_3\Big]^+_{12}\Big[\not{p}_1\Big]^-_{34}\Big[\not{p}_1\Big]^-_{56}\,.
\end{aligned} \qquad (3.34)$$

The entire reduction algorithm, described in the three steps above, reduces the spinor chains of the considered processes to the SMEs (3.26) and about 35 different $A^{a\,b\,c\,\pm}_{i\,j\,k\,l}$. When inserting the results into the amplitudes, further simplifications between contributions of different spinor structures can be performed owing to the simple structure of the SMEs. This speeds up the calculations considerably.

The spinor structures could alternatively be evaluated directly in the Weyl–van der Waerden spinor formalism, as described in some detail in the appendix. Although most of the relations given in this section can be easily derived using the spinor formalism, many simplifications that are based on four-momenta are harder to perform in that approach.

3.3 Alternative strategy for reducing Dirac structures

In this section we describe an alternative strategy for the reduction of Dirac structures. In this approach we take care that no quantities are introduced in the denominator that can lead to numerical problems, like scalar products or Gram determinants. As a consequence, the Dirac structures are not reduced to the minimal set, but to a small set of standard structures. Moreover, the coefficients in front of these standard structures only involve Lorentz products, but no contractions with ϵ-tensors, facilitating further simplifications in amplitudes.[8]

Step 1 *Reduction of multiple contractions between spinor chains*

Multiple Lorentz contractions between two spinor chains can be reduced to single contractions using (3.7) and (3.8). A typical example is given by

$$\Big[A\gamma^{\mu}\not{p}_i\gamma^{\nu}\Big]^{\pm}_{12}\Big[B\gamma_{\mu}\not{p}_j\gamma_{\nu}\Big]^{\pm}_{34} \overset{(3.7)}{=} 4(p_ip_j)\Big[A\gamma^{\mu}\Big]^{\pm}_{12}\Big[B\gamma_{\mu}\Big]^{\pm}_{34}. \tag{3.35}$$

This procedure leaves only products of spinor chains with (i) no contractions, (ii) exactly one contraction between two spinor chains, or (iii) the case in which one spinor chain is singly contracted with each of the two other chains.

Case (iii) can be reduced to (i) and (ii) as follows. Each spinor chain of type (iii) can be brought to the form $[A\gamma^{\mu}\not{p}_i\gamma^{\nu}]^{\rho}_{12}\,[B\gamma_{\mu}]^{\sigma}_{34}\,[C\gamma_{\nu}]^{\tau}_{56}$ or to one of the analogous forms with external fermions interchanged. The transformation to this standard form produces only terms of types (i) and (ii). The factor $\not{p}_i$ in the first chain is always present, because the number of Dirac matrices in the chain is at least three. We can assume that p_i is the momentum of a spinor belonging to the other chains, i.e. $i = 3, 4, 5$, or 6. Otherwise we could eliminate it with the Dirac equation after anticommuting it to the left or right in the spinor chain $[\ldots]_{12}$. The trick to get rid of the two Lorentz contractions is to apply (3.6) in order to shift the factor $\not{p}_i$ to the spinor chain where it can be eliminated with its Dirac equation. This means, if $i = 3$ or 4, $\not{p}_i$ is shifted into $[\ldots]_{34}$; if $i = 5$ or 6, it is shifted into $[\ldots]_{56}$. We give a simple example:

$$\begin{aligned}
\Big[A\gamma^{\mu}\not{p}_4\gamma^{\nu}\Big]^{\pm}_{12}\Big[B\gamma_{\mu}\Big]^{\mp}_{34}\Big[C\gamma_{\nu}\Big]^{\tau}_{56} &\overset{(3.6)}{=} \Big[A\gamma^{\mu}\Big]^{\pm}_{12}\Big[B\not{p}_4\gamma^{\nu}\gamma_{\mu}\Big]^{\mp}_{34}\Big[C\gamma_{\nu}\Big]^{\tau}_{56} \\
&= \Big[A\gamma^{\mu}\Big]^{\pm}_{12}\Big[B(2p_4^{\nu}\gamma_{\mu} - 2p_{4,\mu}\gamma^{\nu})\Big]^{\mp}_{34}\Big[C\gamma_{\nu}\Big]^{\tau}_{56} \\
&= 2\Big[A\gamma^{\mu}\Big]^{\pm}_{12}\Big[B\gamma_{\mu}\Big]^{\mp}_{34}\Big[C\not{p}_4\Big]^{\tau}_{56} - 2\Big[A\not{p}_4\Big]^{\pm}_{12}\Big[B\gamma^{\nu}\Big]^{\mp}_{34}\Big[C\gamma_{\nu}\Big]^{\tau}_{56}.
\end{aligned} \tag{3.36}$$

Step 2 *Reduction of single contractions to standard form*

After the first step, the only contractions between spinor chains are of the form $[A\gamma^{\mu}]^{\rho}_{12}\,[B\gamma_{\mu}]^{\sigma}_{34}\,[C]^{\tau}_{56}$ (or with fermions interchanged), where the matrices A, B, C are products of slashed momenta. The matrices A and B can be systematically eliminated as follows.

We reduce the number of slashed momenta in A until $A = \mathbf{1}$. If $A = \mathbf{1}$, there is nothing to do. Otherwise A is of the form $A'\not{p}_i\not{p}_j$ with A' containing two slashed momenta less than A. If either i or j is 3 or 4, we shift $\not{p}_i\not{p}_j$ to the spinor chain $[\ldots]_{34}$ with the help of (3.6) and eliminate $\not{p}_3$ or $\not{p}_4$ with its Dirac equation. This leaves the cases $\not{p}_i\not{p}_j = \not{p}_5\not{p}_6$ or $\not{p}_6\not{p}_5$ (since $\not{p}_i\not{p}_i = 0$), which can be reduced by momentum conservation, e.g., $\not{p}_5\not{p}_6 = \not{p}_5(-\not{p}_1 - \not{p}_2 - \not{p}_3 - \not{p}_4)$. The terms $\not{p}_3$ and $\not{p}_4$ are again shifted to $[\ldots]_{34}$, while $\not{p}_1$ and $\not{p}_2$ can be eliminated with their Dirac equations in $[\ldots]_{12}$ directly. The whole procedure reduces the number of slashed momenta in $[A\gamma^\mu]^\rho_{12}$ by two and can be repeated until $A = \mathbf{1}$.

---

[8] In this approach all explicit ϵ-tensors are eliminated with the Chisholm identity (3.4) at the beginning of the reduction.

The same procedure can be applied to $[B\gamma_\mu]^\sigma_{34}$ until $B = \mathbf{1}$. Finally, all products of spinor chains containing a Lorentz contraction between two chains are of the form $[\gamma^\mu]^\rho_{12}\,[\gamma_\mu]^\sigma_{34}\,[C]^\tau_{56}$ (or with fermions interchanged). Again, we give an illustrative example:

$$
\begin{aligned}
&\big[\not{p}_4\not{p}_5\gamma^\mu\big]^\pm_{12}\big[\not{p}_5\not{p}_6\gamma_\mu\big]^\mp_{34}\big[C\big]^\tau_{56}\\
&\quad\overset{(3.6)}{=}\ \big[\gamma^\mu\big]^\pm_{12}\big[\not{p}_5\not{p}_6\gamma_\mu\not{p}_4\not{p}_5\big]^\mp_{34}\big[C\big]^\tau_{56}\\
&\quad=\ 2(p_4p_5)\big[\gamma^\mu\big]^\pm_{12}\big[\not{p}_5\not{p}_6\gamma_\mu\big]^\mp_{34}\big[C\big]^\tau_{56}\\
&\quad=\ -2(p_4p_5)\big[\gamma^\mu\big]^\pm_{12}\big[(\not{p}_1+\not{p}_2+\not{p}_3+\not{p}_4)\not{p}_6\gamma_\mu\big]^\mp_{34}\big[C\big]^\tau_{56}\\
&\quad\overset{(3.6)}{=}\ -2(p_4p_5)\Big\{\big[\gamma^\mu(\not{p}_1+\not{p}_2)\not{p}_6\big]^\pm_{12}\big[\gamma_\mu\big]^\mp_{34}+\big[\gamma^\mu\big]^\pm_{12}\big[(\not{p}_3+\not{p}_4)\not{p}_6\gamma_\mu\big]^\mp_{34}\Big\}\big[C\big]^\tau_{56}\\
&\quad=\ -4(p_4p_5)\Big\{\big[\not{p}_6\big]^\pm_{12}\big[\not{p}_1\big]^\mp_{34}+(p_2p_6)\big[\gamma^\mu\big]^\pm_{12}\big[\gamma_\mu\big]^\mp_{34}\\
&\qquad\qquad+(p_4p_6)\big[\gamma^\mu\big]^\pm_{12}\big[\gamma_\mu\big]^\mp_{34}-\big[\not{p}_4\big]^\pm_{12}\big[\not{p}_6\big]^\mp_{34}\Big\}\big[C\big]^\tau_{56}.
\end{aligned}
\tag{3.37}
$$

Step 3 *Reduction of products of slashed momenta*

First we write all products of slashed momenta in a standard form. After the preceding steps, we are left with spinor chains of the form $[A]^\rho_{12}\,[\gamma^\mu]^\sigma_{34}\,[\gamma_\mu]^\tau_{56}$, $[\gamma^\mu]^\rho_{12}\,[B]^\sigma_{34}\,[\gamma_\mu]^\tau_{56}$, $[\gamma^\mu]^\rho_{12}\,[\gamma_\mu]^\sigma_{34}\,[C]^\tau_{56}$, or $[A]^\rho_{12}\,[B]^\sigma_{34}\,[C]^\tau_{56}$. None of the A, B, C contains open Dirac indices, i.e. they are products of slashed momenta and chirality projectors. With the help of Dirac algebra and of momentum conservation the spinor chains can be brought into the form of a linear combination of terms $[\not{p}_i]^\rho_{ab}$ and $[\not{p}_i\not{p}_j\not{p}_k]^\rho_{ab}$. For $[A]^\rho_{12}$, e.g., we substitute $p_6 = -p_1 - p_2 - p_3 - p_4 - p_5$, eliminate all $\not{p}_1$ and $\not{p}_2$ with their Dirac equations by anticommuting them to the left or right and reorder the remaining $\not{p}_i$ terms according to increasing i. Owing to the relation $\not{p}\not{p} = p^2$, this leaves only $[\not{p}_i]^\rho_{12}$ with $i = 3, 4, 5$ and $[\not{p}_3\not{p}_4\not{p}_5]^\rho_{12}$. In the same way we reduce the other uncontracted spinor chains to $[\not{p}_j]^\rho_{34}$, $[\not{p}_5\not{p}_6\not{p}_1]^\rho_{34}$, $[\not{p}_k]^\rho_{56}$, and $[\not{p}_1\not{p}_2\not{p}_3]^\rho_{56}$ with $j = 5, 6, 1$ and $k = 1, 2, 3$.

We now eliminate all chains of the form $[\not{p}_i\not{p}_j\not{p}_k]^\rho_{ab}\,[\not{p}_l\not{p}_m\not{p}_n]^\sigma_{cd}$ by making use of the Chisholm identity (3.4) which can be written as

$$
\not{p}_i\not{p}_j\not{p}_k = E_{ijk} + G_{ijk} \tag{3.38}
$$

with the shorthands

$$
\begin{aligned}
E_{ijk} &= \mathrm{i}\epsilon^{\alpha\beta\gamma\delta}p_{i,\alpha}p_{j,\beta}p_{k,\gamma}\gamma_\delta\gamma_5,\\
G_{ijk} &= (p_ip_j)\not{p}_k - (p_ip_k)\not{p}_j + (p_jp_k)\not{p}_i.
\end{aligned}
\tag{3.39}
$$

Thus, we can write

$$
\begin{aligned}
\big[\not{p}_i\not{p}_j\not{p}_k\big]^\rho_{ab}\big[\not{p}_l\not{p}_m\not{p}_n\big]^\sigma_{cd} = {}&\big[E_{ijk}\big]^\rho_{ab}\big[E_{lmn}\big]^\sigma_{cd}+\big[\not{p}_i\not{p}_j\not{p}_k\big]^\rho_{ab}\big[G_{lmn}\big]^\sigma_{cd}\\
&+\big[G_{ijk}\big]^\rho_{ab}\big[\not{p}_l\not{p}_m\not{p}_n\big]^\sigma_{cd}-\big[G_{ijk}\big]^\rho_{ab}\big[G_{lmn}\big]^\sigma_{cd}.
\end{aligned}
\tag{3.40}
$$

In the first term on the r.h.s. we can express the product of ϵ-tensors,

$$\Big[E_{ijk}\Big]^{\rho}_{ab}\Big[E_{lmn}\Big]^{\sigma}_{cd} = -\epsilon^{\alpha\beta\gamma\delta}\epsilon^{\alpha'\beta'\gamma'\delta'} p_{i,\alpha}p_{j,\beta}p_{k,\gamma}p_{l,\alpha'}p_{m,\beta'}p_{n,\gamma'}\Big[\gamma_\delta\gamma_5\Big]^{\rho}_{ab}\Big[\gamma_{\delta'}\gamma_5\Big]^{\sigma}_{cd}, \tag{3.41}$$

in terms of ordinary Lorentz products because of (3.14). This means, after exploiting (3.40) products of slashed momenta only occur in terms of the forms: (i) $[\not{p}_3\not{p}_4\not{p}_5]^{\rho}_{12}\,[\gamma^\mu]^{\sigma}_{34}\,[\gamma_\mu]^{\tau}_{56}$, (ii) $[\not{p}_3\not{p}_4\not{p}_5]^{\rho}_{12}\,[\not{p}_j]^{\sigma}_{34}\,[\not{p}_k]^{\tau}_{56}$, and similar terms with products of slashed momenta in the other spinor chains.

Terms of type (ii) can always be simplified with (3.10). If one of the indices j, k is 1 or 2, then $\not{p}_3\not{p}_4\not{p}_5$ can always be reordered such that one of the relations in (3.10) applies (if necessary momentum conservation has to be used). We illustrate this by a simple example:

$$\begin{aligned}
\Big[\not{p}_3\not{p}_4\not{p}_5\Big]^{+}_{12}\Big[\not{p}_2\Big]^{-}_{34}\Big[\not{p}_k\Big]^{\tau}_{56} &= 2(p_4p_5)\Big[\not{p}_3\Big]^{+}_{12}\Big[\not{p}_2\Big]^{-}_{34}\Big[\not{p}_k\Big]^{\tau}_{56} - \Big[\not{p}_3\not{p}_5\not{p}_4\Big]^{+}_{12}\Big[\not{p}_2\Big]^{-}_{34}\Big[\not{p}_k\Big]^{\tau}_{56}\\
&\overset{(3.10)}{=} 2(p_4p_5)\Big[\not{p}_3\Big]^{+}_{12}\Big[\not{p}_2\Big]^{-}_{34}\Big[\not{p}_k\Big]^{\tau}_{56} - (p_2p_4)\Big[\not{p}_3\not{p}_5\gamma^\mu\Big]^{+}_{12}\Big[\gamma_\mu\Big]^{-}_{34}\Big[\not{p}_k\Big]^{\tau}_{56}\\
&\overset{(3.6)}{=} 2(p_4p_5)\Big[\not{p}_3\Big]^{+}_{12}\Big[\not{p}_2\Big]^{-}_{34}\Big[\not{p}_k\Big]^{\tau}_{56} - (p_2p_4)\Big[\gamma^\mu\Big]^{+}_{12}\Big[\gamma_\mu\not{p}_3\not{p}_5\Big]^{-}_{34}\Big[\not{p}_k\Big]^{\tau}_{56}\\
&= 2(p_4p_5)\Big[\not{p}_3\Big]^{+}_{12}\Big[\not{p}_2\Big]^{-}_{34}\Big[\not{p}_k\Big]^{\tau}_{56} - 2(p_2p_4)\Big[\not{p}_3\Big]^{+}_{12}\Big[\not{p}_5\Big]^{-}_{34}\Big[\not{p}_k\Big]^{\tau}_{56}.
\end{aligned} \tag{3.42}$$

If neither j or k has the value 1 or 2 in terms of type (ii), then one of the relations in (3.10) applies to the product $[\not{p}_j]^{\sigma}_{34}\,[\not{p}_k]^{\tau}_{56}$ (if necessary momentum conservation has to be used). In this case terms of type (ii) transform into terms of type (i) and terms without products of slashed momenta.

Finally, we have to reduce terms of type (i), which turns out to be a tedious task. We illustrate the basic steps for the following example,

$$\begin{aligned}
\Big[\not{p}_3\not{p}_4\not{p}_5\Big]^{-}_{12}\Big[\gamma^\mu\Big]^{-}_{34}\Big[\gamma_\mu\Big]^{-}_{56} &= \frac{1}{2}\Big[\not{p}_3\not{p}_4\gamma^\nu\Big]^{-}_{12}\Big[\gamma^\mu\Big]^{-}_{34}\Big[\gamma_\nu\not{p}_5\gamma_\mu\Big]^{-}_{56}\\
&= -\frac{1}{2}\Big[\not{p}_3\not{p}_4\gamma^\nu\Big]^{-}_{12}\Big[\gamma^\mu\Big]^{-}_{34}\Big[\gamma_\nu\not{p}_6\gamma_\mu\Big]^{-}_{56}\\
&\quad -\frac{1}{2}\Big[\not{p}_3\not{p}_4\gamma^\nu\Big]^{-}_{12}\Big[\gamma^\mu\Big]^{-}_{34}\Big[\gamma_\nu(\not{p}_1+\not{p}_2+\not{p}_3+\not{p}_4)\gamma_\mu\Big]^{-}_{56}\\
&\overset{(3.6)}{=} -\Big[\not{p}_3\not{p}_4\gamma^\nu\Big]^{-}_{12}\Big[\not{p}_6\Big]^{-}_{34}\Big[\gamma_\nu\Big]^{-}_{56}\\
&\quad -\frac{1}{2}\Big[\not{p}_3\not{p}_4\gamma^\nu\gamma_\mu(\not{p}_1+\not{p}_2+\not{p}_3+\not{p}_4)\Big]^{-}_{12}\Big[\gamma^\mu\Big]^{-}_{34}\Big[\gamma_\nu\Big]^{-}_{56}.
\end{aligned} \tag{3.43}$$

At first sight, we have made the expression more complicated by using the Dirac equation and some rearrangements for $\not{p}_5$, which was then eliminated by momentum conservation in the second equality. The last expression in (3.43) can be simplified by anticommuting the terms in $(\not{p}_1+\not{p}_2+\not{p}_3+\not{p}_4)$ in such a way that the Dirac equations for $\not{p}_1$ and $\not{p}_2$ apply and that the terms $\not{p}_3$ and $\not{p}_4$ drop out via $\not{p}_i\not{p}_i = 0$. The various terms that survive this procedure can all be further reduced as described in the previous steps. After some tedious algebra, we get

$$\Big[\not{p}_3\not{p}_4\not{p}_5\Big]^{-}_{12}\Big[\gamma^\mu\Big]^{-}_{34}\Big[\gamma_\mu\Big]^{-}_{56} = -2(p_3p_5)\Big[\gamma^\mu\Big]^{-}_{12}\Big[\gamma_\mu\Big]^{-}_{34}\Big[\not{p}_4\Big]^{-}_{56} + 2(p_4p_5)\Big[\not{p}_3\Big]^{-}_{12}\Big[\gamma^\mu\Big]^{-}_{34}\Big[\gamma_\mu\Big]^{-}_{56}. \tag{3.44}$$

Note, however, that the explicit form of this result is not unique, i.e. it might look different if other algebraic manipulations had been made.

Step 4 *Reducing products of the form* $[\not{p}_i]^\rho_{12}\,[\not{p}_j]^\sigma_{34}\,[\not{p}_k]^\tau_{56}$

Obviously, momentum conservation can be used such that the indices i, j, k take only the following values, $i = 3,4,5$, $j = 5,6,1$, and $k = 1,2,3$. Equations (3.10) provide $2 \times 3 \times 3 = 18$ relations per chirality which can be used to reduce the number of these 27 (ijk) values to 9.

There are, however, still some relations among the structures $[\not{p}_i]^\rho_{12}\,[\not{p}_j]^\sigma_{34}\,[\not{p}_k]^\tau_{56}$ and $[\not{p}_i]^\rho_{12}\,[\gamma^\mu]^\sigma_{34}\,[\gamma_\mu]^\tau_{56}$, etc., which can be exploited to eliminate some (ijk) values. Such relations can be deduced as in the following example,

$$
\begin{aligned}
0 &= \Big[\not{p}_1\not{p}_6\gamma^\nu\not{p}_4\gamma^\mu\Big]^-_{12}\Big[\gamma_\mu\Big]^-_{34}\Big[\gamma_\nu\Big]^-_{56} \\
&\overset{(3.6)}{=} \Big[\gamma^\nu\not{p}_4\gamma^\mu\Big]^-_{12}\Big[\gamma_\mu\Big]^-_{34}\Big[\not{p}_6\not{p}_1\gamma_\nu\Big]^-_{56} \\
&\overset{(3.6)}{=} \Big[\gamma^\mu\Big]^-_{12}\Big[\not{p}_4\gamma^\nu\gamma_\mu\Big]^-_{34}\Big[\not{p}_6\not{p}_1\gamma_\nu\Big]^-_{56} \\
&= \Big[\gamma^\mu\Big]^-_{12}\Big[2p_4^\nu\gamma_\mu - 2p_{4,\mu}\gamma^\nu\Big]^-_{34}\Big[2(p_1p_6)\gamma_\nu - 2p_{6,\nu}\not{p}_1\Big]^-_{56} \\
&= 4(p_1p_6)\Big[\gamma^\mu\Big]^-_{12}\Big[\gamma_\mu\Big]^-_{34}\Big[\not{p}_4\Big]^-_{56} - 4(p_4p_6)\Big[\gamma^\mu\Big]^-_{12}\Big[\gamma_\mu\Big]^-_{34}\Big[\not{p}_1\Big]^-_{56} \\
&\quad - 4(p_1p_6)\Big[\not{p}_4\Big]^-_{12}\Big[\gamma^\nu\Big]^-_{34}\Big[\gamma_\nu\Big]^-_{56} + 4\Big[\not{p}_4\Big]^-_{12}\Big[\not{p}_6\Big]^-_{34}\Big[\not{p}_1\Big]^-_{56}.
\end{aligned}
\tag{3.45}
$$

This expresses the last term in terms of $[\not{p}_i]^-_{12}\,[\gamma^\mu]^-_{34}\,[\gamma_\mu]^-_{56}$, etc. In total we find 7 such relations per chirality, so that the number of structures $[\not{p}_i]^\rho_{12}\,[\not{p}_j]^\sigma_{34}\,[\not{p}_k]^\tau_{56}$ can be reduced to 2 combinations (ijk) per chirality configuration $(\rho\sigma\tau)$.

Step 5 *Reducing products of the form* $[\not{p}_i]^\rho_{12}\,[\gamma^\mu]^\sigma_{34}\,[\gamma_\mu]^\tau_{56}$*, etc.*

As in the previous step, we use momentum conservation to constrain the indices i, j, k in the structures $[\not{p}_i]^\rho_{12}\,[\gamma^\mu]^\sigma_{34}\,[\gamma_\mu]^\tau_{56}$, $[\gamma^\mu]^\rho_{12}\,[\not{p}_j]^\pm_{34}\,[\gamma_\mu]^\tau_{56}$, and $[\gamma^\mu]^\rho_{12}\,[\gamma_\mu]^\sigma_{34}\,[\not{p}_k]^\tau_{56}$ to the values $i = 3,4,5$, $j = 5,6,1$, and $k = 1,2,3$. One out of these 9 resulting structures (per chirality) is, however, redundant and can be easily eliminated as follows,

$$
\begin{aligned}
0 &= \Big[\gamma^\mu(\not{p}_1+\not{p}_2+\not{p}_3+\not{p}_4+\not{p}_5+\not{p}_6)\gamma^\nu\Big]^\pm_{12}\Big[\gamma_\mu\Big]^\pm_{34}\Big[\gamma_\nu\Big]^\pm_{56} \\
&\overset{(3.6)}{=} \Big[\gamma^\mu(\not{p}_1+\not{p}_2)\gamma^\nu\Big]^\pm_{12}\Big[\gamma_\mu\Big]^\pm_{34}\Big[\gamma_\nu\Big]^\pm_{56} + \Big[\gamma^\mu\Big]^\pm_{12}\Big[\gamma_\mu\gamma^\nu(\not{p}_3+\not{p}_4)\Big]^\pm_{34}\Big[\gamma_\nu\Big]^\pm_{56} \\
&\quad + \Big[\gamma^\nu\Big]^\pm_{12}\Big[\gamma_\mu\Big]^\pm_{34}\Big[(\not{p}_5+\not{p}_6)\gamma^\mu\gamma_\nu\Big]^\pm_{56} \\
&= 2\Big[\gamma^\mu\Big]^\pm_{12}\Big[(\not{p}_1+\not{p}_6)\Big]^\pm_{34}\Big[\gamma_\mu\Big]^\pm_{56} + 2\Big[\gamma^\mu\Big]^\pm_{12}\Big[\gamma_\mu\Big]^\pm_{34}\Big[(\not{p}_2+\not{p}_3)\Big]^\pm_{56} \\
&\quad - 2\Big[(\not{p}_3+\not{p}_6)\Big]^\pm_{12}\Big[\gamma^\mu\Big]^\pm_{34}\Big[\gamma_\mu\Big]^\pm_{56} \\
&= 2\Big[\gamma^\mu\Big]^\pm_{12}\Big[(\not{p}_1+\not{p}_6)\Big]^\pm_{34}\Big[\gamma_\mu\Big]^\pm_{56} + 2\Big[\gamma^\mu\Big]^\pm_{12}\Big[\gamma_\mu\Big]^\pm_{34}\Big[(\not{p}_2+\not{p}_3)\Big]^\pm_{56} \\
&\quad + 2\Big[(\not{p}_4+\not{p}_5)\Big]^\pm_{12}\Big[\gamma^\mu\Big]^\pm_{34}\Big[\gamma_\mu\Big]^\pm_{56}.
\end{aligned}
\tag{3.46}
$$

Relations for the other chirality configurations can be obtained in the same way.

We note that there are further relations among the spinor structures considered in this step. The remaining relations, however, involve coefficients with Lorentz products, so that their use to further eliminate some structures would lead to Lorentz products in the denominator, which we want to avoid. Nevertheless we give two such relations for illustration:

$$\begin{aligned}
&(p_1p_5)\Big[\not{p}_3\Big]^{\pm}_{12}\Big[\gamma^{\mu}\Big]^{\pm}_{34}\Big[\gamma_{\mu}\Big]^{\pm}_{56}+(p_3p_5)\Big[\gamma^{\mu}\Big]^{\pm}_{12}\Big[\not{p}_1\Big]^{\pm}_{34}\Big[\gamma_{\mu}\Big]^{\pm}_{56}\\
&\quad=(p_1p_3)\Big[\gamma^{\mu}\Big]^{\pm}_{12}\Big[\not{p}_5\Big]^{\pm}_{34}\Big[\gamma_{\mu}\Big]^{\pm}_{56}+(p_1p_5)\Big[\gamma^{\mu}\Big]^{\pm}_{12}\Big[\gamma_{\mu}\Big]^{\pm}_{34}\Big[\not{p}_3\Big]^{\pm}_{56}\\
&\quad=(p_3p_5)\Big[\gamma^{\mu}\Big]^{\pm}_{12}\Big[\gamma_{\mu}\Big]^{\pm}_{34}\Big[\not{p}_1\Big]^{\pm}_{56}+(p_1p_3)\Big[\not{p}_5\Big]^{\pm}_{12}\Big[\gamma^{\mu}\Big]^{\pm}_{34}\Big[\gamma_{\mu}\Big]^{\pm}_{56}.
\end{aligned}\tag{3.47}$$

Summary: *Final set of spinor structures*

After applying the steps described above, all Dirac structures occurring in one-loop amplitudes for processes with six external fermions can be expressed as linear combinations of the following SMEs with coefficients that do not involve any denominators,

$$\begin{aligned}
\hat{\mathcal{M}}^{\rho\sigma\tau}_{\{1,2\}}&=\Big[\gamma^{\mu}\Big]^{\rho}_{12}\Big[\gamma_{\mu}\Big]^{\sigma}_{34}\Big[\not{p}_{\{1,2\}}\Big]^{\tau}_{56},\\
\hat{\mathcal{M}}^{\rho\sigma\tau}_{\{3,4,5\}}&=\Big[\not{p}_{\{3,4,5\}}\Big]^{\rho}_{12}\Big[\gamma^{\mu}\Big]^{\sigma}_{34}\Big[\gamma_{\mu}\Big]^{\tau}_{56},\\
\hat{\mathcal{M}}^{\rho\sigma\tau}_{\{6,7,8\}}&=\Big[\gamma^{\mu}\Big]^{\rho}_{12}\Big[\not{p}_{\{5,6,1\}}\Big]^{\sigma}_{34}\Big[\gamma_{\mu}\Big]^{\tau}_{56},\\
\hat{\mathcal{M}}^{\rho\sigma\tau}_{9}&=\Big[\not{p}_4\Big]^{\rho}_{12}\Big[\not{p}_6\Big]^{\sigma}_{34}\Big[\not{p}_2\Big]^{\tau}_{56},\\
\hat{\mathcal{M}}^{\rho\sigma\tau}_{10}&=\Big[\not{p}_3\Big]^{\rho}_{12}\Big[\not{p}_5\Big]^{\sigma}_{34}\Big[\not{p}_1\Big]^{\tau}_{56}.
\end{aligned}\tag{3.48}$$

4 The complex mass scheme at one loop

The description of resonances in perturbation theory requires at least a partial Dyson summation of self-energy insertions. This leads to a mixing of perturbative orders and, if done carelessly, can easily jeopardise gauge invariance [26, 27]. Therefore, the proper introduction of finite-width effects is a non-trivial problem. While several solutions have been described for lowest-order predictions [23, 27, 28, 29, 30, 31, 32, 33, 34, 35], no viable, universally valid scheme exists so far for a consistent evaluation of radiative corrections in the presence of resonances. A pole expansion [28, 30, 31, 35] provides a gauge-invariant answer and is applicable to radiative corrections, but restricts the validity of the result to the resonance region only and is not reliable in threshold regions. In our calculation we want to cover both the threshold region, where the pole approximation is not applicable, and the continuum above threshold, where threshold expansions are not valid. Moreover, the calculation should be valid both for resonant and non-resonant regions in phase space. In other words, we are after a unified description that is applicable in the complete phase space and does not require any matching between different treatments for different regions.

Such a description is provided by the "complex-mass scheme" (CMS), which was introduced in Ref. [23] for lowest-order calculations. In this approach the W- and Z-boson masses are consistently considered as complex quantities, defined as the locations of the poles in the complex k^2 plane of the corresponding propagators with momentum k. Gauge invariance is preserved if the complex masses are introduced everywhere in the Feynman rules, in particular in the definition of the weak mixing angle,

$$\cos^2\theta_{\mathrm{W}} \equiv c_{\mathrm{w}}^2 = 1 - s_{\mathrm{w}}^2 = \frac{\mu_{\mathrm{W}}^2}{\mu_{\mathrm{Z}}^2}, \tag{4.1}$$

which is derived from the ratio of the complex mass squares of the gauge bosons,[9]

$$\mu_{\mathrm{W}}^2 = M_{\mathrm{W}}^2 - \mathrm{i}M_{\mathrm{W}}\Gamma_{\mathrm{W}}, \qquad \mu_{\mathrm{Z}}^2 = M_{\mathrm{Z}}^2 - \mathrm{i}M_{\mathrm{Z}}\Gamma_{\mathrm{Z}}. \tag{4.2}$$

The (algebraic) relations, such as Ward identities, that follow from gauge invariance remain valid, because the gauge-boson masses are modified only by an analytic continuation. As a consequence unitarity cancellations are respected, and the amplitudes have a decent high-energy behaviour.

While necessary in the resonant propagators, the consistent introduction of complex gauge-boson masses introduces spurious terms in other places, as e.g. in the weak mixing angle (4.1). When using the CMS at tree level, which amounts to replacing the real gauge-boson masses by the complex masses (4.2) and the weak mixing angle by (4.1) in tree-level amplitudes, the spurious terms are of order $\mathcal{O}(\Gamma_{\mathrm{W}}/M_{\mathrm{W}}) = \mathcal{O}(\alpha)$ relative to the lowest-order term (both in resonant and non-resonant regions).

Here we propose a generalization of the CMS to higher orders. The complex masses are introduced directly at the level of the Lagrangian by splitting the bare masses into complex renormalized masses and complex counterterms. This scheme has the following properties:

- From the Lagrangian we obtain Feynman rules with complex masses and counterterms with which we can perform perturbative calculations as usual. Since we do not change the theory at all, but only rearrange its perturbative expansion, no double counting of terms occurs.

- For each unstable particle mass, we add and subtract the same imaginary part in the Lagrangian. One of these terms provides the imaginary part for the mass parameter and becomes part of the free propagator, while the other becomes part of a counterterm vertex. The first term is, thus, resummed but the second is not. Independently of the imaginary part that is added and subtracted, this procedure does not spoil the algebraic relations that govern gauge invariance, and unitarity cancellations are exactly respected. In practice, this means that we can insert values for the gauge-boson widths that are not directly related to the one-loop order to which the corrections for the process are calculated. We could even go beyond one loop in the calculation of the widths or take an empirical value.

---

[9] While it is generally accepted that the mass and width of unstable particles are related to the pole of the propagator in the complex plane, this does not define the mass and the width separately. This arbitrariness is discussed in detail in Ref. [55], where also a definition of the mass and width is proposed such that the width is given by the inverse lifetime. We have chosen the popular definition (4.2), but the complex renormalization scheme is applicable to other definitions as well.

- Performing an $\mathcal{O}(\alpha)$ calculation in the CMS yields $\mathcal{O}(\alpha)$ accuracy everywhere in phase space provided the width that enters in the resonant propagators via the complex mass is calculated including at least $\mathcal{O}(\alpha)$ corrections. This is evident away from the resonances, where one could expand in terms of the width, thus recovering the usual perturbative expansion. In the resonance region, where the resonant contributions dominate, both the prefactors of the resonant propagators and the resonant propagators themselves are taken into account in $\mathcal{O}(\alpha)$ and our results differ by $\mathcal{O}(\alpha^2)$ terms from a leading pole approximation where this is applicable. Thus, any spurious terms are of order $\mathcal{O}(\alpha^2)$.

Introducing complex masses and couplings seems to violate unitarity. Obviously, the Cutkosky cutting equations [56] are no longer valid, and unitarity cannot simply be proven order by order anymore. However, since we do not modify the bare Lagrangian, the unitarity-violating terms are of higher order, i.e. of $\mathcal{O}(\alpha^2)$ in an $\mathcal{O}(\alpha)$ calculation. Moreover, this unitarity violation cannot be enhanced, because all Ward identities are exactly preserved. In this respect one should also mention that unstable particles should be excluded as external states and only the S-matrix connecting stable particle states needs to be unitary, as has already been pointed out by Veltman in the sixties [57]. Of course, before the described CMS can be viewed as a rigorous procedure to define a renormalized quantum field theory it has to be clarified whether one can directly prove unitarity order by order in this formalism. In particular, it is an interesting question whether one can construct modified cutting equations in the CMS.

(i) Complex renormalization – 't Hooft–Feynman gauge

The consistent introduction of complex masses in loop calculations necessitates the formulation of an appropriate renormalization prescription. To this end, we generalize the on-shell renormalization scheme formulated in Refs. [40, 44, 58] at the one-loop level in a straight-forward way. A generalization to higher orders should be possible, but this is beyond the scope of this paper.

Following the conventions of Ref. [44], the renormalized transverse (T) gauge-boson self-energies read

$$\begin{aligned}
\hat{\Sigma}_{\mathrm{T}}^{W}(k^2) &= \Sigma_{\mathrm{T}}^{W}(k^2) - \delta\mu_{\mathrm{W}}^2 + (k^2 - \mu_{\mathrm{W}}^2)\delta\mathcal{Z}_{W},\\
\hat{\Sigma}_{\mathrm{T}}^{ZZ}(k^2) &= \Sigma_{\mathrm{T}}^{ZZ}(k^2) - \delta\mu_{\mathrm{Z}}^2 + (k^2 - \mu_{\mathrm{Z}}^2)\delta\mathcal{Z}_{ZZ},\\
\hat{\Sigma}_{\mathrm{T}}^{AA}(k^2) &= \Sigma_{\mathrm{T}}^{AA}(k^2) + k^2\delta\mathcal{Z}_{AA},\\
\hat{\Sigma}_{\mathrm{T}}^{AZ}(k^2) &= \Sigma_{\mathrm{T}}^{AZ}(k^2) + k^2\frac{1}{2}\delta\mathcal{Z}_{AZ} + (k^2 - \mu_{\mathrm{Z}}^2)\frac{1}{2}\delta\mathcal{Z}_{ZA},
\end{aligned} \tag{4.3}$$

where A denotes the photon field, and the hat indicates renormalized self-energies. Compared to Ref. [44], the renormalized on-shell masses and mass counterterms are replaced by the renormalized complex masses μ_{W} and μ_{Z} everywhere, i.e. also within the self-energies. We denote the field renormalization constants in the CMS by calligraphic letters. The complex renormalized masses and mass counterterms result from a splitting of the real bare masses squared,[10]

$$M_{\mathrm{W},0}^2 = \mu_{\mathrm{W}}^2 + \delta\mu_{\mathrm{W}}^2, \qquad M_{\mathrm{Z},0}^2 = \mu_{\mathrm{Z}}^2 + \delta\mu_{\mathrm{Z}}^2, \tag{4.4}$$

---

[10] Similar ideas were proposed in Ref. [59].

where here and in the following bare quantities are indicated by a subscript 0. Similarly, splitting the bare fields in complex field renormalization constants and renormalized fields

$$\begin{aligned} W_0^{\pm} &= (1+\tfrac{1}{2}\delta\mathcal{Z}_W)W^{\pm}, \\ \begin{pmatrix} Z_0 \\ A_0 \end{pmatrix} &= \begin{pmatrix} 1+\frac{1}{2}\delta\mathcal{Z}_{ZZ} & \frac{1}{2}\delta\mathcal{Z}_{ZA} \\ \frac{1}{2}\delta\mathcal{Z}_{AZ} & 1+\frac{1}{2}\delta\mathcal{Z}_{AA} \end{pmatrix} \begin{pmatrix} Z \\ A \end{pmatrix}, \end{aligned} \tag{4.5}$$

implies that the bare and renormalized fields have different phases. Thus, for instance, the renormalized Z-boson field becomes complex, while the corresponding bare field is real. As a consequence, the renormalized Lagrangian, i.e. the Lagrangian in terms of renormalized fields without counterterms, is not hermitian, but the total Lagrangian (which is equal to the bare Lagrangian) of course is.

In order to fix the counterterms, we generalize the renormalization conditions of the complete on-shell scheme [44, 58] and require

$$\begin{aligned} \hat{\Sigma}_{\mathrm{T}}^{W}(\mu_{\mathrm{W}}^2) &= 0, \qquad \hat{\Sigma}_{\mathrm{T}}^{ZZ}(\mu_{\mathrm{Z}}^2) = 0, \\ \hat{\Sigma}_{\mathrm{T}}^{AZ}(0) &= 0, \qquad \hat{\Sigma}_{\mathrm{T}}^{AZ}(\mu_{\mathrm{Z}}^2) = 0, \\ \hat{\Sigma}_{\mathrm{T}}^{\prime W}(\mu_{\mathrm{W}}^2) &= 0, \qquad \hat{\Sigma}_{\mathrm{T}}^{\prime ZZ}(\mu_{\mathrm{Z}}^2) = 0, \qquad \hat{\Sigma}_{\mathrm{T}}^{\prime AA}(0) = 0, \end{aligned} \tag{4.6}$$

where the prime denotes differentiation with respect to the argument. The conditions (4.6), in particular the first two, fix the mass counterterms in such a way that the renormalized mass is equal to the location of the propagator pole in the complex plane. This is a gauge-invariant quantity, as pointed out and shown in Refs. [30, 60]. The last five renormalization conditions in (4.6) fix the field renormalization constants. Note that the field renormalization constants of the gauge-boson fields exactly drop out in all S-matrix elements that do not involve external gauge bosons, but allow to render all vertex functions finite. This generally holds for all field renormalization constants of unstable particles as long as one does not consider S-matrix elements for external unstable particles. Unlike in Refs. [44, 58], we did not take real parts in the renormalization conditions (4.6), and thus not only the mass renormalization constants but also the field renormalization constants become in general complex. This ansatz is supported by the fact that the imaginary part of one-loop scattering amplitudes involving unstable external particles becomes gauge dependent if the imaginary parts of the counterterms are not included [61]. For the definition of the renormalized mass and width this scheme is exactly the one described in Appendix D of Ref. [29]. We stress the fact that the renormalization constant $\delta\mathcal{Z}_W$ applies to both the W^+ and W^- field, i.e. the imaginary part of $\delta\mathcal{Z}_W$ is fixed by the renormalization condition and does not change sign when going from the W^+ to the W^- field.

The renormalization conditions (4.6) have the solutions

$$\begin{aligned} \delta\mu_{\mathrm{W}}^2 &= \Sigma_{\mathrm{T}}^{W}(\mu_{\mathrm{W}}^2), \qquad \delta\mu_{\mathrm{Z}}^2 = \Sigma_{\mathrm{T}}^{ZZ}(\mu_{\mathrm{Z}}^2), \\ \delta\mathcal{Z}_{ZA} &= \frac{2}{\mu_{\mathrm{Z}}^2}\Sigma_{\mathrm{T}}^{AZ}(0), \qquad \delta\mathcal{Z}_{AZ} = -\frac{2}{\mu_{\mathrm{Z}}^2}\Sigma_{\mathrm{T}}^{AZ}(\mu_{\mathrm{Z}}^2), \\ \delta\mathcal{Z}_W &= -\Sigma_{\mathrm{T}}^{\prime W}(\mu_{\mathrm{W}}^2), \qquad \delta\mathcal{Z}_{ZZ} = -\Sigma_{\mathrm{T}}^{\prime ZZ}(\mu_{\mathrm{Z}}^2), \qquad \delta\mathcal{Z}_{AA} = -\Sigma_{\mathrm{T}}^{\prime AA}(0), \end{aligned} \tag{4.7}$$

which require to calculate the self-energies for complex squared momenta. This would demand an analytic continuation of the 2-point functions entering the self-energies in the momentum variable to the unphysical Riemann sheet. In order to avoid this complication, we perform appropriate expansions about real arguments,

$$\begin{aligned}
\Sigma_{\mathrm{T}}^{W}(\mu_{\mathrm{W}}^2) &= \Sigma_{\mathrm{T}}^{W}(M_{\mathrm{W}}^2) + (\mu_{\mathrm{W}}^2 - M_{\mathrm{W}}^2)\Sigma_{\mathrm{T}}^{\prime W}(M_{\mathrm{W}}^2) + \mathcal{O}(\alpha^3),\\
\Sigma_{\mathrm{T}}^{ZZ}(\mu_{\mathrm{Z}}^2) &= \Sigma_{\mathrm{T}}^{ZZ}(M_{\mathrm{Z}}^2) + (\mu_{\mathrm{Z}}^2 - M_{\mathrm{Z}}^2)\Sigma_{\mathrm{T}}^{\prime ZZ}(M_{\mathrm{Z}}^2) + \mathcal{O}(\alpha^3),\\
\frac{1}{\mu_{\mathrm{Z}}^2}\Sigma_{\mathrm{T}}^{AZ}(\mu_{\mathrm{Z}}^2) &= \frac{1}{\mu_{\mathrm{Z}}^2}\Sigma_{\mathrm{T}}^{AZ}(0) + \frac{1}{M_{\mathrm{Z}}^2}\Sigma_{\mathrm{T}}^{AZ}(M_{\mathrm{Z}}^2) - \frac{1}{M_{\mathrm{Z}}^2}\Sigma_{\mathrm{T}}^{AZ}(0) + \mathcal{O}(\alpha^2),
\end{aligned} \tag{4.8}$$

as done similarly in Appendix D of Ref. [29]. The $\mathcal{O}(\alpha^2)$ and $\mathcal{O}(\alpha^3)$ contributions result from products of terms $\Sigma^W = \mathcal{O}(\alpha)$, $\Sigma^{ZZ} = \mathcal{O}(\alpha)$, $\Sigma^{AZ} = \mathcal{O}(\alpha)$, $(\mu_{\mathrm{W}}^2 - M_{\mathrm{W}}^2) = \mathcal{O}(\alpha)$, and $(\mu_{\mathrm{Z}}^2 - M_{\mathrm{Z}}^2) = \mathcal{O}(\alpha)$ and are UV-finite by construction at the one-loop level.

By neglecting these $\mathcal{O}(\alpha^2)$ and $\mathcal{O}(\alpha^3)$ terms, we can replace (4.7) by

$$\begin{aligned}
\delta\mu_{\mathrm{W}}^2 &= \Sigma_{\mathrm{T}}^{W}(M_{\mathrm{W}}^2) + (\mu_{\mathrm{W}}^2 - M_{\mathrm{W}}^2)\Sigma_{\mathrm{T}}^{\prime W}(M_{\mathrm{W}}^2),\\
\delta\mu_{\mathrm{Z}}^2 &= \Sigma_{\mathrm{T}}^{ZZ}(M_{\mathrm{Z}}^2) + (\mu_{\mathrm{Z}}^2 - M_{\mathrm{Z}}^2)\Sigma_{\mathrm{T}}^{\prime ZZ}(M_{\mathrm{Z}}^2),
\end{aligned} \tag{4.9}$$

and

$$\begin{aligned}
\delta\mathcal{Z}_{ZA} &= \frac{2}{\mu_{\mathrm{Z}}^2}\Sigma_{\mathrm{T}}^{AZ}(0), \qquad \delta\mathcal{Z}_{AZ} = -\frac{2}{M_{\mathrm{Z}}^2}\Sigma_{\mathrm{T}}^{AZ}(M_{\mathrm{Z}}^2) + \left(\frac{\mu_{\mathrm{Z}}^2}{M_{\mathrm{Z}}^2} - 1\right)\delta\mathcal{Z}_{ZA},\\
\delta\mathcal{Z}_{W} &= -\Sigma_{\mathrm{T}}^{\prime W}(M_{\mathrm{W}}^2), \qquad \delta\mathcal{Z}_{ZZ} = -\Sigma_{\mathrm{T}}^{\prime ZZ}(M_{\mathrm{Z}}^2).
\end{aligned} \tag{4.10}$$

We use these counterterms in our calculation. While the missing $\mathcal{O}(\alpha^2)$ terms in $\delta\mathcal{Z}_{AZ}$ do not influence our results, since the gauge-boson field renormalization constants drop out as there is no external gauge boson in the process under consideration, the missing (finite) $\mathcal{O}(\alpha^3)$ terms in the mass counterterms are beyond the accuracy of our calculation. The counterterms (4.9) involve only functions that appear also in the usual on-shell renormalization scheme [44, 58], but consistently take into account the imaginary parts.

When inserting the counterterms (4.9) and (4.10) into (4.3), we can rewrite the renormalized self-energies in the CMS as

$$\begin{aligned}
\hat{\Sigma}_{\mathrm{T}}^{W}(k^2) &= \Sigma_{\mathrm{T}}^{W}(k^2) - \delta M_{\mathrm{W}}^2 + (k^2 - M_{\mathrm{W}}^2)\delta Z_{W},\\
\hat{\Sigma}_{\mathrm{T}}^{ZZ}(k^2) &= \Sigma_{\mathrm{T}}^{ZZ}(k^2) - \delta M_{\mathrm{Z}}^2 + (k^2 - M_{\mathrm{Z}}^2)\delta Z_{ZZ},\\
\hat{\Sigma}_{\mathrm{T}}^{AA}(k^2) &= \Sigma_{\mathrm{T}}^{AA}(k^2) + k^2\delta Z_{AA},\\
\hat{\Sigma}_{\mathrm{T}}^{AZ}(k^2) &= \Sigma_{\mathrm{T}}^{AZ}(k^2) + k^2\frac{1}{2}\delta Z_{AZ} + (k^2 - M_{\mathrm{Z}}^2)\frac{1}{2}\delta Z_{ZA}
\end{aligned} \tag{4.11}$$

with

$$\begin{aligned}
\delta M_{\mathrm{W}}^2 &= \Sigma_{\mathrm{T}}^{W}(M_{\mathrm{W}}^2), \qquad \delta M_{\mathrm{Z}}^2 = \Sigma_{\mathrm{T}}^{ZZ}(M_{\mathrm{Z}}^2),\\
\delta Z_{ZA} &= \frac{2}{M_{\mathrm{Z}}^2}\Sigma_{\mathrm{T}}^{AZ}(0), \qquad \delta Z_{AZ} = -\frac{2}{M_{\mathrm{Z}}^2}\Sigma_{\mathrm{T}}^{AZ}(M_{\mathrm{Z}}^2),\\
\delta Z_{W} &= -\Sigma_{\mathrm{T}}^{\prime W}(M_{\mathrm{W}}^2), \qquad \delta Z_{ZZ} = -\Sigma_{\mathrm{T}}^{\prime ZZ}(M_{\mathrm{Z}}^2), \qquad \delta Z_{AA} = -\Sigma_{\mathrm{T}}^{\prime AA}(0).
\end{aligned} \tag{4.12}$$

Equations (4.11) with (4.12) have exactly the form of the renormalized self-energies in the usual on-shell scheme, but without taking the real part of the counterterms. While in the on-shell scheme the self-energies are calculated in terms of the real renormalized masses M_{Z}^2 and M_{W}^2, in (4.11) and (4.12) the self-energies are to be calculated in terms of the complex masses μ_{Z}^2 and μ_{W}^2, although with real squared momenta. Note that this difference between usual on-shell and complex renormalization also changes the form of the IR divergence appearing in the W-field renormalization constant δZ_W. In the former scheme, it appears as logarithm $\ln m_\gamma$ of an infinitesimally small photon mass (or as the related $1/(4-D)$ pole in dimensional regularization); in the latter, the W width regularizes the singularity via $\ln \Gamma_{\mathrm{W}}$.

Owing to its definition (4.1), the renormalization of the complex weak mixing angle is determined by

$$\frac{\delta s_{\mathrm{w}}}{s_{\mathrm{w}}} = -\frac{c_{\mathrm{w}}^2}{s_{\mathrm{w}}^2}\frac{\delta c_{\mathrm{w}}}{c_{\mathrm{w}}} = -\frac{c_{\mathrm{w}}^2}{2s_{\mathrm{w}}^2}\left(\frac{\delta\mu_{\mathrm{W}}^2}{\mu_{\mathrm{W}}^2} - \frac{\delta\mu_{\mathrm{Z}}^2}{\mu_{\mathrm{Z}}^2}\right). \tag{4.13}$$

The electric charge is fixed in the on-shell scheme by requiring that there are no higher-order corrections to the $ee\gamma$ vertex in the Thomson limit. In the CMS this condition reads

$$\frac{\delta e}{e} = \frac{1}{2}\Sigma'^{AA}(0) - \frac{s_{\mathrm{w}}}{c_{\mathrm{w}}}\frac{\Sigma_{\mathrm{T}}^{AZ}(0)}{\mu_{\mathrm{Z}}^2}. \tag{4.14}$$

Because of the presence of the complex masses in the loop integrals, the charge renormalization constant and thus the renormalized charge become complex. Since the imaginary part of the bare charge vanishes, the imaginary part of the charge renormalization constant is directly fixed by the imaginary part of self-energies. In a one-loop calculation, the imaginary part of the renormalized charge drops out in the corrections to the absolute square of the matrix element, because the charge factorizes from the lowest-order matrix element. Starting from the two-loop level, the imaginary part has to be taken into account.

For a correct description of the resonances at the $\mathcal{O}(\alpha)$ level, we need the width including $\mathcal{O}(\alpha)$ corrections. The width is defined via (4.9). Using $\delta\mu_{\mathrm{W}}^2 = M_{\mathrm{W},0}^2 - \mu_{\mathrm{W}}^2$ and taking the imaginary part of (4.9) yields

$$M_{\mathrm{W}}\Gamma_{\mathrm{W}} = \mathrm{Im}\{\Sigma_{\mathrm{T}}^{W}(M_{\mathrm{W}}^2)\} - M_{\mathrm{W}}\Gamma_{\mathrm{W}}\,\mathrm{Re}\{\Sigma_{\mathrm{T}}'^{W}(M_{\mathrm{W}}^2)\} + \mathcal{O}(\alpha^3), \tag{4.15}$$

which can be iteratively solved for Γ_{W}. In $\mathcal{O}(\alpha^2)$, i.e. including first-order corrections to the width, the result is equivalent to the one obtained in the usual on-shell scheme. To this order the imaginary part of the self-energy is required in two-loop accuracy, but it can be more easily obtained by calculating the one-loop corrections to the decay processes $\mathrm{W} \to \bar{f}f'$ [29]. In our numerical calculation, we calculate the width from the decay processes including $\mathcal{O}(\alpha)$ corrections [12].

In our calculation we consider external fermions only in the massless limit, in which these fermions are stable. Therefore, the corresponding on-shell self-energies do not involve any absorptive parts. Nevertheless they become complex via the complex renormalized weak mixing angle and the complex gauge-boson masses, and thus the field renormalization constants $\delta\mathcal{Z}_{f,\sigma}$ of the fermion fields f^σ, defined by

$$f_0^\sigma = (1 + \tfrac{1}{2}\delta\mathcal{Z}_{f,\sigma})f^\sigma, \qquad \sigma = \mathrm{R}, \mathrm{L}, \tag{4.16}$$

become complex. As in the case of $\delta\mathcal{Z}_W$, also these complex field renormalization constants apply both for fermions and antifermions, i.e. fields and antifields are not connected by complex conjugation anymore. Explicitly the $\delta\mathcal{Z}_{f,\sigma}$ are given by

$$\delta\mathcal{Z}_{f,\sigma} = -\Sigma^{f,\sigma}(m_f^2) - m_f^2\left[\Sigma'^{f,\mathrm{R}}(m_f^2) + \Sigma'^{f,\mathrm{L}}(m_f^2) + 2\Sigma'^{f,\mathrm{S}}(m_f^2)\right], \tag{4.17}$$

where $\sigma = \mathrm{R}, \mathrm{L}$ refers to the right- and left-handed components of the fermion self-energy $\Sigma^f(p)$ following the conventions of Ref. [44]. Note that again no real part was taken in this relation in contrast to the usual on-shell renormalization. In contrast to $\delta\mathcal{Z}_W$, there are soft IR divergences in the field renormalization constants $\delta\mathcal{Z}_f$ that are not regularized by finite widths but by the usual IR regulators such as m_γ.

In the massless limit, the fermion-mass renormalization constant δm_f tends to zero, and the quark-mixing matrix, if assumed to be different from the unit matrix, need not be renormalized.

(ii) Complex renormalization for the Higgs sector and the top quark

Since the top-quark and the Higgs boson do not appear in the lowest-order matrix elements for the processes under consideration, the corresponding mass and field counterterms are not needed in our calculation. Nevertheless, for completeness we define the corresponding renormalization constants here.

For the Higgs boson the whole renormalization proceeds along the same lines as for the gauge bosons above. The complex Higgs mass squared

$$\mu_\mathrm{H}^2 = M_\mathrm{H}^2 - \mathrm{i}M_\mathrm{H}\Gamma_\mathrm{H} = M_{\mathrm{H},0}^2 - \delta\mu_\mathrm{H}^2 \tag{4.18}$$

is defined as the location of the zero in k^2 in the renormalized Higgs-boson self-energy

$$\hat{\Sigma}^H(k^2) = \Sigma^H(k^2) - \delta\mu_\mathrm{H}^2 + (k^2 - \mu_\mathrm{H}^2)\delta\mathcal{Z}_H. \tag{4.19}$$

Fixing the Higgs field renormalization as above, we obtain the renormalization constants

$$\begin{aligned}\delta\mu_\mathrm{H}^2 &= \Sigma^H(\mu_\mathrm{H}^2) = \Sigma^H(M_\mathrm{H}^2) + (\mu_\mathrm{H}^2 - M_\mathrm{H}^2)\Sigma'^H(M_\mathrm{H}^2) + \mathcal{O}(\alpha^3),\\ \delta\mathcal{Z}_H &= -\Sigma'^H(\mu_\mathrm{H}^2) = -\Sigma'^H(M_\mathrm{H}^2) + \mathcal{O}(\alpha^2),\end{aligned} \tag{4.20}$$

so that the renormalized Higgs-boson self-energy up to finite $\mathcal{O}(\alpha^2)$ terms can be written as

$$\hat{\Sigma}^H(k^2) = \Sigma^H(k^2) - \delta M_\mathrm{H}^2 + (k^2 - M_\mathrm{H}^2)\delta Z_H. \tag{4.21}$$

with

$$\delta M_\mathrm{H}^2 = \Sigma^H(M_\mathrm{H}^2), \qquad \delta Z_H = -\Sigma'^H(M_\mathrm{H}^2). \tag{4.22}$$

For the top quark the renormalization procedure works analogously, i.e. we introduce the complex mass via

$$\mu_\mathrm{t}^2 = m_\mathrm{t}^2 - \mathrm{i}m_\mathrm{t}\Gamma_\mathrm{t}, \qquad m_{\mathrm{t},0} = \mu_\mathrm{t} + \delta\mu_\mathrm{t}. \tag{4.23}$$

The renormalized top-quark self-energy reads

$$\begin{aligned}\hat{\Sigma}^t(p) = {} & \left[\Sigma^{t,\mathrm{R}}(p^2) + \delta\mathcal{Z}_{t,\mathrm{R}}\right] \not{p}\omega_+ + \left[\Sigma^{t,\mathrm{L}}(p^2) + \delta\mathcal{Z}_{t,\mathrm{L}}\right] \not{p}\omega_- \\ & + \mu_\mathrm{t}\left[\Sigma^{t,\mathrm{S}}(p^2) - \frac{1}{2}(\delta\mathcal{Z}_{t,\mathrm{R}} + \delta\mathcal{Z}_{t,\mathrm{L}}) - \frac{\delta\mu_\mathrm{t}}{\mu_\mathrm{t}}\right] \end{aligned} \qquad (4.24)$$

in the conventions of Ref. [44]. Generalizing the on-shell renormalization conditions to complex renormalization as

$$\begin{aligned}\delta\mu_\mathrm{t} &= \frac{\mu_\mathrm{t}}{2}\left[\Sigma^{t,\mathrm{R}}(\mu_\mathrm{t}^2) + \Sigma^{t,\mathrm{L}}(\mu_\mathrm{t}^2) + 2\Sigma^{t,\mathrm{S}}(\mu_\mathrm{t}^2)\right], \\ \delta\mathcal{Z}_{t,\sigma} &= -\Sigma^{t,\sigma}(\mu_\mathrm{t}^2) - \mu_\mathrm{t}^2\left[\Sigma'^{t,\mathrm{R}}(\mu_\mathrm{t}^2) + \Sigma'^{t,\mathrm{L}}(\mu_\mathrm{t}^2) + 2\Sigma'^{t,\mathrm{S}}(\mu_\mathrm{t}^2)\right], \qquad \sigma = \mathrm{R},\mathrm{L}, \end{aligned} \qquad (4.25)$$

fixes μ_t^2 as the location of the complex pole in p^2 in the top propagator. Expanding the self-energies appearing in the renormalization constants (4.25) about m_t^2 and neglecting (UV-finite) terms of order $\mathcal{O}(\alpha^2)$, the renormalized top-quark self-energy can be expressed as

$$\begin{aligned}\hat{\Sigma}^t(p) = {} & \left[\Sigma^{t,\mathrm{R}}(p^2) + \delta Z_{t,\mathrm{R}}\right] \not{p}\omega_+ + \left[\Sigma^{t,\mathrm{L}}(p^2) + \delta Z_{t,\mathrm{L}}\right] \not{p}\omega_- \\ & + \mu_\mathrm{t}\left[\Sigma^{t,\mathrm{S}}(p^2) - \frac{1}{2}(\delta Z_{t,\mathrm{R}} + \delta Z_{t,\mathrm{L}}) - \frac{\delta m_\mathrm{t}}{m_\mathrm{t}}\right] \end{aligned} \qquad (4.26)$$

with

$$\begin{aligned}\delta m_\mathrm{t} &= \frac{m_\mathrm{t}}{2}\left[\Sigma^{t,\mathrm{R}}(m_\mathrm{t}^2) + \Sigma^{t,\mathrm{L}}(m_\mathrm{t}^2) + 2\Sigma^{t,\mathrm{S}}(m_\mathrm{t}^2)\right], \\ \delta Z_{t,\sigma} &= -\Sigma^{t,\sigma}(m_\mathrm{t}^2) - m_\mathrm{t}^2\left[\Sigma'^{t,\mathrm{R}}(m_\mathrm{t}^2) + \Sigma'^{t,\mathrm{L}}(m_\mathrm{t}^2) + 2\Sigma'^{t,\mathrm{S}}(m_\mathrm{t}^2)\right], \qquad \sigma = \mathrm{R},\mathrm{L}. \end{aligned} \qquad (4.27)$$

Finally, we complete the renormalization in the scalar sector. The field renormalization for the would-be Goldstone bosons can simply be set equal to the Higgs field renormalization constant $\delta\mathcal{Z}_H$, which is sufficient to cancel all UV divergences in vertex functions. The tadpole counterterm δt is again introduced to cancel explicitly occurring tadpole graphs, i.e. we set $\delta t = -t$, where $\Gamma^H = \mathrm{i}t$ is the one-point vertex function for the Higgs boson at one loop. The gauge-fixing term need not be renormalized.

In summary, in the CMS the usual renormalization conditions of the on-shell scheme can be used, but without taking any real parts. All parameters, in particular also the renormalization points, become complex. The calculation of self-energies with complex momentum arguments can be avoided by expanding these about real values. Performing these expansions appropriately and neglecting (UV-finite) higher-order terms, the renormalized self-energies are obtained just as in the usual on-shell scheme with renormalization constants determined for real momenta. However, all the mass arguments are complex and no real parts must be taken.

(iii) Complex renormalization – background-field gauge

Using the background-field method, the gauge-boson field renormalization constants can be determined in terms of the parameter renormalization in such a way that Ward identities possess the same form before and after renormalization [40]. Real parameters have to be substituted by the corresponding complex parameters everywhere when the complex renormalization is employed. The complex parameter renormalization is fixed as above in (4.9), (4.13), (4.14), (4.20), and (4.25). Note that $\Sigma_{\mathrm{T}}^{AZ}(0)$ vanishes in the background-field gauge as a consequence of the background-field gauge invariance of the effective action, which in particular simplifies the charge renormalization constant (4.14).

Since the gauge-boson field renormalization constants drop out in the S-matrix elements without external gauge-boson fields, we can alternatively also use the definitions in (4.10) in the calculation.

(iv) Loop integrals with complex masses

The consistent use of complex gauge-boson masses requires to use these also in the loop integrals. Thus, we need one-loop integrals with complex internal masses. The IR-singular integrals can be found in Ref. [49]. Concerning the non-IR singular cases, we have analytically continued the results of Ref. [48] for the 2-point and 3-point functions[11], and the relevant results of Ref. [50] for the 4-point functions. We have checked all these results by independent direct calculation of the Feynman-parameter integrals. These results will be published elsewhere.

5 Numerical results

5.1 Input parameters and setup

The numerical results are based on the same set of input parameters as in Ref. [37]:

$$
\begin{array}{lll}
G_\mu = 1.16637\times 10^{-5}\,\mathrm{GeV}^{-2}, & \alpha(0) = 1/137.03599911, & \alpha_{\mathrm{s}} = 0.1187, \\
M_{\mathrm{W}} = 80.425\,\mathrm{GeV}, & M_{\mathrm{Z}} = 91.1876\,\mathrm{GeV}, & \Gamma_{\mathrm{Z}} = 2.4952\,\mathrm{GeV}, \\
M_{\mathrm{H}} = 115\,\mathrm{GeV}, & & \\
m_{\mathrm{e}} = 0.51099892\,\mathrm{MeV}, & m_\mu = 105.658369\,\mathrm{MeV}, & m_\tau = 1.77699\,\mathrm{GeV}, \\
m_{\mathrm{u}} = 66\,\mathrm{MeV}, & m_{\mathrm{c}} = 1.2\,\mathrm{GeV}, & m_{\mathrm{t}} = 178\,\mathrm{GeV}, \\
m_{\mathrm{d}} = 66\,\mathrm{MeV}, & m_{\mathrm{s}} = 150\,\mathrm{MeV}, & m_{\mathrm{b}} = 4.3\,\mathrm{GeV},
\end{array} \qquad (5.1)
$$

which essentially follows Ref. [62]. For the top-quark mass m_{t} we have taken the more recent value of Ref. [63]. The masses of the light quarks are adjusted to reproduce the hadronic contribution to the photonic vacuum polarization of Ref. [64]. Since we parametrize the lowest-order cross section with the Fermi constant G_μ (G_μ scheme), i.e. we derive the electromagnetic coupling α according to $\alpha_{G_\mu} = \sqrt{2}G_\mu M_{\mathrm{W}}^2(1-M_{\mathrm{W}}^2/M_{\mathrm{Z}}^2)/\pi$, the results are practically independent of the masses of the light quarks. Moreover, this procedure absorbs the corrections proportional to $m_{\mathrm{t}}^2/M_{\mathrm{W}}^2$ in the fermion–W-boson couplings and the running of $\alpha(Q^2)$ from $Q^2=0$ to the electroweak scale. In the relative radiative corrections, we use, however, $\alpha(0)$ as coupling parameter, which is the correct effective coupling for real photon emission.

---

[11] Note that the result of Ref. [48] for the scalar two-point function is not valid in general for complex masses. In this case an extra η function has to be added. The same comment applies to the results for the 2-point tensor integrals in Ref. [47].

QCD corrections are treated in the "naive" approach of multiplying cross sections and partial decay rates by factors $(1+\alpha_{\mathrm{s}}/\pi)$ per hadronically decaying W boson. The W-boson width Γ_{W} is calculated from the above input including electroweak $\mathcal{O}(\alpha)$ and QCD corrections, yielding

$$\Gamma_{\mathrm{W}} = 2.09269848\ldots\ \mathrm{GeV}. \tag{5.2}$$

This procedure ensures that the effective branching ratios for the leptonic, semileptonic, and hadronic W decays, which result from the integration over the decay fermions, add up to 1. The value for the Z decay width Γ_{Z}, which is needed because of the Z resonance in the ISR convolution below the W-pair threshold, is taken from experiment [62]. All other particles, including the top quark and the Higgs boson, are taken as stable.

The setup differs from the one of Ref. [37] only in the event selection. In contrast to Ref. [37], where no phase-space cuts were applied at all, we now impose selection cuts in conjunction with a photon recombination procedure. In detail, we adopt the same procedure as in Ref. [21]:

1. All bremsstrahlung photons within a cone of 5 degrees around the beams are treated as invisible, i.e. their momenta are disregarded when calculating angles, energies, and invariant masses.

2. Next, the invariant masses $M_{f\gamma}$ of the photon with each of the charged final-state fermions are calculated. If the smallest $M_{f\gamma}$ is smaller than $M_{\mathrm{rec}} = 25\,\mathrm{GeV}$ or if the energy of the photon is smaller than $1\,\mathrm{GeV}$, the photon is combined with the charged final-state fermion that leads to the smallest $M_{f\gamma}$, i.e. the momenta of the photon and the fermion are added and associated with the momentum of the fermion, and the photon is discarded[12].

3. Finally, all events are discarded in which one of the charged final-state fermions is within a cone of 10 degrees around the beams (after a possible recombination with a photon). No other cuts are applied.

The presented results have been obtained with 10^8 events, using the subtraction method. All but the lowest-order predictions include naive QCD corrections and improvements by ISR beyond $\mathcal{O}(\alpha)$, as described in Ref. [21].

5.2 Results for differential cross sections

In this section we consider results for various distributions at $\sqrt{s} = 200\,\mathrm{GeV}$ and $\sqrt{s} = 500\,\mathrm{GeV}$ in the setup described above. For reference, in Table 1 we provide the corresponding integrated cross sections for the final states $\nu_\tau\tau^+\mu^-\bar{\nu}_\mu$, $\mathrm{u}\bar{\mathrm{d}}\mu^-\bar{\nu}_\mu$, and $\mathrm{u}\bar{\mathrm{d}}\mathrm{s}\bar{\mathrm{c}}$ in various approximations for different CM energies $\sqrt{s}$. The numbers in parentheses represent the uncertainties from Monte Carlo integration in the last digits of the predictions. Columns two and three in each table contain the two versions of the lowest-order cross section for the full $\mathrm{e}^+\mathrm{e}^- \to 4f$ processes corresponding to the different treatments of finite-width effects as provided by the "fixed-width scheme" (FW) and the complex-mass scheme (CMS). In the FW scheme the finite constant width, and thus the complex mass,

---

[12] Except for the $1\,\mathrm{GeV}$ cut, the described cut and recombination procedure coincides with the one used in the first two papers of Ref. [20].

$\sqrt{s}$/GeV	Born(FW)	Born(CMS)	DPA	ee4f
$\mathrm{e}^+\mathrm{e}^- \to \nu_\tau\tau^+\mu^-\bar{\nu}_\mu$				
200	211.52(3)	211.40(3) [−0.06%]	191.98(3) [−9.24(1)%]	191.18(3) [−9.57(1)%]
500	62.17(1)	62.14(1) [−0.05%]	65.48(2) [+5.32(1)%]	64.96(2) [+4.54(1)%]
$\mathrm{e}^+\mathrm{e}^- \to \mathrm{u\bar{d}}\mu^-\bar{\nu}_\mu$				
200	628.72(9)	628.37(9) [−0.06%]	591.55(9) [−5.91(1)%]	589.11(10) [−6.25(1)%]
500	180.83(4)	180.73(4) [−0.06%]	197.87(5) [+9.42(1)%]	196.20(5) [+8.56(2)%]
$\mathrm{e}^+\mathrm{e}^- \to \mathrm{u\bar{d}s\bar{c}}$				
200	1868.9(3)	1867.8(3) [−0.06%]	1822.6(3) [−2.48(1)%]	1815.3(3) [−2.81(1)%]
500	526.1(1)	525.8(1) [−0.06%]	597.1(2) [+13.50(2)%]	591.9(2) [+12.58(2)%]

Table 1: Integrated cross sections in fb for $\mathrm{e}^+\mathrm{e}^- \to \nu_\tau\tau^+\mu^-\bar{\nu}_\mu$, $\mathrm{u\bar{d}}\mu^-\bar{\nu}_\mu$, and $\mathrm{u\bar{d}s\bar{c}}$ in Born approximation (in the fixed-width and complex-mass schemes), in DPA, and using the full $\mathcal{O}(\alpha)$ correction (ee4f); all but the Born cross sections include higher-order ISR and (if relevant) naive QCD corrections.

is only inserted into the propagators. The relative difference $\sigma_{\mathrm{Born}}(\mathrm{CMS})/\sigma_{\mathrm{Born}}(\mathrm{FW}) - 1$ of the schemes in lowest order is given by the numbers in square brackets in the third columns. We have not given an error on this difference, because the two Born predictions are strongly correlated. The last-but-one columns show the DPA of RacoonWW which also includes some effects beyond DPA, as described in Ref. [21]; the numbers in square brackets are defined as $\delta_{\mathrm{DPA}} = \sigma_{\mathrm{DPA}}/\sigma_{\mathrm{Born}}(\mathrm{FW}) - 1$. We normalize σ_{DPA} to $\sigma_{\mathrm{Born}}(\mathrm{FW})$, because the lowest-order part of the DPA is per default evaluated in the FW scheme in RacoonWW. Finally, the last columns (ee4f) contain the full one-loop corrections to $\mathrm{e}^+\mathrm{e}^- \to 4f$; the numbers in square brackets are defined as $\delta_{\mathrm{ee4f}} = \sigma_{\mathrm{ee4f}}/\sigma_{\mathrm{Born}}(\mathrm{CMS}) - 1$. Here we normalize to $\sigma_{\mathrm{Born}}(\mathrm{CMS})$, because the full $\mathrm{e}^+\mathrm{e}^- \to 4f$ calculation is consistently performed in the CMS. For $\sqrt{s} = 500\,\mathrm{GeV}$ the difference between the predictions based on the full $\mathcal{O}(\alpha)$ corrections and on the DPA slightly increases by $\sim 0.1\%$ with respect to the results without cuts [37]. This tendency can be attributed to the fact that at high energies the cross section is dominated by forward-scattered nearly on-shell W-bosons. Such events are discarded by the cuts thus reducing the contribution of on-shell W-boson pairs and worsening the quality of the DPA.

For the differential distributions, we focus on the semileptonic process $\mathrm{e}^+\mathrm{e}^- \to \mathrm{u\bar{d}}\mu^-\bar{\nu}_\mu$ in the following. The respective results for the final states $\nu_\tau\tau^+\mu^-\bar{\nu}_\mu$ and $\mathrm{u\bar{d}s\bar{c}}$ look similar, up to an offset resulting from the QCD corrections; in particular, the difference between the DPA and the full $\mathcal{O}(\alpha)$ calculation are almost identical. We always display the lowest-order prediction (Born) and the result of the full one-loop calculation (ee4f) in the upper row of each figure. The relative corrections (in per cent) in the DPA approach (DPA), $\delta_{\mathrm{DPA}} = \mathrm{d}\sigma_{\mathrm{DPA}}/\mathrm{d}\sigma_{\mathrm{Born}}(\mathrm{FW}) - 1$, and in the full one-loop calculation (ee4f), $\delta_{\mathrm{ee4f}} = \mathrm{d}\sigma_{\mathrm{ee4f}}/\mathrm{d}\sigma_{\mathrm{Born}}(\mathrm{CMS}) - 1$, are shown in the lower rows of the figures. These additionally include an inset depicting the relative difference between the full one-loop and the DPA calculation with respect to the DPA calculation, $\Delta = \mathrm{d}\sigma_{\mathrm{ee4f}}/\mathrm{d}\sigma_{\mathrm{DPA}} - 1$. We define all angles in the laboratory system, which is the CM system of the initial state. The momenta of the W^+ and W^- bosons are defined as

$$k_+ = k_1 + k_2, \qquad k_- = k_3 + k_4, \tag{5.3}$$

respectively, after a possible photon recombination. From these momenta the invariant masses of the virtual W bosons and their angles are calculated.

The invariant-mass distributions for the W^+ and W^- bosons are shown in Figures 10 and 11. From the plots for the relative corrections, it can be seen that the full one-loop corrections are smaller than the DPA corrections for invariant masses bigger than M_{W} and vice versa for invariant masses smaller than M_{W}. If neglected, this effect will give rise to a small shift in the direct reconstruction of the W-boson mass. The distribution in the cosine of the W^+ production angle θ_{W^+} is shown in Figure 12. While at LEP energies there is hardly any distortion of the shape induced by corrections beyond DPA, at 500 GeV the difference of the corrections in DPA and the complete $\mathcal{O}(\alpha)$ corrections rises from -1% to about -2.5% with increasing scattering angle. Note that such a distortion of the shape of the angular distribution can be a signal for anomalous triple gauge-boson couplings. The angular dependence of Δ is even more pronounced in the distribution in the decay angle $\theta_{\mathrm{W}^-\mu^-}$ presented in Figure 13. Note, however, that as a general feature the cross section is smallest where the corrections beyond DPA are largest. The distribution in the energy E_{μ^-} of the muon can be found in Figure 14. Again, for $\sqrt{s} = 200\,\mathrm{GeV}$ the corrections beyond DPA hardly depend on the muon energy in the interval $20\,\mathrm{GeV} \lesssim E_\mu \lesssim 80\,\mathrm{GeV}$, where two resonant W bosons are kinematically possible. Outside this interval, the DPA runs out of control, and the difference to the full calculation becomes big; but there the cross section is very small.

Finally, we consider the distributions in azimuthal angles that were also discussed in Ref. [21] including corrections in DPA. In Figure 15 we show the distributions in the azimuthal decay angle ϕ_{W^+} of the W^+ boson, i.e. the angle between the decay plane of the W^+ and the plane of W-pair production,

$$\begin{aligned} \cos\phi_{\mathrm{W}^+} &= \frac{(\mathbf{k}_+ \times \mathbf{p}_+)(\mathbf{k}_+ \times \mathbf{k}_1)}{|\mathbf{k}_+ \times \mathbf{p}_+||\mathbf{k}_+ \times \mathbf{k}_1|}, \\ \mathrm{sgn}(\sin\phi_{\mathrm{W}^+}) &= \mathrm{sgn}\left\{\mathbf{k}_+ \cdot [(\mathbf{k}_+ \times \mathbf{p}_+) \times (\mathbf{k}_+ \times \mathbf{k}_1)]\right\}. \end{aligned} \tag{5.4}$$

Here, in particular at 200 GeV the difference between DPA and the full $\mathcal{O}(\alpha)$ corrections is approximately proportional to $\sin\phi_{\mathrm{W}^+}$ plus some constant offset. In the DPA, it can be deduced from Appendix A of Ref. [18], that the contributions of the imaginary parts of the one-loop coefficient functions always involve a factor $\sin\phi_{\mathrm{W}^+}$ or a factor $\sin\phi_{\mathrm{W}^-}$ together

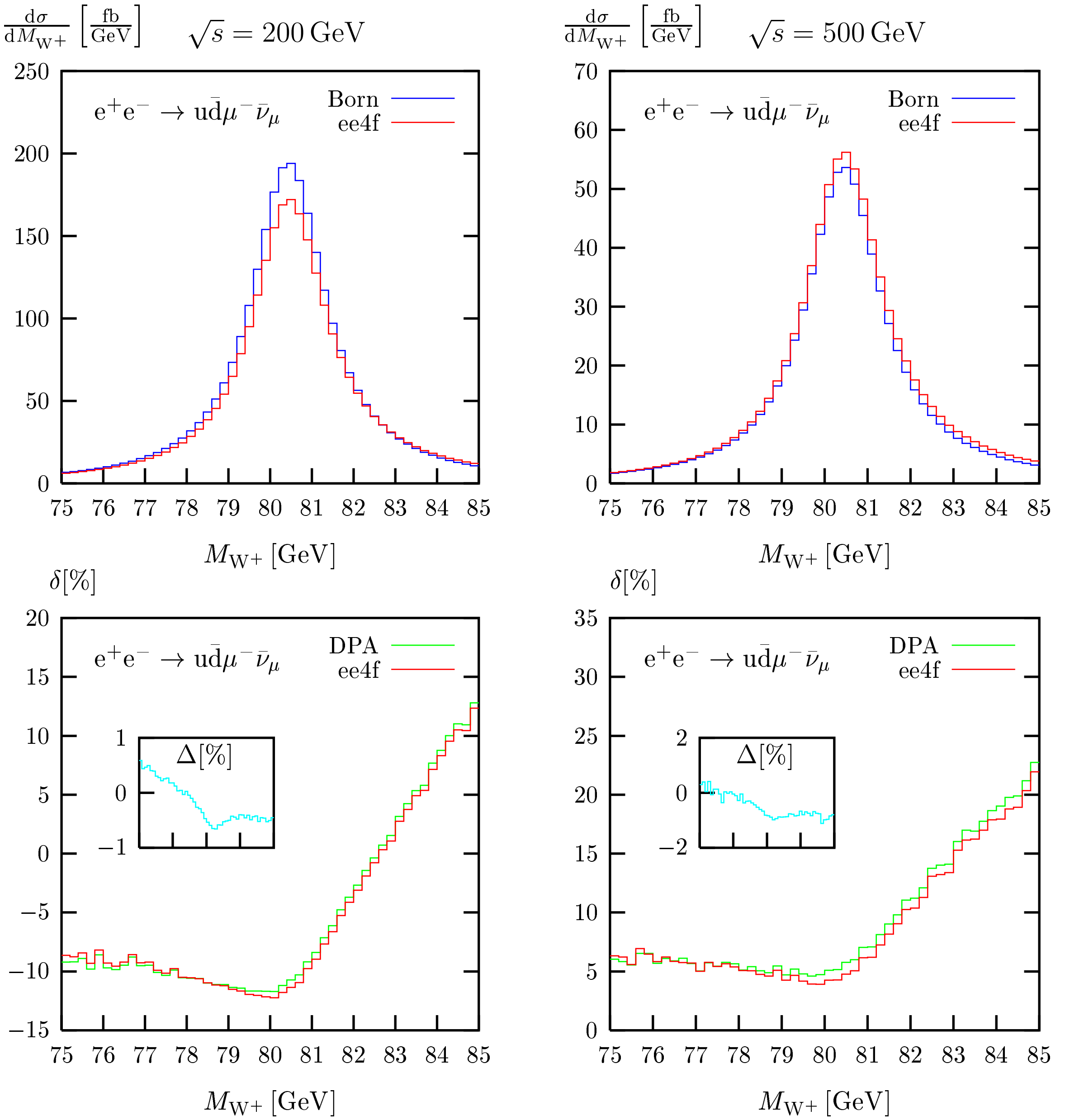

Figure 10: Distribution in the invariant mass of the W$^+$ boson (upper row) and the corresponding corrections (lower row) at $\sqrt{s} = 200\,\mathrm{GeV}$ (l.h.s.) and $\sqrt{s} = 500\,\mathrm{GeV}$ (r.h.s.) for $e^+e^- \to u\bar{d}\mu^-\bar{\nu}_\mu$. The inset plot shows the difference between the full $\mathcal{O}(\alpha)$ corrections and those in DPA.

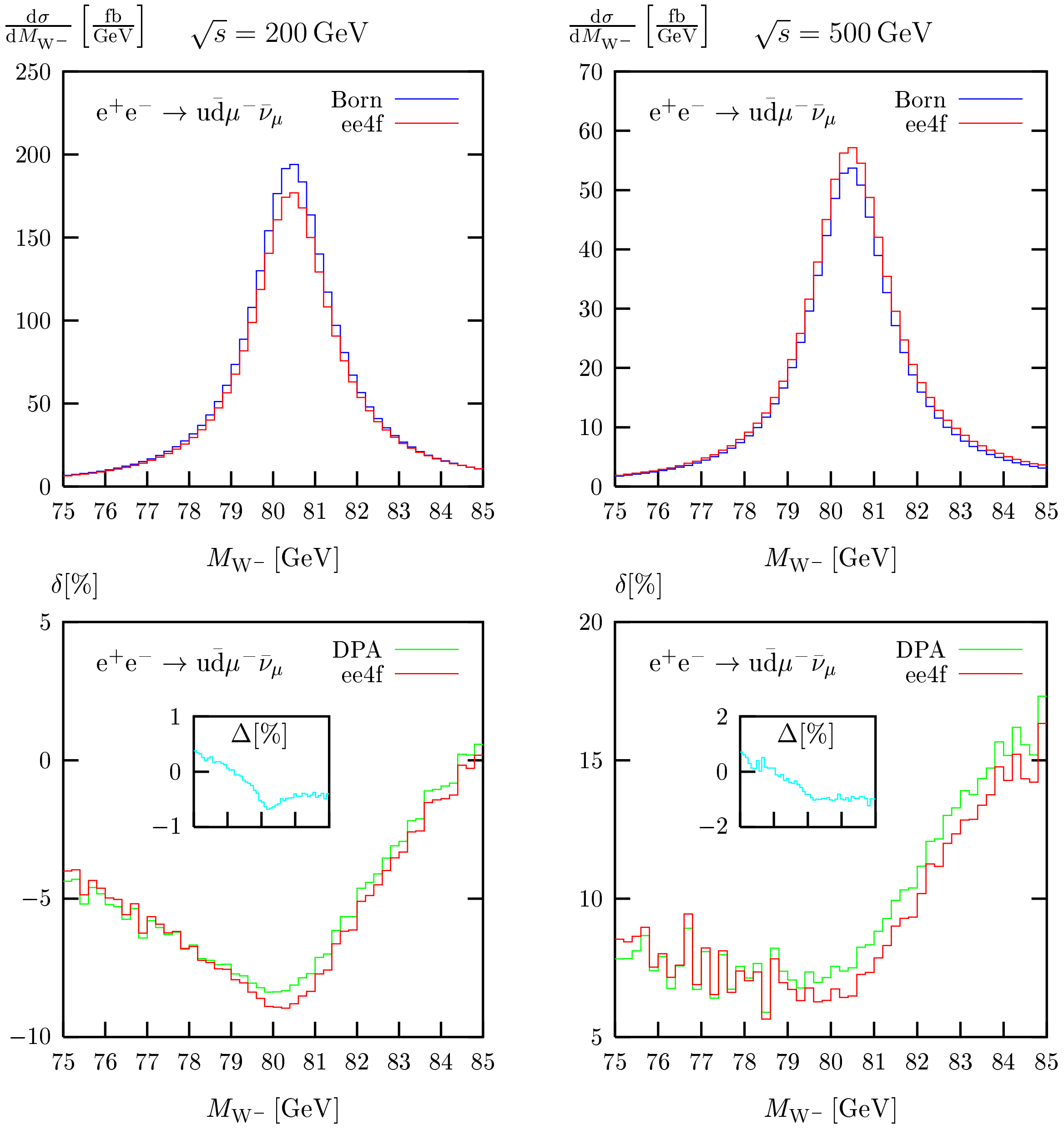

Figure 11: Distribution in the invariant mass of the W^- boson (upper row) and the corresponding corrections (lower row) at $\sqrt{s} = 200\,GeV$ (l.h.s.) and $\sqrt{s} = 500\,GeV$ (r.h.s.) for $e^+e^- \to u\bar{d}\mu^-\bar{\nu}_\mu$. The inset plot shows the difference between the full $\mathcal{O}(\alpha)$ corrections and those in DPA.

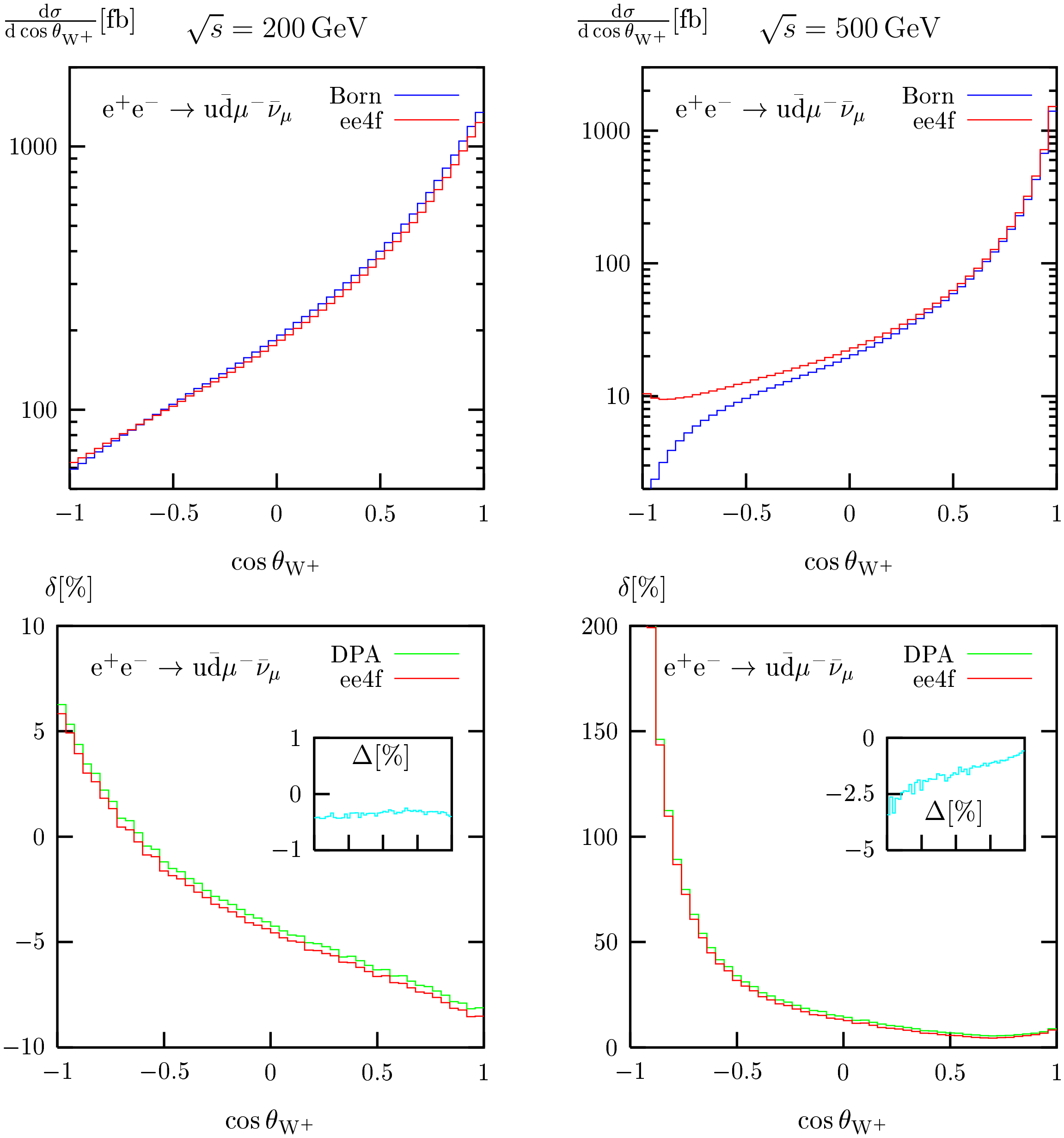

Figure 12: Distribution in the cosine of the W^+ production angle with respect to the e^+ beam (upper row) and the corresponding corrections (lower row) at $\sqrt{s} = 200\,\mathrm{GeV}$ (l.h.s.) and $\sqrt{s} = 500\,\mathrm{GeV}$ (r.h.s.) for $e^+e^- \to u\bar{d}\mu^-\bar{\nu}_\mu$. The inset plot shows the difference between the full $\mathcal{O}(\alpha)$ corrections and those in DPA.

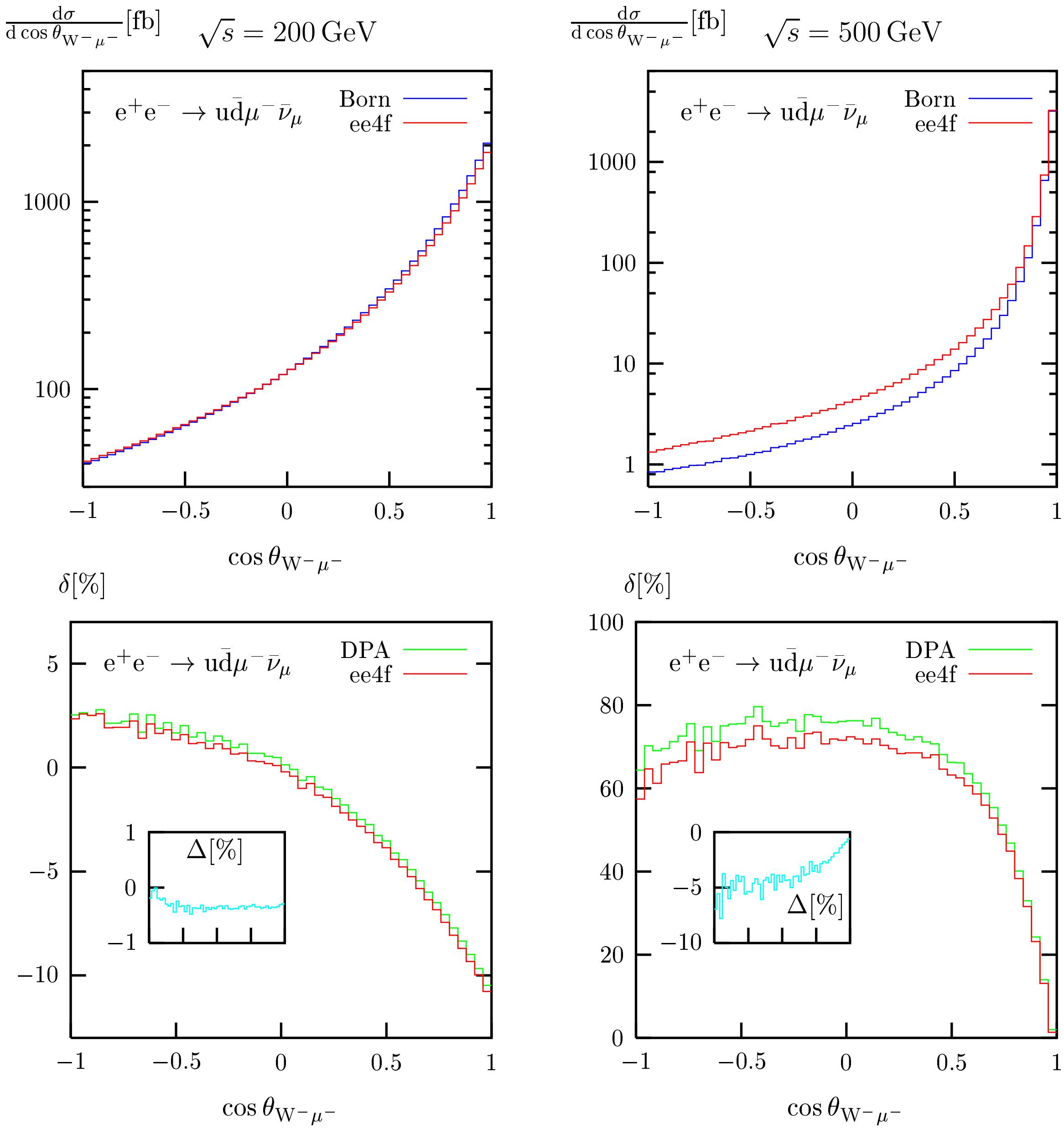

Figure 13: Distribution in the cosine of the μ^- decay angle with respect to the W^- direction (upper row) and the corresponding corrections (lower row) at $\sqrt{s} = 200\,\text{GeV}$ (l.h.s.) and $\sqrt{s} = 500\,\text{GeV}$ (r.h.s.) for $e^+e^- \to u\bar{d}\mu^-\bar{\nu}_\mu$. The inset plot shows the difference between the full $\mathcal{O}(\alpha)$ corrections and those in DPA.

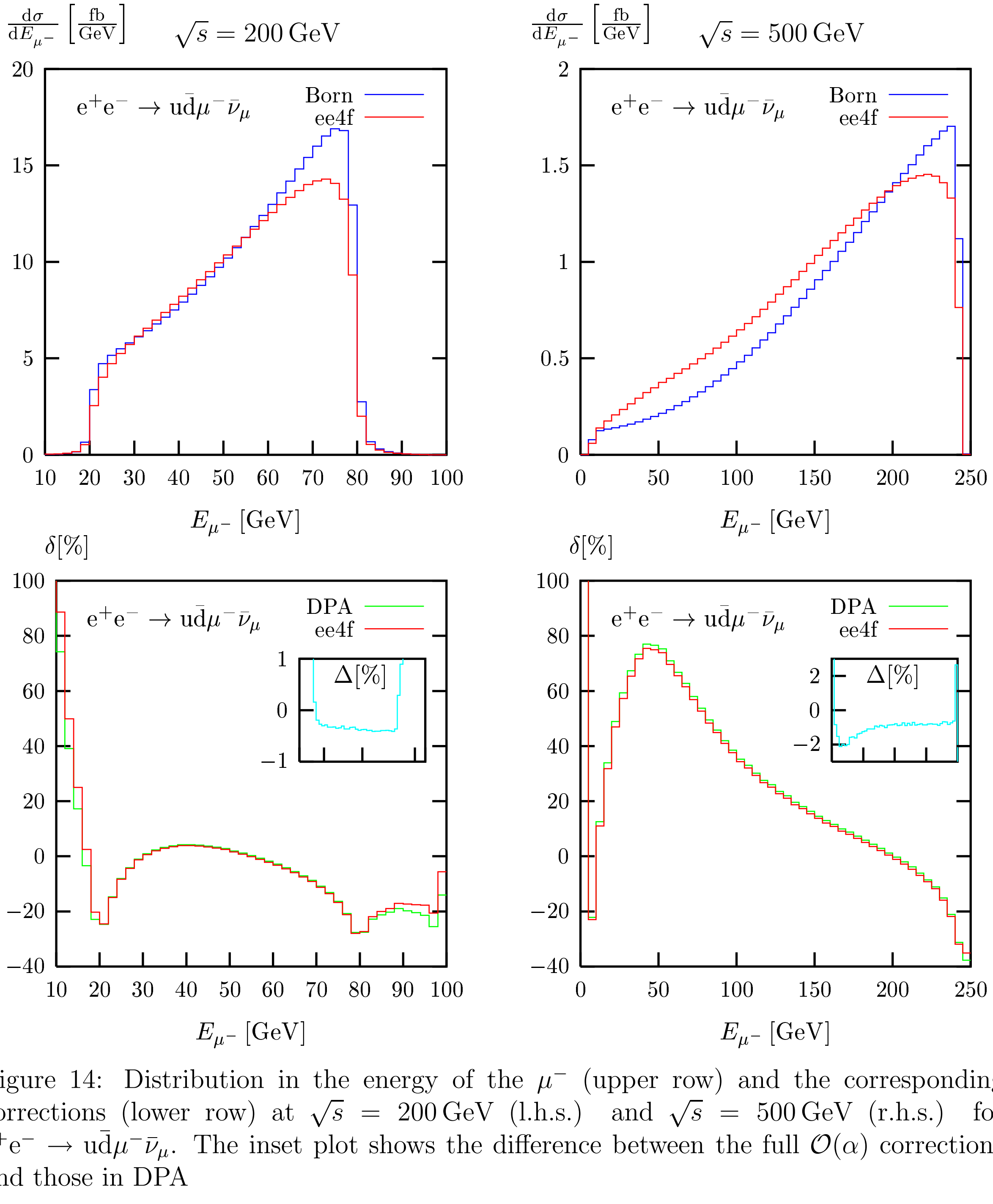

Figure 14: Distribution in the energy of the μ^- (upper row) and the corresponding corrections (lower row) at $\sqrt{s} = 200\,\mathrm{GeV}$ (l.h.s.) and $\sqrt{s} = 500\,\mathrm{GeV}$ (r.h.s.) for $\mathrm{e^+e^-} \to \mathrm{u\bar{d}}\mu^-\bar{\nu}_\mu$. The inset plot shows the difference between the full $\mathcal{O}(\alpha)$ corrections and those in DPA

with symmetric functions in these angles. Contributions of real parts, on the other hand, are symmetric in these angles. In order to illustrate this feature, we have included an extra curve in the plots for the relative corrections to this distribution labelled "DPA (real)". In this curve, we have switched off all imaginary parts in the DPA calculation, apart from the finite width in the resonant propagators. As expected, these results are symmetric in the angle ϕ_{W^+} about 180°. The contribution proportional to $\sin\phi_{\mathrm{W}^+}$ in the difference of the full $\mathcal{O}(\alpha)$ calculation with respect to the DPA (real) is even larger than the corresponding difference with respect to the complete DPA. These properties of the DPA suggest, that also the sinusoidal dependence on ϕ_{W^+} in the latter difference results from imaginary parts. A possible source could be the missing imaginary parts of the counterterms in DPA.

The distributions in the angle ϕ between the two planes spanned by the momenta of the two fermion pairs in which the W bosons decay, i.e. (note that $\mathbf{k}_+ = -\mathbf{k}_-$ for non-photonic events)

$$\begin{aligned} \cos\phi &= \frac{(\mathbf{k}_+ \times \mathbf{k}_1)(-\mathbf{k}_- \times \mathbf{k}_3)}{|\mathbf{k}_+ \times \mathbf{k}_1||-\mathbf{k}_- \times \mathbf{k}_3|}, \\ \mathrm{sgn}(\sin\phi) &= \mathrm{sgn}\left\{\mathbf{k}_+ \cdot [(\mathbf{k}_+ \times \mathbf{k}_1) \times (-\mathbf{k}_- \times \mathbf{k}_3)]\right\}, \end{aligned} \tag{5.5}$$

are presented in Figure 16. The large corrections for angles ϕ near 0° or 180°, i.e. if the two decay planes coincide, result from the suppression of hard photonic corrections [21]. The corrections beyond DPA do hardly depend on ϕ.

6 Conclusions

We have presented technical and conceptual details as well as further numerical results of a calculation of the complete electroweak $\mathcal{O}(\alpha)$ corrections to the charged-current four-fermion production processes $\mathrm{e}^+\mathrm{e}^- \to \nu_\tau\tau^+\mu^-\bar{\nu}_\mu$, $\mathrm{u}\bar{\mathrm{d}}\mu^-\bar{\nu}_\mu$, and $\mathrm{u}\bar{\mathrm{d}}\mathrm{s}\bar{\mathrm{c}}$.

In particular, we have described methods how the $\mathcal{O}(10^3)$ occurring different spinor structures can be algebraically reduced to a few simple standard structures. The presented algorithms, which shorten the analytical results considerably and thereby render the resulting computer code relatively short, should be useful for other future calculations.

Moreover, a concept for consistently performing one-loop calculations with complex masses for unstable particles is presented. Technically the complex masses are introduced via an appropriate complex renormalization prescription at the level of the Lagrangian, so that the usual machinery of perturbation theory (Feynman rules etc.) can be used to organize the calculation. Since the theory is not changed at all, there is no danger of double counting terms. The complex mass parameters, which also enter the weak mixing angle and coupling constants, can be viewed as an analytical continuation of the real masses. Consequently, all algebraic relations that follow from gauge invariance (Slavnov–Taylor identities, Ward identities, cancellation of gauge-parameter dependences) are valid in spite of the complex masses which incorporate finite-width effects. The price to pay for this achievement is that all one-loop integrals have to be performed with complex mass parameters.

Finally, we have completed our discussion of numerical results, which was started in Ref. [37] by considering total cross sections, by showing the effects of the complete $\mathcal{O}(\alpha)$

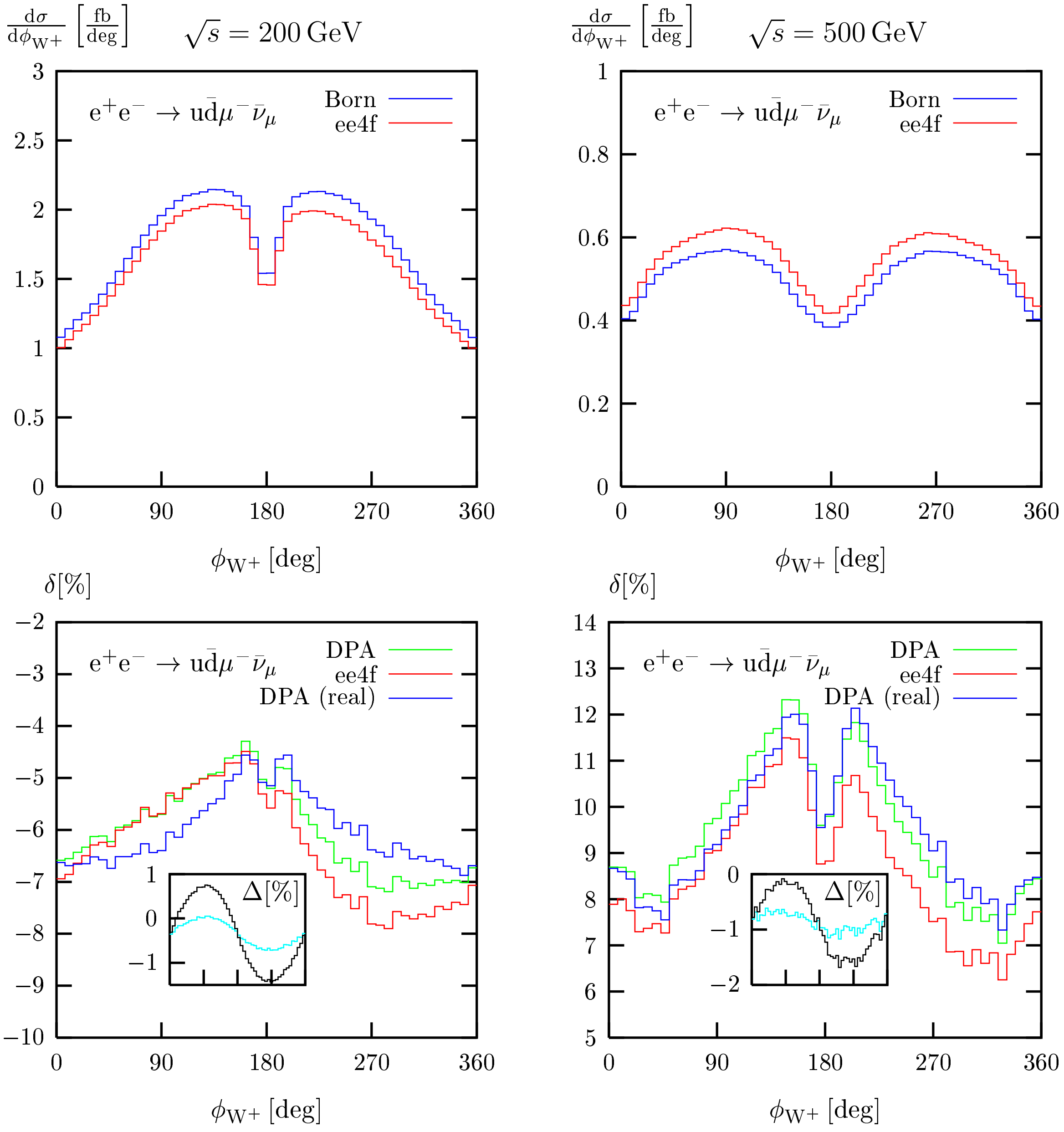

Figure 15: Distribution in the azimuthal decay angle of the W^+ (upper row) and the corresponding corrections (lower row) at $\sqrt{s} = 200\,\text{GeV}$ (l.h.s.) and $\sqrt{s} = 500\,\text{GeV}$ (r.h.s.) for $e^+e^- \to u\bar{d}\mu^-\bar{\nu}_\mu$. The inset plot shows the difference of the full $\mathcal{O}(\alpha)$ corrections to those in DPA and the larger difference to those in DPA (real), which is calculated without imaginary parts.

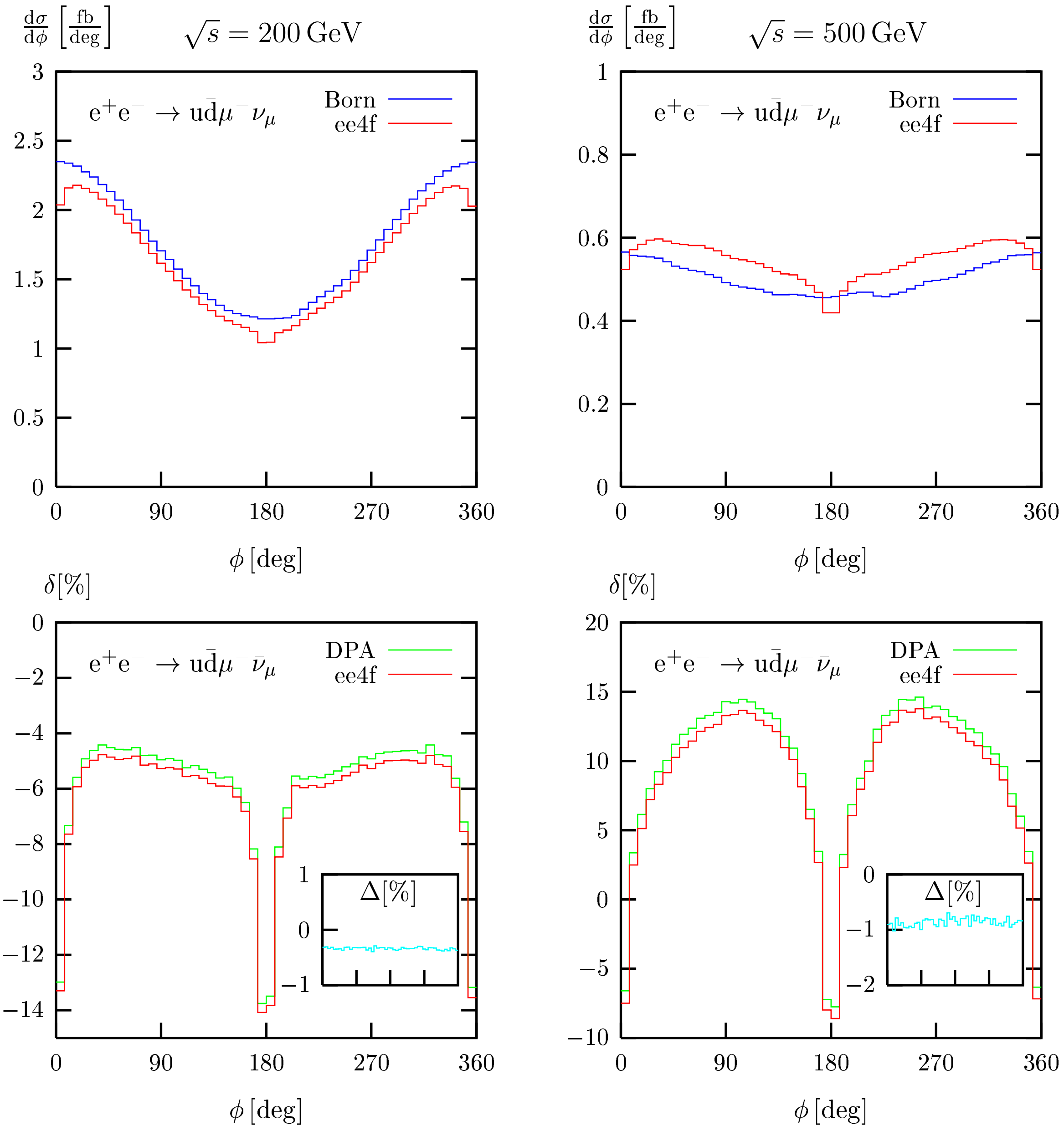

Figure 16: Distribution in the azimuthal angle ϕ (upper row) and the corresponding corrections (lower row) at $\sqrt{s} = 200\,\mathrm{GeV}$ (l.h.s.) and $\sqrt{s} = 500\,\mathrm{GeV}$ (r.h.s.) for $e^+e^- \to u\bar{d}\mu^-\bar{\nu}_\mu$. The inset plot shows the difference between the full $\mathcal{O}(\alpha)$ corrections and those in DPA.

corrections to various differential cross sections of physical interest. In particular, we have considered differential cross sections sensitive to imaginary parts. Our results have also been compared to predictions based on the double-pole approximation, revealing that the latter approximation is not sufficient to fully exploit the potential of a future linear collider in an analysis of W-boson pairs at high energies. Specifically, at (and above) a CM energy of 500 GeV the corrections beyond DPA induce a non-negligible distortion in angular distributions that could be misinterpreted as signal for anomalous triple gauge-boson couplings if not taken into account. The remaining theoretical uncertainties for the total cross section have been discussed in Ref. [37]. For differential distributions the uncertainties from QCD effects are even more relevant.

In this paper we have presented methods that were successfully used for the first complete $\mathcal{O}(\alpha)$ calculation of electroweak corrections to a process with six external particles and involving unstable particles in intermediate states. Processes of this type will become more and more important in the future. Our methods are not specifically adapted to the considered process and therefore should be helpful in precision calculations for similar processes at future colliders.

Acknowledgements

This work was supported in part by the Swiss National Science Foundation, by the Swiss Bundesamt für Bildung und Wissenschaft, and by the European Union under contract HPRN-CT-2000-00149. A.D. thanks the Lehrstuhl für Theoretische Physik II of the University of Würzburg, where part of this work has been done, for its kind hospitality.

Appendix

Interpretation of the reduction algorithm of Section 3.2 in the Weyl–van der Waerden spinor formalism

In this appendix we inspect the reduction algorithm of Section 3.2 within the Weyl–van der Waerden (WvdW) spinor formalism, which is particularly simple for massless particles. We consistently employ the conventions of Ref. [65] for the spinor method and highlight only those features that are crucial for our manipulations.

In this formalism, Dirac spinors and momenta of massless fermions are described by Weyl spinors p_A, $p_{\dot{A}} = (p_A)^*$ which are related to the four-momentum p_μ according to

$$p_\mu \sigma^\mu_{\dot{A}B} = p_{\dot{A}} p_B, \tag{A.1}$$

where $\sigma^\mu_{\dot{A}B}$ denote the unit matrix ($\mu = 0$) and the Pauli matrices ($\mu = 1, 2, 3$). The matrices σ^μ also appear as the non-vanishing blocks in the Dirac matrices γ^μ. Thus, Dirac spinor chains translate into chains involving Weyl spinors and σ^μ matrices. Coupled chains can be separated by using the relation

$$\sigma^\mu_{\dot{A}B} \sigma_{\mu,\dot{C}D} = 2\epsilon_{\dot{A}\dot{C}} \epsilon_{BD}, \tag{A.2}$$

where ϵ_{AB} is the totally antisymmetric tensor in two dimensions and $\epsilon_{\dot{A}\dot{B}}$ is its complex conjugate. In this way, all Weyl spinors get contracted in so-called spinor products

$$\langle p_i p_j \rangle = \epsilon^{AB} p_{i,A} p_{j,B} \tag{A.3}$$

or their complex conjugates. Using (A.2), Lorentz products can also be translated into spinor products. We illustrate the above considerations by the simplest examples:

$$\begin{aligned} (p_i p_j) &= \frac{1}{2} \langle p_i p_j \rangle \langle p_i p_j \rangle^*, \\ \Big[\not{p}_k\Big]^-_{ij} &= \langle p_k p_i \rangle \langle p_k p_j \rangle^*, \\ \Big[\not{p}_k\Big]^+_{ij} &= \langle p_k p_i \rangle^* \langle p_k p_j \rangle. \end{aligned} \tag{A.4}$$

Dirac chains of the form (3.3) involving no additional $\epsilon^{\mu\nu\rho\sigma}$ can thus be directly reduced to a product of (at least four) spinor products. The totally antisymmetric tensor $\epsilon^{\mu\nu\rho\sigma}$ is translated into WvdW objects according to

$$\epsilon^{\mu\nu\rho\kappa} = \frac{\mathrm{i}}{4} \left(\sigma^{\mu}_{\dot{A}B} \sigma^{\nu,B\dot{C}} \sigma^{\kappa}_{\dot{C}D} \sigma^{\rho,D\dot{A}} - \sigma^{\mu}_{\dot{A}B} \sigma^{\rho,B\dot{C}} \sigma^{\kappa}_{\dot{C}D} \sigma^{\nu,D\dot{A}} \right), \tag{A.5}$$

so that contractions with $\epsilon^{\mu\nu\rho\sigma}$ can also be expressed in terms of WvdW spinor products. The two-dimensionality of the WvdW spinor space is rather restrictive and leads to the identity

$$\langle p_i p_j \rangle \langle p_k p_l \rangle + \langle p_i p_k \rangle \langle p_l p_j \rangle + \langle p_i p_l \rangle \langle p_j p_k \rangle = 0, \tag{A.6}$$

which frequently admits simplifications in complicated expressions. In the cases relevant for the considered processes, these identities allow to combine the sums that result from the application of (A.5), so that also all spinorial expressions involving contractions with $\epsilon^{\mu\nu\rho\sigma}$ can be reduced to a product of spinor products.

The identities (A.5) and (A.6) also allow to write the combinations $A^{a\,b\,c\,d}_{i\,j\,k\,l}$ of (3.21) as simple factors of spinor products:

$$\begin{aligned} A^{++-+}_{i\,j\,k\,l} &= \frac{1}{2} \langle p_i p_j \rangle \langle p_k p_l \rangle \langle p_i p_k \rangle^* \langle p_j p_l \rangle^*, \\ A^{+-++}_{i\,j\,k\,l} &= \frac{1}{2} \langle p_i p_l \rangle \langle p_k p_j \rangle \langle p_i p_j \rangle^* \langle p_k p_l \rangle^*, \\ A^{-+++}_{i\,j\,k\,l} &= \frac{1}{2} \langle p_i p_k \rangle \langle p_j p_l \rangle \langle p_i p_l \rangle^* \langle p_j p_k \rangle^*, \\ A^{a\,b\,c\,-}_{i\,j\,k\,l} &= (A^{a\,b\,c\,+}_{i\,j\,k\,l})^*. \end{aligned} \tag{A.7}$$

When expressing the $A^{a\,b\,c\,d}_{i\,j\,k\,l}$ in terms of spinor products, the relations (3.30)–(3.33) become trivial. The relations (A.7) and the fact that in the WvdW formalism all spinor chains can be expressed in terms of products of spinor products explains why in the formalism of Section 3.2 all spinor chains could be reduced to a simple product of $A^{a\,b\,c\,d}_{i\,j\,k\,l}$ and scalar products. The results of (3.34) read in the WvdW formalism

$$\Big[\gamma^\mu \gamma^\nu \gamma^\rho\Big]^\sigma_{12} \Big[\gamma_\mu \gamma_\nu \gamma_\rho\Big]^\tau_{34} = 32 \langle p_2 p_4 \rangle \langle p_1 p_3 \rangle^* \delta_{\sigma+} \delta_{\tau+} + 32 \langle p_2 p_4 \rangle^* \langle p_1 p_3 \rangle \delta_{\sigma-} \delta_{\tau-}$$

$$
\begin{aligned}
&\quad + 8\langle p_2p_3\rangle\langle p_1p_4\rangle^*\delta_{\sigma+}\delta_{\tau-} + 8\langle p_2p_3\rangle^*\langle p_1p_4\rangle\delta_{\sigma-}\delta_{\tau+}, \\
\Big[\not{p}_3\gamma^\mu\gamma^\nu\Big]^\sigma_{12}\Big[\gamma_\nu\gamma^\rho\gamma^\kappa\Big]^-_{34}\Big[\gamma_\mu\gamma_\rho\gamma_\kappa\Big]^-_{56} &= 32\langle p_3p_5\rangle\langle p_4p_6\rangle^* \\
&\quad \times \left(\delta_{\sigma+}\langle p_2p_3\rangle\langle p_1p_3\rangle^* + \delta_{\sigma-}\langle p_1p_3\rangle\langle p_2p_3\rangle^*\right), \\
\Big[\not{p}_3\gamma^\mu\gamma^\nu\gamma^\rho\gamma^\kappa\Big]^-_{12}\Big[\gamma_\nu\gamma_\rho\gamma_\kappa\Big]^-_{34}\Big[\gamma_\mu\Big]^-_{56} &= 64\langle p_1p_3\rangle\langle p_3p_5\rangle\langle p_2p_4\rangle^*\langle p_3p_6\rangle^*, \\
-\mathrm{i}\epsilon^{\mu\nu\rho\sigma}\, p_{1,\sigma}\Big[\gamma_\mu\Big]^+_{12}\Big[\gamma_\nu\Big]^-_{34}\Big[\gamma_\rho\Big]^-_{56} &= -2\langle p_1p_2\rangle\langle p_3p_5\rangle\langle p_1p_4\rangle^*\langle p_1p_6\rangle^*. \qquad \text{(A.8)}
\end{aligned}
$$

Finally, the relevant SMEs (3.26) read in the WvdW formalism

$$
\begin{aligned}
\hat{\mathcal{M}}^{---} &= \langle p_1p_3\rangle\langle p_2p_3\rangle^*\langle p_1p_3\rangle\langle p_1p_4\rangle^*\langle p_1p_5\rangle\langle p_1p_6\rangle^*, \\
\hat{\mathcal{M}}^{+--} &= \langle p_1p_3\rangle^*\langle p_2p_3\rangle\langle p_1p_3\rangle\langle p_1p_4\rangle^*\langle p_1p_5\rangle\langle p_1p_6\rangle^*. \qquad \text{(A.9)}
\end{aligned}
$$

Of course, it would have been possible to translate each spinor chain into WvdW spinor products directly after performing the loop integration, i.e. skipping the steps described in Section 3.2. However, it would have been hard to perform all the manipulations with WvdW objects made there in terms of Lorentz products. For instance, it is practically impossible to make full use of momentum conservation in very involved expressions in terms of WvdW spinor products. It turned out in many examples given in the literature that no algorithmic recipe has been found yet yielding the most compact expressions in complicated amplitudes. Moreover, the generalization to massive fermions is more complicated in the WvdW formalism than in the method described in Section 3.2. In fact a variant of this method has already been used in Ref. [54] for the process $\mathrm{e^+e^-} \to \mathrm{t\bar{t}H}$.

References

[1] The LEP Collaborations ALEPH, DELPHI, L3, OPAL, the LEP EWWG, and the SLD Heavy Flavor and Electroweak Groups, hep-ex/0412015.

[2] J. A. Aguilar-Saavedra *et al.*, TESLA Technical Design Report Part III: Physics at an $\mathrm{e^+e^-}$ Linear Collider, hep-ph/0106315.

[3] T. Abe *et al.* [American Linear Collider Working Group Collaboration], in *Proc. of the APS/DPF/DPB Summer Study on the Future of Particle Physics (Snowmass 2001)* ed. R. Davidson and C. Quigg, SLAC-R-570, *Resource book for Snowmass 2001*, [hep-ex/0106055, hep-ex/0106056, hep-ex/0106057, hep-ex/0106058].

[4] K. Abe *et al.* [ACFA Linear Collider Working Group Collaboration], ACFA Linear Collider Working Group report, [hep-ph/0109166].

[5] K. Mönig and A. Tonazzo, talk given by K. Mönig at the *2nd ECFA/DESY Study on Physics and Detectors for a Linear Electron–Positron Collider*, Padova, Italy, 2000.

[6] W. Alles, C. Boyer and A. J. Buras, Nucl. Phys. B **119** (1977) 125;
K. J. F. Gaemers and G. J. Gounaris, Z. Phys. C **1** (1979) 259.

[7] M. Lemoine and M. J. G. Veltman, Nucl. Phys. B **164** (1980) 445;
R. Philippe, Phys. Rev. D **26** (1982) 1588;
J. Fleischer, F. Jegerlehner and M. Zrałek, Z. Phys. C **42** (1989) 409.

[8] M. Böhm *et al.*, Nucl. Phys. B **304** (1988) 463.

[9] W. Beenakker, K. Kołodziej and T. Sack, Phys. Lett. B **258** (1991) 469;
W. Beenakker, F. A. Berends and T. Sack, Nucl. Phys. B **367** (1991) 287;
H. Tanaka, T. Kaneko and Y. Shimizu, Comput. Phys. Commun. **64** (1991) 149;
K. Kołodziej and M. Zrałek, Phys. Rev. D **43** (1991) 3619;
J. Fleischer, K. Kołodziej and F. Jegerlehner, Phys. Rev. D **47** (1993) 830.

[10] S. Dittmaier, M. Böhm and A. Denner, Nucl. Phys. B **376** (1992) 29 [Erratum-ibid. B **391** (1993) 483];
M. Kuroda, I. Kuss and D. Schildknecht, Phys. Lett. B **409** (1997) 405 [hep-ph/9705294].

[11] W. Beenakker *et al.*, Nucl. Phys. B **410** (1993) 245; Phys. Lett. B **317** (1993) 622;
M. Kuroda and D. Schildknecht, Nucl. Phys. B **531** (1998) 24 [hep-ph/9807250].

[12] D. Y. Bardin, S. Riemann and T. Riemann, Z. Phys. C **32** (1986) 121;
F. Jegerlehner, Z. Phys. C **32** (1986) 425 [Erratum-ibid. C **38** (1988) 519];
A. Denner and T. Sack, Z. Phys. C **46** (1990) 653.

[13] F. A. Berends, R. Pittau and R. Kleiss, Comput. Phys. Commun. **85** (1995) 437 [hep-ph/9409326];
M. Skrzypek, S. Jadach, W. Płaczek and Z. Wąs, Comput. Phys. Commun. **94** (1996) 216;
G. Passarino, Comput. Phys. Commun. **97** (1996) 261 [hep-ph/9602302];
E. Accomando and A. Ballestrero, Comput. Phys. Commun. **99** (1997) 270 [hep-ph/9607317];
J. Fujimoto *et al.*, Comput. Phys. Commun. **100** (1997) 128 [hep-ph/9605312];
D. Y. Bardin *et al.*, Comput. Phys. Commun. **104** (1997) 161 [hep-ph/9612409];
S. Jadach *et al.*, Comput. Phys. Commun. **119** (1999) 272 [hep-ph/9906277];
F. A. Berends, C. G. Papadopoulos and R. Pittau, Comput. Phys. Commun. **136** (2001) 148 [hep-ph/0011031];
E. Accomando, A. Ballestrero and E. Maina, Comput. Phys. Commun. **150** (2003) 166 [hep-ph/0204052].

[14] W. Beenakker *et al.*, in *Physics at LEP2*, eds. G. Altarelli, T. Sjöstrand and F. Zwirner (CERN 96-01, Geneva, 1996), Vol. 1, p. 79 [hep-ph/9602351].

[15] D. Y. Bardin *et al.*, in *Physics at LEP2*, eds. G. Altarelli, T. Sjöstrand and F. Zwirner (CERN 96-01, Geneva, 1996), Vol. 2, p. 3 [hep-ph/9709270].

[16] M. W. Grünewald *et al.*, in *Reports of the Working Groups on Precision Calculations for LEP2 Physics*, eds. S. Jadach, G. Passarino and R. Pittau (CERN 2000-009, Geneva, 2000), p. 1 [hep-ph/0005309].

[17] V. S. Fadin, V. A. Khoze and A. D. Martin, Phys. Lett. B **311** (1993) 311;
D. Y. Bardin, W. Beenakker and A. Denner, Phys. Lett. B **317** (1993) 213.

[18] W. Beenakker, F. A. Berends and A. P. Chapovsky, Nucl. Phys. B **548** (1999) 3 [hep-ph/9811481].

[19] S. Jadach *et al.*, Phys. Rev. D **61** (2000) 113010 [hep-ph/9907436]; Comput. Phys. Commun. **140** (2001) 432 [hep-ph/0103163]; Comput. Phys. Commun. **140** (2001) 475 [hep-ph/0104049]; Phys. Rev. D **65** (2002) 093010 [hep-ph/0007012].

[20] A. Denner, S. Dittmaier, M. Roth and D. Wackeroth, Phys. Lett. B **475** (2000) 127 [hep-ph/9912261]; Eur. Phys. J. direct C **2** (2000) 4 [hep-ph/9912447]; in *Proc. of the 5th International Symposium on Radiative Corrections (RADCOR 2000)*, ed. H. E. Haber, hep-ph/0101257; Comput. Phys. Commun. **153** (2003) 462 [hep-ph/0209330].

[21] A. Denner, S. Dittmaier, M. Roth and D. Wackeroth, Nucl. Phys. B **587** (2000) 67 [hep-ph/0006307].

[22] Y. Kurihara, M. Kuroda and D. Schildknecht, Phys. Lett. B **509** (2001) 87 [hep-ph/0104201].

[23] A. Denner, S. Dittmaier, M. Roth and D. Wackeroth, Nucl. Phys. B **560** (1999) 33 [hep-ph/9904472].

[24] S. Jadach *et al.*, Phys. Lett. B **523** (2001) 117 [hep-ph/0109072];
F. Cossutti, DELPHI note 2004-050 PHYS 944, hep-ph/0505232;
R. Brunelière *et al.*, Phys. Lett. B **533** (2002) 75 [hep-ph/0201304].

[25] A. Vicini, Acta Phys. Polon. B **29** (1998) 2847.

[26] F. A. Berends and G. B. West, Phys. Rev. D **1** (1970) 122;
Y. Kurihara, D. Perret-Gallix and Y. Shimizu, Phys. Lett. B **349** (1995) 367 [hep-ph/9412215].

[27] E. N. Argyres *et al.*, Phys. Lett. B **358**(1995) 339 [hep-ph/9507216].

[28] A. Aeppli, F. Cuypers and G. J. van Oldenborgh, Phys. Lett. B **314** (1993) 413 [hep-ph/9303236].

[29] W. Beenakker *et al.*, Nucl. Phys. B **500** (1997) 255 [hep-ph/9612260].

[30] R. G. Stuart, Phys. Lett. B **262** (1991) 113.

[31] A. Aeppli, G. J. van Oldenborgh and D. Wyler, Nucl. Phys. B **428** (1994) 126 [hep-ph/9312212].

[32] U. Baur and D. Zeppenfeld, Phys. Rev. Lett. **75** (1995) 1002 [hep-ph/9503344].

[33] G. Passarino, Nucl. Phys. B **574** (2000) 451 [hep-ph/9911482];
E. Accomando, A. Ballestrero and E. Maina, Phys. Lett. B **479** (2000) 209 [hep-ph/9911489].

[34] W. Beenakker, F. A. Berends and A. P. Chapovsky, Nucl. Phys. B **573** (2000) 503 [hep-ph/9909472];
W. Beenakker *et al.*, Nucl. Phys. B **667** (2003) 359 [hep-ph/0303105].

[35] M. Beneke, A. P. Chapovsky, A. Signer and G. Zanderighi, Phys. Rev. Lett. **93** (2004) 011602 [hep-ph/0312331] and Nucl. Phys. B **686** (2004) 205 [hep-ph/0401002].

[36] F. Boudjema *et al.*, Nucl. Phys. Proc. Suppl. **135** (2004) 323 [hep-ph/0407079].

[37] A. Denner, S. Dittmaier, M. Roth and L. H. Wieders, Phys. Lett. B **612** (2005) 223 [hep-ph/0502063].

[38] S. Dittmaier, Nucl. Phys. B **565** (2000) 69 [hep-ph/9904440];
M. Roth, PhD thesis, ETH Zürich No. 13363 (1999), hep-ph/0008033.

[39] W. F. L. Hollik, Fortschr. Phys. **38** (1990) 165.

[40] A. Denner, S. Dittmaier and G. Weiglein, Nucl. Phys. B **440** (1995) 95 [hep-ph/9410338].

[41] J. Küblbeck, M. Böhm and A. Denner, Comput. Phys. Commun. **60** (1990) 165;
H. Eck and J. Küblbeck, *Guide to FeynArts 1.0*, University of Würzburg, 1992.

[42] T. Hahn, Comput. Phys. Commun. **140** (2001) 418 [hep-ph/0012260].

[43] T. Hahn and M. Perez-Victoria, Comput. Phys. Commun. **118** (1999) 153 [hep-ph/9807565];
T. Hahn, Nucl. Phys. Proc. Suppl. **89** (2000) 231 [hep-ph/0005029].

[44] A. Denner, Fortsch. Phys. **41** (1993) 307.

[45] D. B. Melrose, Nuovo Cimento **XL A** (1965) 181.

[46] A. Denner and S. Dittmaier, Nucl. Phys. B **658** (2003) 175 [hep-ph/0212259].

[47] G. Passarino and M. Veltman, Nucl. Phys. B **160** (1979) 151.

[48] G. 't Hooft and M. Veltman, Nucl. Phys. B **153** (1979) 365.

[49] W. Beenakker and A. Denner, Nucl. Phys. B **338** (1990) 349.

[50] A. Denner, U. Nierste and R. Scharf, Nucl. Phys. B **367** (1991) 637.

[51] A. Vicini, Phys. Lett. B **531** (2002) 83 [hep-ph/0104164].

[52] A. Sirlin, Nucl. Phys. B **192** (1981) 93.

[53] A. Denner, S. Dittmaier, M. Roth and M. M. Weber, Nucl. Phys. B **660** (2003) 289 [hep-ph/0302198].

[54] A. Denner, S. Dittmaier, M. Roth and M. M. Weber, Nucl. Phys. B **680** (2004) 85 [hep-ph/0309274].

[55] A. R. Bohm and Y. Sato, Phys. Rev. D **71** (2005) 085018 [hep-ph/0412106].

[56] R. E. Cutkosky, J. Math. Phys. **1** (1960) 429.

[57] M. J. G. Veltman, Physica **29** (1963) 186.

[58] K. I. Aoki *et al.*, Prog. Theor. Phys. **65** (1981) 1001; Prog. Theor. Phys. Suppl. **73** (1982) 1.

[59] R. G. Stuart, in Proceedings of the XXVth Rencontre de Moriond, Z^0 *physics*, ed. J. Trân Thanh Vân, (Editions Frontières, Gif-sur-Yvette, 1990), p. 41.

[60] A. Sirlin, Phys. Rev. Lett. **67** (1991) 2127; Phys. Lett. B **267** (1991) 240;
R. G. Stuart, Phys. Rev. Lett. **70** (1993) 3193;
M. Passera and A. Sirlin, Phys. Rev. Lett. **77** (1996) 4146 [hep-ph/9607253];
P. Gambino and P. A. Grassi, Phys. Rev. D **62** (2000) 076002 [hep-ph/9907254];
P. A. Grassi, B. A. Kniehl and A. Sirlin, Phys. Rev. D **65** (2002) 085001 [hep-ph/0109228];
A. Freitas, W. Hollik, W. Walter and G. Weiglein, Nucl. Phys. B **632** (2002) 189 [Erratum-ibid. B **666** (2003) 305] [hep-ph/0202131].

[61] A. Denner and T. Hahn, Nucl. Phys. B **525** (1998) 27 [hep-ph/9711302];
A. Bredenstein, S. Dittmaier and M. Roth, hep-ph/0506005, to appear in Eur. Phys. J. C.

[62] S. Eidelman *et al.* [Particle Data Group Collaboration], Phys. Lett. B **592** (2004) 1.

[63] P. Azzi *et al.* [CDF and D0 Collaborations, and Tevatron Electroweak Working Group], hep-ex/0404010.

[64] F. Jegerlehner, DESY 01-029, LC-TH-2001-035, hep-ph/0105283.

[65] S. Dittmaier, Phys. Rev. D **59** (1999) 016007 [hep-ph/9805445].